



National Library  
of Canada

Acquisitions and  
Bibliographic Services Branch

395 Wellington Street  
Ottawa, Ontario  
K1A 0N4

Bibliothèque nationale  
du Canada

Direction des acquisitions et  
des services bibliographiques

395, rue Wellington  
Ottawa (Ontario)  
K1A 0N4

*Your file    Votre référence*

*Our file    Notre référence*

## NOTICE

The quality of this microform is heavily dependent upon the quality of the original thesis submitted for microfilming. Every effort has been made to ensure the highest quality of reproduction possible.

If pages are missing, contact the university which granted the degree.

Some pages may have indistinct print especially if the original pages were typed with a poor typewriter ribbon or if the university sent us an inferior photocopy.

Reproduction in full or in part of this microform is governed by the Canadian Copyright Act, R.S.C. 1970, c. C-30, and subsequent amendments.

## AVIS

La qualité de cette microforme dépend grandement de la qualité de la thèse soumise au microfilmage. Nous avons tout fait pour assurer une qualité supérieure de reproduction.

S'il manque des pages, veuillez communiquer avec l'université qui a conféré le grade.

La qualité d'impression de certaines pages peut laisser à désirer, surtout si les pages originales ont été dactylographiées à l'aide d'un ruban usé ou si l'université nous a fait parvenir une photocopie de qualité inférieure.

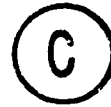
La reproduction, même partielle, de cette microforme est soumise à la Loi canadienne sur le droit d'auteur, SRC 1970, c. C-30, et ses amendements subséquents.

UNIVERSITY OF ALBERTA

Pressure Transient Analysis of Non-Newtonian Power-Law  
Fluid Flow in Fractal Reservoirs

by

Chayan Chakrabarty



A THESIS

SUBMITTED TO THE FACULTY OF GRADUATE STUDIES AND RESEARCH  
IN PARTIAL FULFILMENT OF THE REQUIREMENTS FOR THE DEGREE OF

Doctor of Philosophy

IN

Petroleum Engineering

Department of Mining, Metallurgical & Petroleum Engineering

Edmonton, Alberta

Spring 1993



National Library  
of Canada

Acquisitions and  
Bibliographic Services Branch

395 Wellington Street  
Ottawa, Ontario  
K1A 0N4

Bibliothèque nationale  
du Canada

Direction des acquisitions et  
des services bibliographiques

395, rue Wellington  
Ottawa (Ontario)  
K1A 0N4

*Your file / Votre référence*

*Our file / Notre référence*

**The author has granted an irrevocable non-exclusive licence allowing the National Library of Canada to reproduce, loan, distribute or sell copies of his/her thesis by any means and in any form or format, making this thesis available to interested persons.**

**L'auteur a accordé une licence irrévocable et non exclusive permettant à la Bibliothèque nationale du Canada de reproduire, prêter, distribuer ou vendre des copies de sa thèse de quelque manière et sous quelque forme que ce soit pour mettre des exemplaires de cette thèse à la disposition des personnes intéressées.**

**The author retains ownership of the copyright in his/her thesis. Neither the thesis nor substantial extracts from it may be printed or otherwise reproduced without his/her permission.**

**L'auteur conserve la propriété du droit d'auteur qui protège sa thèse. Ni la thèse ni des extraits substantiels de celle-ci ne doivent être imprimés ou autrement reproduits sans son autorisation.**

ISBN 0-315-82165-5

**Canada**

THE UNIVERSITY OF ALBERTA

RELEASE FORM

NAME OF AUTHOR Chayan Chakrabarty

TITLE OF THESIS Pressure Transient Analysis of Non-Newtonian  
Power-Law Fluid Flow in Fractal Reservoirs

DEGREE FOR WHICH THESIS WAS PRESENTED Doctor of Philosophy

YEAR THIS DEGREE GRANTED Spring 1993

Permission is hereby granted to THE UNIVERSITY OF ALBERTA LIBRARY to reproduce single copies of this thesis and to lend or sell such copies for private, scholarly or scientific research purposes only.

The author reserves other publication rights, and neither the thesis nor extensive extracts from it may be printed or otherwise reproduced without the author's written permission.

(SIGNED) Chayan Chakrabarty

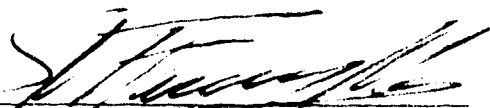
PERMANENT ADDRESS:

c/o Mr. B. Chakrabarty  
Flat 8C, 5<sup>th</sup> Phase  
Jamshedpur - 831 011, INDIA

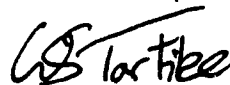
DATED April 22, 1993

THE UNIVERSITY OF ALBERTA  
FACULTY OF GRADUATE STUDIES AND RESEARCH

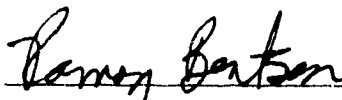
The undersigned certify that they have read, and recommend to the Faculty of Graduate Studies and Research, for acceptance, a thesis entitled Pressure Transient Analysis of Non-Newtonian Power-Law Fluid Flow in Fractal Reservoirs submitted by Chayan Chakrabarty in partial fulfilment of the requirements for the degree of Doctor of Philosophy in Petroleum Engineering.



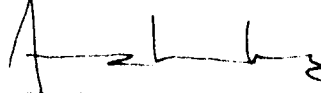
Professor S. M. Farouq Ali (Co-supervisor)



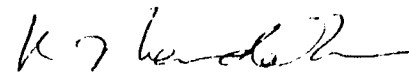
Professor W. S. Tortike (Co-supervisor)



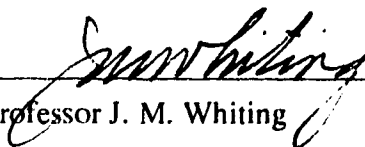
Professor R. G. Bentsen



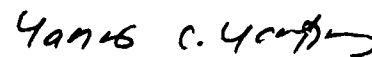
Professor A. Chakma



Professor K. Nandakumar



Professor J. M. Whiting



Professor Y. C. Yortsos

Date April 15, 93

*TO*

*MY PARENTS*

*AND*

*MY TEACHER*

## ABSTRACT

Analytical modelling of heterogeneous and, especially, fractured reservoir systems constitutes an important aspect of petroleum reservoir engineering and formation evaluation and environmental engineering studies. Fractal geometry has been used in some recent studies to help define hydrologic conceptual models for a certain class of fractured systems. However, transient pressure behaviour during the flow of non-Newtonian power-law fluids in homogeneous systems has often been misinterpreted as flow in fractures when using Newtonian-based theory. Thus, use of the existing fractal pressure transient models may not be appropriate when analyzing pressure transient data during non-Newtonian fluid flow through a network of fractures.

The principal objective of the present study is to examine the basic characteristics of transient flow of non-Newtonian power-law fluids in a fractal network of fractures. The theoretical basis for analyzing transient pressure and rate data under such situations are presented. Analytical and finite-difference solutions of the partial differential equations describing the single-phase flow of a slightly compressible, power-law fluid in an infinitely large fractal reservoir are obtained.

Transient pressure behaviour for finite reservoir cases is studied. Analytical solutions are also presented for the case of a two-zone composite reservoir, with the inner zone being completely fractal and the outer zone homogeneous. Finally, an analytical model is presented for Newtonian fluid flow in a "double-porosity" situation where the fracture network is characterized by a particular type of fractal geometry and the matrix is homogeneous. The sensitivity of the system response to the various relevant parameters is also examined in detail.

## ACKNOWLEDGEMENTS

The author wishes to express sincere gratitude and appreciation to his supervisors, Drs. S. M. Farouq Ali and W. S. Tortike, for their guidance, interest and encouragement extended throughout the course of this study. The successful completion of this work owes immensely to their extraordinary support and their belief in the author's capabilities.

The author is indebted to his friend and partner, Romita Choudhury, for her warm and unquestioning support, continued encouragement and for the stimulating discussions on the various connotative aspects of "fractures".

The author is especially grateful to Dr. Yanis Yortsos of the University of Southern California, who is responsible to a great extent for bringing the concepts of fractals and percolation networks to the attention of the petroleum reservoir engineering and well-testing communities, for his frequent and detailed communications and advice regarding the approach followed in this work. Heartfelt thanks are also due to Drs. Ramon Bentsen and Jerry Whiting of the Department of Mining, Metallurgical and Petroleum Engineering, Dr. K. Nandakumar of the Department of Chemical Engineering and Dr. Amit Chakma of the University of Calgary for their comments and suggestions.

Finally, the author wishes to gratefully thank the Society of Petroleum Engineers and the University of Alberta for financial assistance which made this study possible.



# TABLE OF CONTENTS

	Page
List of Tables	x
List of Figures	xi
NOMENCLATURE	xv
Chapter I: Introduction	1
Chapter II: Review of Literature	3
Literature survey of pressure transient models for power-law fluid flow	3
Literature survey of fractal pressure transient analysis	5
Chapter III: Objectives and Applications	10
Purpose and scope of present study	10
Potential applications	11
Chapter IV: Mathematical Model for Power-Law Flow Through Fractal Porous Media	12
Flow of non-Newtonian power-law fluids through porous media	12
Flow properties of fractal fracture networks: theoretical background	16
Assumptions	21
Some comments about the use of Equation (4-15)	22
Partial differential equation	25
Dimensionless variables	29

<b>Chapter V: Solutions for the Infinite Reservoir Case</b>	<b>31</b>
Constant rate case	31
Constant pressure case	49
<b>Chapter VI: Numerical Pressure Solution of the Nonlinear Equation Governing Power-Law Flow Through Fractal Porous Media</b>	<b>53</b>
Dimensionless nonlinear equation	53
Douglas-Jones predictor-corrector method	54
<b>Chapter VII: Analytical Solutions for Power-Law Flow Through a Finite-Sized Fractal Reservoir</b>	<b>59</b>
Constant-rate inner boundary, closed outer boundary	59
Constant-rate inner boundary, constant-pressure outer boundary	64
Constant-pressure inner boundary, closed outer boundary	65
Constant-pressure inner boundary, constant-pressure outer boundary	69
<b>Chapter VIII: Analytical Solutions for Power-Law Flow Through a Two-Zone Composite Reservoir</b>	<b>70</b>
Mathematical formulation	70
<b>Chapter IX: Pressure Transients with Matrix Participation in Flow: A Special Case</b>	<b>82</b>
Mathematical formulation	82
Analytical solutions for a special case	85
<b>Chapter X: Results and Discussion</b>	<b>96</b>
Transient flow through a fractal medium	98
Transient flow through a fractal fracture/homogeneous matrix system	142

<b>Chapter XI: Conclusions</b>	<b>156</b>
<b>REFERENCES</b>	<b>158</b>
<b>Appendix A: Computer Program for Generating Dimensionless Pressures for Power-Law Flow in an Infinite Fractal Reservoir</b>	<b>164</b>
<b>Appendix B: Computer Program for Numerical Solution of the Nonlinear Partial Differential Equation for Flow of a Power-Law Fluid in an Infinite Fractal Reservoir</b>	<b>168</b>
<b>Appendix C: Computer Program for Generating Dimensionless Pressures for Power-Law Flow in a Finite Fractal Reservoir</b>	<b>172</b>

## LIST OF TABLES

Table	Page
10-1. Comparison of analytical and numerical solutions at two different dimensionless times	124

## LIST OF FIGURES

Figure	Page
4-1. Three different fracture networks embedded into a medium of dimension $d = 2$ (after Acuña <i>et al.</i> , 1992 b)	17
8-1. Schematic representation of a two-zone composite reservoir	71
10-1. An organizational map depicting the situations considered in this study	97
10-2. Dimensionless wellbore pressure versus time for an infinite system; pseudoplastic fluids, $d_f = 2$	99
10-3. Dimensionless wellbore pressure derivative versus time for an infinite system; pseudoplastic fluids, $d_f = 2$	100
10-4. Dimensionless wellbore pressure derivative to pressure ratio versus time for an infinite system; pseudoplastic fluids, $d_f = 2$	101
10-5. Dimensionless wellbore pressure versus time for an infinite system; dilatant fluids, $d_f = 1.75$	103
10-6. Dimensionless wellbore pressure versus time for an infinite system with varying $d_f$ ; $n = 0.75$	105
10-7. Dimensionless wellbore pressure versus time for the flow of a dilatant fluid ( $n = 1.25$ ) in a fractal reservoir; infinite system, varying $d_f$	106
10-8. Pressure and pressure-derivative solutions for two different cases	108
10-9. Dimensionless rate versus time in an infinite system; $n = 0.75$	110
10-10. Dimensionless rate versus time in an infinite system; $d_f = 1.75$	111

10-11. Comparison of wellbore pressure solutions using Equations (5-30) and (5-43)	113
10-12. Comparison of wellbore pressure solutions using Equations (5-30) and (5-43)	114
10-13. Plot of dimensionless time at the beginning of log-log straight line against parameter $\nu$	116
10-14. Comparison of analytical and numerical solutions for dimensionless wellbore pressure variation ( $n = 0.75, d_f = 2$ )	118
10-15. Comparison of analytical and numerical solutions for dimensionless wellbore pressure variation ( $d_f = 2, d_s = 1.75$ )	119
10-16. Comparison of analytical and numerical solutions for dimensionless wellbore pressure variation ( $n = 0.5, d_s = 2$ )	120
10-17. Comparison of analytical and numerical solutions for dimensionless wellbore pressure variation ( $d_f = 2$ )	122
10-18. Comparison of analytical and numerical solutions for dimensionless wellbore pressure variation ( $d_f = d_s = 2$ )	123
10-19. Plots of pressure drop and pressure-derivative for a closed circular system: $n = 1, d_s = 2, r_{eD} = 100$	126
10-20. Effect of $d_f$ on $d\ln(p_{wD})/d\ln(t_D)$ for a closed reservoir	127
10-21. Plots of pressure drop and pressure-derivative for a closed reservoir: $n = 1, d_s = 2, r_{eD} = 200$	129
10-22. Effect of $d_f$ on $d\ln(p_{wD})/d\ln(t_D)$ for a closed circular reservoir	130

10-23. Effect of $d_f$ on the pressure behaviour of a circular reservoir with constant pressure outer boundary: $n = 1, d_s = 2, r_{eD} = 200$	131
10-24. Effect of permeability and diffusivity ratios on pressure solution for a composite system: $n = 1, d_f = 2, d_s = 1.5, a = 2$	133
10-25. Effect of permeability and diffusivity ratios on pressure derivative for a composite system: $n = 1, d_f = 2, d_s = 1.5, a = 2$	134
10-26. Effect of permeability and diffusivity ratios on pressure derivative for a composite system: $n = 1, d_f = 2, d_s = 1.5, a = 10$	136
10-27. Effect of $d_f$ on pressure derivative for a composite system: $n = 1, d_s = 1.5, a = 5, k_w/k' = 100$	138
10-28. Effect of $d_s$ on pressure derivative for a composite system: $n = 1, d_f = 2, a = 5, k_w/k' = 100$	139
10-29. Pressure derivative behaviour for a composite reservoir: different inner-zone sizes	140
10-30. Effect of $d_f$ and $d_s$ on pressure derivative for a composite system: $n = 1, k_w/k' = 100, F = 0.1$	141
10-31. Pressure drawdown curves for single- and double-porosity systems: $d_s = 1.5, \omega = 10^{-3}, \lambda = 10^{-5}$	143
10-32. Plot of pressure drop for a fracture/matrix system: $\omega = 0.01, \lambda = 10^{-5}$	145
10-33. Plot of pressure-derivative for a fracture/matrix system: $\omega = 0.01, \lambda = 10^{-5}$	146
10-34. Plot of $d \ln(p_{wD})/d \ln(\tau)$ for a fracture/matrix system:	

$\omega = 0.01, \lambda = 10^{-5}$	147
10-35. Effect of $\omega$ on plot of $p_{wD}$ versus $\tau$ for fracture/matrix system: $\nu = 0.25, \lambda = 10^{-5}$	148
10-36. Effect of $\omega$ on $dp_{wD}/d\ln(\tau)$ for fracture/matrix system: $\nu = 0.25, \lambda = 10^{-5}$	150
10-37. Effect of $\omega$ on plot of $p_{wD}$ versus $t_D$ for fracture/matrix system: $\nu = 0.25, \lambda = 10^{-5}$	151
10-38. Effect of $\omega$ on plot of pressure derivative for fracture/matrix system: $\nu = 0.25, \lambda = 10^{-5}$	152
10-39. Effect of $\lambda$ on pressure solution for a fracture/matrix system: $\omega = 0.01, \nu = 0.25$	154
10-40. Effect of $\lambda$ on pressure derivative for a fracture/matrix system: $\omega = 0.01, \nu = 0.25$	155



## NOMENCLATURE

$a$	dimensionless radius of the inner region in a two-region composite system
$a_1, a_2$	dimensionless groups defined by Equations (8-41) and (8-42), respectively
$A$	group defined by Equation (4-17) [ $\text{Pa.s}^n.\text{m}^{1-n}$ ]
$A_1, A_2, A_3$	dimensionless groups defined by Equations (6-3), (6-4) and (6-5), respectively
$c$	fluid compressibility [ $\text{Pa}^{-1}$ ]
$c_f$	pore compressibility [ $\text{Pa}^{-1}$ ]
$C_p$	group defined by Equation (5-60) [ $\text{Pa}^{-1}$ ]
$c_t$	system compressibility [ $\text{Pa}^{-1}$ ]
$d$	embedding medium dimension
$d_f$	mass fractal dimension
$d_s$	spectral dimension
$E_1(x)$	exponential-integral function
$G$	group defined by Equation (4-32) [ $\text{m}^{n-3}.\text{s}$ ]
$h$	formation thickness [m]
$H$	consistency (power-law parameter) [ $\text{Pa.s}^n$ ]
$I_\nu$	modified Bessel function
$k'$	permeability of the homogeneous outer region in a two-region composite system [ $\text{m}^2$ ]
$k(r)$	permeability defined by Equation (4-12) [ $\text{m}^2$ ]
$k_w$	permeability @ $r = r_w$ [ $\text{m}^2$ ]
$K$	effective hydraulic conductivity [ $\text{m}^2.\text{Pa}^{-1}.\text{s}^{-1}$ ]
$K_\nu$	modified Bessel function
$l$	Laplace-space variable
$m$	slope of linear plot of $p_{wD}$ vs. $t_D^\nu$ , given by Equation (5-44)
$n$	flow behaviour index (power-law parameter)
$N$	number of equal space-increments
$p$	pressure, Pa
$p^*$	dimensionless pressure defined by Equation (10-7)
$p_D$	dimensionless pressure defined by Equation (4-33)

$\bar{p}_D$	dimensionless pressure in Laplace space
$p_{Df}$	dimensionless pressure in fracture
$\bar{p}_{Df}$	dimensionless fracture pressure in Laplace space
$p_{Dm}$	dimensionless pressure in matrix
$\bar{p}_{Dm}$	dimensionless matrix pressure in Laplace space
$p_f$	pressure in fracture [Pa]
$p_i$	initial pressure [Pa]
$p_m$	pressure in matrix [Pa]
$p_w$	constant wellbore pressure [Pa]
$p_{wD}$	dimensionless transient wellbore pressure
$p_{wf}$	transient wellbore pressure [Pa]
$\bar{p}_{wD}$	dimensionless transient wellbore pressure in Laplace space
$q$	constant rate (constant rate case); variable rate (constant pressure case) [m <sup>3</sup> /s]
$q_D$	transient dimensionless rate
$Q_D$	transient dimensionless cumulative production
$\bar{Q}_D$	transient dimensionless cumulative production in Laplace space
$q_{mf}$	interporosity fluid exchange rate [m.m <sup>1/n</sup> .s <sup>-1/n</sup> ]
$r$	radius [m]
$r_I$	radius of the inner region in a two-region composite system [m]
$r_{Di}$	dimensionless radius of investigation
$r_D$	dimensionless radius defined by Equation (4-34)
$r_e$	outer boundary radius [m]
$r_{eD}$	dimensionless outer boundary radius
$r_{inv}$	radius of investigation [m]
$r_w$	wellbore radius [m]
$t$	time [s]
$t(n)$	conductivity scaling exponent for non-Newtonian power-law flows in a percolation system
$t^*$	dimensionless time defined by Equation (10-8)
$t_D$	dimensionless time defined by Equation (4-35)
$s$	dimensionless skin factor
$u_r$	superficial velocity in the radial direction [m/s]
$v$	dimensionless parameter defined by Equation (5-21)

$v'$	dimensionless parameter defined by Equation (8-30)
$x$	variable defined by Equation (6-1)
$\alpha$	parameter defined by Equation (5-17); also group defined by Equation (6-18)
$\alpha'$	parameter defined by Equation (8-26)
$\beta$	parameter defined by Equation (5-18)
$\beta'$	parameter defined by Equation (8-27)
$\gamma$	parameter defined by Equation (5-19)
$\gamma'$	parameter defined by Equation (8-28)
$\Gamma(x)$	gamma function
$\Gamma(b, x)$	incomplete gamma function
$\Delta$	parameter defined by Equation (8-38)
$\Delta p$	pressure drop [Pa]
$\Delta p_o$	pressure drop at $t = 0$ [Pa]
$\Delta p_s$	skin pressure drop given by Equation (5-61) [Pa]
$\kappa, \nu$	conductivity scaling exponents of a percolation system for Newtonian flows
$\theta$	conductivity index (fractal exponent)
$\lambda$	matrix/fracture interaction parameter
$\mu$	viscosity [Pa.s]
$\mu_{app}$	apparent viscosity [Pa.s]
$\mu_{eff}$	"effective viscosity" defined by Equation (4-16) [Pa.s <sup>n</sup> .m <sup>1-n</sup> ]
$\rho$	density [Kg.m <sup>-3</sup> ]; dimensionless variable defined by Equation (5-13)
$\rho'$	dimensionless variable defined by Equation (8-24)
$\sigma$	fracture/matrix interaction index
$\sigma_1$	dimensionless group defined by Equation (8-7)
$\sigma_2$	dimensionless group defined by Equation (8-14)
$\phi$	porosity
$\phi_f$	fracture porosity
$\phi_m$	matrix porosity
$\omega$	dimensionless storage parameter
$\tau$	dimensionless time defined by Equation (9-12)
$\xi$	group defined by Equation (9-19)

## Chapter I

### INTRODUCTION

Research in modelling of pressure transient behaviour of fractured hydrocarbon reservoirs has advanced considerably over the past few decades. In 1963, the now classical study of Warren and Root's two-scale model of naturally fractured reservoirs was published. Since then, most conceptual models of flow in fissured systems have generally centred on various forms and modifications of the original double-porosity model envisaged by Warren and Root (1963). These conventionally accepted models for interpretation of transient pressure data from naturally fractured reservoirs usually involve simplistic assumptions regarding the geometry and transport behaviour of fracture networks. More importantly, pressure transient responses predicted by these models are sometimes not observed in actual well tests in naturally fractured reservoirs.

In a few recent studies (Chang and Yortsos, 1990; Beier, 1990a; Beier, 1990b; Acuña *et al.*, 1992a; Acuña *et al.*, 1992b), the concept of fractal geometry has been made use of in order to develop new models for interpretation of pressure transient tests in fractured media. In these conceptual models, fractal properties have been attributed to networks of fractures in fissured rocks so that the hydraulic response of the fracture system can be analyzed. The application of fractal geometry to the analysis of pressure transient behaviour was the result of an extension of the work of physicists who studied diffusion in disordered media and fractal objects (Orbach, 1986; O'Shaughnessy and Procaccia, 1985). Since pressure for fluid flow in porous media satisfies a diffusion-type equation, scaling principles for diffusion in fractal objects were applied by analogy to fluid flow through porous media (Beier, 1990; Acuña *et al.*, 1992a).

The general theoretical formalism of the application of fractal geometry to pressure transient analysis was presented by Chang and Yortsos (1990). Their approach was applied to analyze real well-test data in a few subsequent studies (Beier, 1990a; Acuña *et al.*, 1992a; Acuña *et al.*, 1992b). However, the analysis presented in these studies is restricted as it applies specifically to the transient flow of a Newtonian fluid in an infinite flow system. The transient injection (or production) behaviour of non-Newtonian fluids is an important and a frequently encountered phenomenon for the petroleum reservoir engineering community, especially during the flow of fluids such as polymer solutions, emulsions, fracturing fluids and oil-sand/fines mixtures through porous media. Without the aid of a proper tool for modelling transient flow behaviour of non-Newtonian fluids, analysis of pressure transient data during the flow of such fluids would be difficult. Moreover, it is to be noted that the results of Chang and Yortsos (1990) apply only for infinite reservoirs and that they also assume that the reservoir exhibits fractal characteristics over all length scales. For reservoirs exhibiting fractal characteristics only over a finite region around the wellbore, alternative approaches must be sought.

The purpose of this investigation is to address some of the concerns mentioned above. Broadly, this work deals with the development of an approach for the interpretation of pressure transient tests during the flow of a non-Newtonian power-law fluid in a totally fractal reservoir. Specifically, this study examines the pressure transient response of a single-well system in a manner consistent with the expectation that the fracture network dominates the flow behaviour in the naturally fractured reservoir.

## Chapter II

### REVIEW OF LITERATURE

The basic aim of this study is to develop a pressure transient model for the flow of a single-phase non-Newtonian power-law fluid through a fractal reservoir. Thus, the topic to be discussed in this research can be described broadly as the incorporation of the rheology of power-law fluids into a pressure transient model for a fractal reservoir. Accordingly, the literature review has been divided into two sections: pressure transient modelling of power-law fluid flow, and fractal pressure transient analysis.

#### *2.1 Literature Survey of Pressure Transient Models for Power-Law Fluid Flow*

The pressure transient modelling and analysis effort in the petroleum industry has generally concentrated on the behaviour of Newtonian fluids in homogeneous and heterogeneous reservoirs. Considerable numbers of exact and approximate models and type-curves exist for the analysis and interpretation of well-test data for various kinds of reservoir systems and wellbore conditions and for different tests. However, not much work or data is available in the petroleum engineering literature on pressure transient modelling of non-Newtonian fluid flow in porous media. In fact, some of the most popular textbooks on well testing (Earlougher, 1977; Streltsova, 1988; Sabet, 1991) do not consider non-Newtonian pressure transient analysis. Most polymer solutions, emulsions (Olaewaju, 1992), aqueous foams (Ikoku, 1978), solid particles suspended in Newtonian liquids (Barnes, 1989) such as heavy oil mixed with fines (Poon and Kisman, 1992), hydraulic fracturing fluids (Torok and Advani, 1987), and so forth, are non-Newtonian. Approximation of the pressure transient behaviour of these fluids by Newtonian fluid flow models, as is commonly done (Olaewaju, 1992), may result in significant errors in the ensuing analysis. Thus, from a

petroleum reservoir engineering point of view, there is a need for a thorough inspection of the transient flow of non-Newtonian fluids in porous media.

A number of articles on the flow behaviour of non-Newtonian fluids through porous media have been published in the chemical engineering, rheology and petroleum engineering literatures. In 1969, Savins presented a review of contemporary literature on the rheological behaviour of non-Newtonian fluids flowing through porous media. He also discussed the relevance of non-Newtonian flow through porous media to various technology areas

McKinley *et al.* (1966) studied the linear flow of a polymer solution in porous media. They proposed a modification of the viscosity to be used in the Newtonian Darcy equation to model linear flow of a non-Newtonian fluid. They suggested that the viscosity should not only be expressed as a function of the rheological properties of the fluid, but also as a function of the characteristics of the porous medium and the pressure gradient. Gogarty (1967) extended the work of McKinley *et al.* (1966) and suggested that the effective viscosity should also be related to the average shear rate in the core.

One of the earliest studies of transient pressure behaviour during the flow of a non-Newtonian power-law fluid in a porous medium was presented by van Poolen and Jargon (1969). They proposed a finite-difference model of a radial system to predict the transient flow behaviour of power-law fluids. Their model made use of Newtonian fluid flow equations, with the non-Newtonian effects being incorporated by means of the viscosity varying as a function of the radial location. A finite-difference model was also presented by Bondor *et al.* (1972) to simulate polymer flooding. However, transient flow was not considered in this study.

Ikoku and Ramey (1979) and Odeh and Yang (1979) presented analytical models for transient flow of non-Newtonian power-law fluids in infinite reservoirs. In these studies,

however, the effect of wellbore storage was not considered. In a subsequent study, Ikoku and Ramey (1980) extended their previous model (1979) to flow in finite circular reservoirs. They also used a wellbore storage simulator to study the effects of skin and wellbore storage during the transient flow of power-law fluids in infinite and finite systems.

Pascal and Pascal (1985) studied the steady and unsteady flow of power-law fluids through porous media. In order to deal with the nonlinearity of the equations describing the transient flow of power-law fluids, they used generalized Boltzman transformations for linear and radial flows. They also discussed the limitations associated with the approximate analytical solutions of the transient power-law flow problem derived by Ikoku and Ramey (1979).

In a recent study, Vongvuthipornchai and Raghavan (1987) examined numerically the pressure falloff behaviour in fractured wells after the injection of a non-Newtonian power-law fluid. The problem was studied previously by Murtha and Ertekin (1983); Murtha and Ertekin, however, did not present a method to analyze the pressure falloff data.

Recently, Olarewaju (1992) presented a study to demonstrate the difference in transient behaviour between a Newtonian and a non-Newtonian power-law type fluid in homogeneous and double-porosity reservoirs. He presented his mathematical solutions to develop pressure and pressure-derivative type curves for such reservoir systems.

## *2.2 Literature Survey of Fractal Pressure Transient Analysis*

The traditional double porosity model (Warren and Root, 1963) has been considered as the standard tool for analysis of pressure transient tests in naturally fractured reservoirs. Essentially, this model assumes that a fractured formation consists of two coexistent components characterized by two distinct permeability and porosity scales. The fracture



system is assumed to be homogeneous (characterized by a Euclidean dimension,  $d_f$ ; e.g.,  $d_f = 1$  for a single fracture) and is embedded within the matrix which is also Euclidean (e.g., of embedding dimension  $d = 2$  for a cylindrical symmetry flow system). An extension of such models was proposed by Abdassah and Ershaghi (1986) who presented a triple-porosity model for analysis of pressure transient behaviour of fractured media. This model assumes that fractures have homogeneous properties throughout and interact with two groups of matrix blocks having different porosities and permeabilities. The approach of Abdassah and Ershaghi (1986), however, is less applicable to systems where the fracture network is not of Euclidean geometry (i.e., the fracture system is non space-filling) (Chang and Yortsos, 1990; Acuña *et al.*, 1992a). In a few recent theoretical studies, several authors (Chang and Yortsos, 1990; Beier, 1990a; Beier, 1990b; Acuña and Yortsos, 1991; Acuña *et al.*, 1992a; Acuña *et al.*, 1992b) have proposed the concept of fractal geometry as an alternative to the classical analysis of pressure transient data for various naturally fractured reservoirs.

The term "fractal" has been used by researchers to characterize geometric objects whose properties show a power-law type spatial dependence (Chang and Yortsos, 1990; Beier, 1990a; Beier, 1990b; Acuña *et al.*, 1992a; Acuña *et al.*, 1992b). Acceptance of a fractal model within the drainage area of a well implies porosity and permeability distributions that exhibit power-law dependence on the distance,  $r$ , from the well. Chang and Yortsos (1990) presented a model for pressure transient analysis of fractal reservoirs where the average porosity and permeability of the fracture network over a region of scale  $r$  vary with  $r$  in a power-law manner. They examined the unsteady-state flow of a slightly compressible fluid in a fractal fracture network embedded in a Euclidean matrix. An appropriate modification of the diffusivity equation for such a case was also undertaken. Solutions of this formulation were obtained for the case where the matrix does not participate in the flow process and also for the case where the matrix exchanges fluid with the fracture network.

Beier (1990a) presented an extension of the work by Chang and Yortsos (1990). Beier's model applies specifically to Newtonian flow in a cylindrical symmetry reservoir ( $d = 2$ ) containing a fractal permeable network. Beier also chose to write the pressure transient equations for a fractal reservoir in a form that required available estimates of "near wellbore porosity and permeability". With a proper choice of dimensionless variables, it can be shown that the dimensionless pressure transient equation derived by Beier (1990a) is quite similar to one of the equations solved by Chang and Yortsos (1990). The main difference in the formulation of these equations lies in the way the dimensionless variables were defined in these two studies. Beier (1990a) also exhibited some field data from the Grayburg and San Andres formations in southeastern New Mexico that apparently do not match solutions from conventional models. Instead, Beier's fractal reservoir model was able to provide a quantitative analysis of the field data. Similar cases have also been observed from some west Texas reservoirs<sup>1</sup> where the use of a fractal reservoir model provided a much superior match to the field pressure data than that provided by any other existing pressure transient models. In a subsequent study, Beier (1990b) presented a model to analyze the pressure response of a well with a vertical fracture in an infinite fractal reservoir. He showed that during the early linear flow period in such a system, the slopes of the log-log plots of pressure and pressure-derivative curves are greater than one-half. Because of negligible wellbore storage effects in these tests, he argued, homogeneous reservoir models could not explain such "anomalous" transient pressure behaviour.

In 1988, Barker presented his "generalized radial flow model" which has since then been of considerable interest and practical use to researchers in hydrogeology and environmental engineering. Barker developed his model for transient flow during hydraulic tests in fractured media having homogeneous and isotropic properties. In Barker's approach

---

<sup>1</sup> R. A. Beier: private communication, 1992.

(1988), the generalized flow equations are developed by assuming that the areas (open to flow) of surfaces perpendicular to flow vary in a power-law fashion with distance from the centre. Theoretically, this is equivalent to assuming that conductivity and storativity have power-law dependence on the radius with the same exponent (Acuña *et al.*, 1992a), so that the diffusivity has no spatial dependence. In a subsequent study, Doe (1991) extended Barker's approach (1988) by considering unusual shapes of drainage volumes which can give rise to power-law variation of flow area with radius. Doe also presented an application of Barker's fractional (or generalized) dimension theory to constant pressure tests. Barker's fractional dimension model has actually been used to match successfully various field hydraulic test data, which could not have been matched by any conventional pressure transient models<sup>2</sup>. Barker's model has also been used in analyzing pressure-transient behaviour of nuclear waste repositories in fractured granite (Long *et al.*, 1990).

The theoretical model of Chang and Yortsos (1990), for the case of a line-source well producing from an infinite medium, was used by Acuña *et al.* (1992a) to interpret the fractal characteristics of a naturally fractured geothermal field. In a more recent study, Acuña *et al.* (1992b) reviewed the theoretical background of fractal analysis. They also demonstrated the application of various diagnostic techniques for fractal pressure transient analysis as developed by Chang and Yortsos (1990). They presented a discussion of various large-time behaviour of the pressure and pressure-derivative responses for a fractal system. The authors also commented on the implications of a transition in flow (fractal) dimensionality during a well test in a fractal reservoir. For example, the early-time response of a well test (in a three-dimensional space) may be characterized by a flow dimensionality indicative of fluid flow not only in the areal plane but also in the vertical direction (caused by, say, a partially-penetrating well in a thick formation); at larger times, however, the pressure

---

<sup>2</sup> T. W. Doe: private communication, 1992.

response may be more likely to be characteristic of cylindrical flow (due to a small/negligible vertical flow component), thereby indicating a different dimensionality. This transition may impart a double porosity-like "V" shape in the pressure-derivative behaviour, causing an incorrect interpretation of the system response.

## Chapter III

### OBJECTIVES AND APPLICATIONS

#### *3.1 Purpose and Scope of Present Study*

Pressure transient analysis is one of the primary tools used by the petroleum reservoir engineering community to characterize the conductive and storage properties of a reservoir. The techniques used to analyze the pressure data collected during a period of production/injection are based on solutions to partial differential equations describing the flow of fluids through porous media. A major assumption incorporated into these solutions is that the conductive and storage properties are uniform in the unit of interest, i.e., the properties are invariant in space. Moreover, the majority of the existing pressure transient models assume Newtonian fluid flow in reservoirs. Although these assumptions have been shown to be viable in many situations, the geological complexity of some units and/or the non-Newtonian characteristics of certain fluids may make these assumptions of dubious validity. More importantly, it has been observed in some previous studies (Odeh and Yang, 1979; Olarewaju, 1992) that pressure data collected during the flow of non-Newtonian power-law fluids may show anomalies when analyzed using methods derived for Newtonian fluids. Such anomalies usually have appearances similar to those for flow in fractures. And as will also be demonstrated in the present study, pressure behaviour during the flow of a power-law fluid in a homogeneous system may appear quite similar to that for Newtonian fluid flow in a fractal reservoir. Thus, use of existing pressure transient models may not be appropriate for the analysis of pressure data for non-Newtonian power-law fluid flow in fractal reservoirs. The purpose of this study is to examine methods for the analysis of non-Newtonian fluid flow data in one class of geological settings that is not amenable to the conventional approach.

In the present study, an investigation of the radial flow of non-Newtonian, power-law, slightly compressible fluids in heterogeneous cylindrical-symmetry reservoirs with a fractal structure is undertaken. The main objectives of this work are to derive a new partial differential equation describing power-law flows in fractal reservoirs and to obtain analytical solutions of this equation for a finite-wellbore case in a single-well situation. Examination of the system response is conducted under the assumption that the fracture network dominates the flow behaviour. Steady and unsteady flow situations in an infinite system are considered. Transient pressure behaviour in finite-sized systems are also dealt with. Analysis of the system response when the matrix participates in the flow is performed for a simple limiting case. Finally, some comments are made on the application of the model to a flow system comprising a two-zone composite reservoir, with the inner zone being totally fractal and the outer zone homogeneous.

### *3.2 Potential Applications*

This study, in effect, extends the modelling effort of non-Newtonian fluid flow to behaviour in fractal reservoirs which so far has been confined to Newtonian flow. The results of this study should prove to be useful to researchers in the areas of petroleum reservoir engineering, hydrogeology and environmental engineering where fracture flow modelling is a subject of considerable theoretical and practical interest. The present model may be used to interpret transient flow of polymer solutions, emulsions and aqueous foams through areally heterogeneous porous media with a fractal structure. The model can be applied also to heavy oil reservoirs, like Lloydminster in Alberta, where the reservoir fluid of heavy oil mixed with sand has been modelled as a non-Newtonian power-law fluid (Poon and Kisman, 1992). The heterogeneous nature of this reservoir may render it to be a probable candidate for representation by fractal geometry.

## Chapter IV

### MATHEMATICAL MODEL FOR POWER-LAW FLOW THROUGH FRACTAL POROUS MEDIA

In this chapter, the rheological properties of non-Newtonian fluids and physical characteristics of fractal permeable networks will be considered first to set the conditions of the present study. Various terms related to the rheology of non-Newtonian fluids and fractal reservoirs will be defined. Subsequently, we will discuss the derivation of a nonlinear partial differential equation describing single-phase flow of a non-Newtonian power-law fluid in a reservoir showing fractal structure. Finally, we will show the use of a "linearizing approximation" that reduces the exact nonlinear equation to a linear one for which closed-form analytical solutions may be obtained.

#### *4.1 Flow of Non-Newtonian Power-Law Fluids Through Porous Media*

##### *4.1.1 Definitions*

A knowledge of the viscosity of various fluids is essential for a study of the flow behaviour of these fluids through porous media. The viscosity of a fluid, a measure of its resistance to flow, is determined by the transport of momentum in a direction perpendicular to the direction of flow. In the viscous region for the flow of a Newtonian fluid, viscosity is defined by

$$\tau = \mu \frac{du}{dy} = \mu \dot{\gamma} \quad (4-1)$$

or

$$\mu = \frac{\tau}{\dot{\gamma}} \quad (4-2)$$

where  $\mu$  is the Newtonian viscosity,  $\tau$  is the shear stress in the shear plane parallel to the flow direction and  $\dot{\gamma}$  is the shear rate perpendicular to the plane of shear. Fluids that obey Equation (4-1) are termed "Newtonian fluids". The connotations of the term "Newtonian" are (Harris, 1977):

1) the stress acting on an element of material is proportional to the shear rate, with the constant of proportionality being called the viscosity;

2) the viscosity is time-independent and is also independent of shear rate and time-derivatives or integrals of shear rate to any order.

The exceptions to Newton's viscous law are not rare. There are fluids like polymer solutions, colloids, foams, solid-liquid suspensions, etc., that do not exhibit Newtonian behaviour. These fluids, called "non-Newtonian fluids", do not show a direct proportionality between the shear rate and the applied shear stress. The viscosity of these fluids changes significantly with shear rate under isothermal conditions. It is often convenient to define an "apparent viscosity" for non-Newtonian fluids as

$$\mu_{app} = \frac{\tau}{\dot{\gamma}} \quad (4-3)$$

which is a function of shear rate. The rheological properties of time-independent non-Newtonian fluids depend only upon the magnitude of the shear stress and not upon the duration of the stress. Shear-thinning (pseudoplastic), shear-thickening (dilatant) and Bingham plastic fluids fall into this category. With increasing shear rate, pseudoplastic and dilatant fluids exhibit decreasing and increasing apparent viscosities, respectively. Bingham plastic fluids are those for which a finite shearing stress is required to initiate motion and for which there exists a linear relationship (beyond the yield stress) between shear stress and shear rate.



#### 4.1.2 The Ostwald-de Waele Power-Law Model

For the purposes of modelling and calculation, the most commonly implemented rheological model used to describe shear-thinning or -thickening behaviour is the Ostwald-de Waele power-law model. This two-parameter function which has been useful in fitting rheological data for a large variety of shear-thickening and shear-thinning flows is often represented by the following (Barnes, 1989; Harris, 1977; Schowalter, 1978; Ikoku and Ramey, 1979; Torok and Advani, 1987; Poon and Kisman, 1992; Olarewaju, 1992):

$$\tau = H\dot{\gamma}^n \quad (4-4)$$

where  $H$  is the consistency and  $n$  is the dimensionless flow behaviour index. Equation (4-4) "is probably the ... most widely used equation in all of rheology" (Schowalter, 1978). The appeal of the power-law is evident. When  $n = 1$ , Equation (4-4) reduces to the description of a Newtonian fluid with viscosity  $H$ . For  $0 < n < 1$ , Equation (4-4) describes a rheogram characteristic of pseudoplastic fluids. For  $n > 1$ , a curve characteristic of dilatant fluids is found. The index  $n$ , thus, is a measure of the degree of non-Newtonian behaviour of the fluid and may often be regarded as constant over several decades of shear rate. Now, for a Newtonian fluid, the viscosity is given by Equation (4-2). Analogously, one can define an "apparent viscosity" for power-law fluids by combining Equations (4-2) and (4-4) to obtain

$$\mu_{app} = H\dot{\gamma}^{n-1} \quad (4-5)$$

The power-law model is an attempt at empirical curve-fitting with maximum simplicity. Even though Equation (4-4) may fail to fit the total range of possible shear rates for some fluids, the expression can be very useful for a two-parameter fit of rheological data over a wide range of shear rates. One of the main objections to the power-law model is that

it does not predict the limiting apparent viscosities (i.e., the apparent viscosities at zero and infinite shear rates).

#### 4.1.3 Generalization of Darcy's Law

The theory of laminar flow of Newtonian fluids through homogeneous porous media is based on the classical experiment of Darcy. Using the modified Blake-Kozeny equation for one-dimensional flow of power-law fluids through porous media (Christopher and Middleman, 1965; Gaitonde and Middleman, 1967; Savins, 1969), the superficial flow velocity can be expressed as (Ikoku and Ramey, 1979; Pascal and Pascal, 1985; Torok and Advani, 1987; Olarewaju, 1992)

$$u_0 = \left( \frac{k}{\mu_{eff}} \frac{\Delta p}{L} \right)^{1/n} \quad (4-6)$$

where the "effective viscosity" ( $\mu_{eff}$ ) is given by (Christopher and Middleman, 1965; Gaitonde and Middleman, 1967; Savins, 1969; Ikoku and Ramey, 1979; Olarewaju, 1992)

$$\mu_{eff} = \frac{H}{12} (9 + 3/n)^n (150k\phi)^{(1-n)/2} \quad (4-7)$$

It is clear from Equation (4-7) that in the Newtonian limit (i.e.,  $n = 1$ )  $\mu_{eff} = H$  = Newtonian (constant) viscosity. From Equation (4-6), an analogy to Darcy's law for power-law fluids, neglecting gravity, can be expressed as (Ikoku and Ramey, 1979; Pascal and Pascal, 1985; Olarewaju, 1992)

$$u_r^n = \frac{k}{\mu_{eff}} \frac{\partial p}{\partial r} \quad (4-8)$$

where  $u_r$  is the superficial velocity in the horizontal (radial) direction.

#### 4.2 Flow Properties of Fractal Fracture Networks: Theoretical Background

When a naturally fractured reservoir is highly disordered and fractal, the geometric and transport properties of the fracture networks differ in a non-trivial way from those for the corresponding Euclidean flow media (Chang and Yortsos, 1990; Acuña *et al.*, 1992a; Acuña *et al.*, 1992b). The theoretical, ideal response of perfect fractal objects is described as follows: many of their basic properties, defined as averages over a region of scale  $r$ , are scale-dependent and are proportional to non-zero powers of  $r$ . For example, the mass density of an arbitrary fractal network of fractures around an arbitrary point decreases in a power-law fashion with respect to the distance  $r$  (Acuña *et al.*, 1992a; Acuña *et al.*, 1992b). The exponent of this power-law is  $(d_f - d)$ , where  $d_f$  is the "mass fractal dimension" of the fractal network of fractures and  $d$  is the Euclidean dimension of the medium in which the fractal object is embedded and is an integer (1, 2 or 3). The physical meaning of the "mass fractal dimension", in the context of well testing, will be discussed subsequently.

The calculation of fracture density is considered in the various fracture networks shown in Figure 4-1 (Acuña *et al.*, 1992b), with the embedding medium being two-dimensional (so that  $d = 2$ ) in every case. The concentric circles are at various radii from the centre (where the well is located) and the fracture densities are calculated within these arbitrary circles. The first network (network (a)) is nothing but a single fracture, the mass of which increases in direct proportion to the distance  $r$ , with the area (volume) of the embedding medium increasing in proportion to  $r^2$ . Thus, the density of the fracture (or the permeable flow path) within the two-dimensional medium varies in proportion to  $r^{-1}$ , or, in more general terms, to  $r^{d_f - d}$ , where  $d_f = 1$  and  $d = 2$ . Figure 4-1(c) exhibits a fracture-matrix system similar to the Warren and Root type double-porosity model with the horizontal and vertical lines representing the uniform fracture system. In this case, the fracture network is equivalent to a two-dimensional homogeneous medium of Euclidean

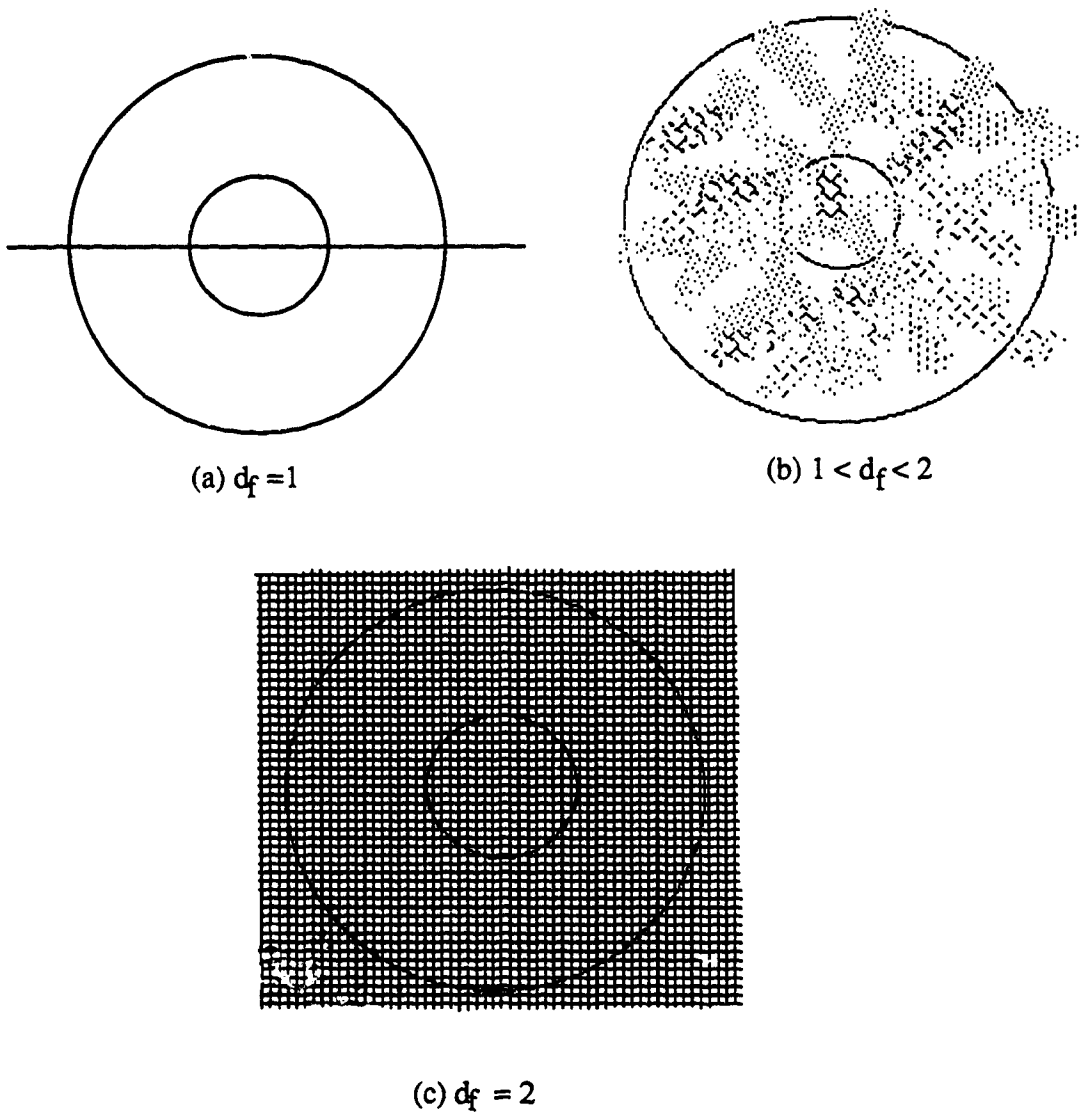


**Figure 4 – 1: Three Different Fracture Networks Embedded into a Medium of Dimension  $d = 2$  (After Acuña *et al.*, 1992 b)**

geometry (Chang and Yortsos, 1990). For this network, the fracture density, again proportional to  $r^{d_f - d}$ , is invariant with distance because of the fact that  $d_f = d = 2$ . In network (b), the indicated mass of dotted lines is assumed to represent a fractal fracture network. This network corresponds to a non-Euclidean case where, even though the same power-law variation of fracture density is exhibited, the value of  $d_f$  lies between one and two; in other words, in this particular case, the cumulative "mass" or length of fractures contained within an observed area grows faster than it does in the case of a line (a single fracture; network (a)) but not as fast as in the case of a plane (a Warren-Root type homogeneous fracture system; network (c)). In a three-dimensional flow space, a value of flow dimensionality ( $d_f$ ) less than or greater than two depends on a combination of wellbore geometry and the nature of the fracture network (Acuña *et al.*, 1992a; Acuña *et al.*, 1992b). For example, the fractal dimension may be less than two if the fracture network exists only in the horizontal plane and the formation is homogeneous in the transverse direction (Acuña *et al.*, 1992b). Similarly,  $d_f$  may be greater than two if flow also occurs parallel to the wellbore as in the case of a partially penetrating well in a relatively thick reservoir (Acuña *et al.*, 1992b). The parameter  $d_f$  is strictly a geometric property of a fractal object and can be estimated by measuring the values of cumulative mass (or length) of fractures contained within circular regions of known radii  $r$  (Acuña *et al.*, 1992a). In fact, as is evident from the discussion presented in this paragraph, the slope of a linear log-log plot of cumulative mass (or length) of fractures against radius would be the mass fractal dimension,  $d_f$ .

Another parameter (of fractal objects) of interest is the fractal exponent,  $\theta$ , which is related to the topology of the fracture network ( $\theta \geq 0$ ) (Beier, 1990a; Beier, 1990b). This parameter characterizes both the geometric and transport properties of the fracture network (Acuña *et al.*, 1992a) and, hence, has a significant role to play in the diffusion of fluid along paths constrained to fractal geometry. During diffusion in fractal objects, the mean square

distance (from the origin) of a single particle diffusing from the origin at time  $t$  is given by the following scaling relation (Orbach, 1986; Acuña *et al.*, 1992a; Acuña *et al.*, 1992b)

$$\langle r^2(t) \rangle \propto t^{2/(2+\theta)} \quad (4-9)$$

When  $\theta = 0$ , Equation (4-9) reduces to  $\langle r^2(t) \rangle \propto t$ , which is the corresponding scaling relation for the "normal situation" of diffusion in Euclidean space (e.g., the cases shown by Figures 4-1a and 4-1c). In these two cases, the fracture connectivity is high and therefore, diffusion is easier. On the other hand, in the fractal network of fractures (represented by Figure 4-1b), there is a diffusion slowdown (for  $\theta > 0$ ) because of poor spatial fracture connectivity and because of a higher degree of tortuosity of the fluid flow path (Orbach, 1986; Beier, 1990a; Beier, 1990b; Acuña *et al.*, 1992a; Acuña *et al.*, 1992b). In general,  $\theta$  increases with poorer fracture connectivity and higher tortuosity of the flow paths (Acuña *et al.*, 1992b).

The spectral dimension of a fractal object,  $d_s$  (Beier, 1990a; Sahimi and Yortsos, 1990; Beier, 1990b), is an extremely important parameter of the flow network, especially in the context of pressure transient analysis. The parameters  $d_f$  and  $\theta$  are related to the spectral dimension  $d_s$  in the following way (Orbach, 1986; Beier, 1990a; Beier, 1990b)

$$d_s = \frac{2 d_f}{2 + \theta} \quad (4-10)$$

Beier (1990a) and Acuña *et al.* (1992a, 1992b) have shown that the asymptotic slope of the transient pressure curve in a fractal reservoir is related to the spectral dimension  $d_s$  and hence, in Beier's studies (1990a, 1990b), the parameter  $d_s$  is used to describe the fractal network instead of  $\theta$ . For a totally areal flow network,  $d_s$  is less than or equal to two (Beier, 1990a; Beier, 1990b; Acuña *et al.*, 1992b); such a situation may occur when the flow medium is homogeneous in the vertical direction or when the producing unit is relatively

thin (Acuña *et al.*, 1992b). The single-well pressure transient behaviour during the flow of a single-phase fluid through a fractal reservoir may differ significantly from its homogeneous radial flow counterpart. The theoretical formulation of the pressure transient behaviour for a fractal fracture network was presented by Chang and Yortsos (1990) who used the following relations for fracture porosity ("mass density") and permeability

$$\phi(r) = \phi_0 \left( \frac{r}{r_0} \right)^{d_f - d} \quad (4-11)$$

and

$$k(r) = k_0 \left( \frac{r}{r_0} \right)^{d_f - d - \theta} \quad (4-12)$$

where  $\phi_0$  and  $k_0$  are the porosity and permeability values at  $r = r_0$ . The defining equation for the permeability of a fractal object was obtained in the study of Chang and Yortsos (1990) by using analogies from the work of physicists who studied the variation of conductance in fractal systems (O'Shaughnessy and Procaccia, 1985; Orbach, 1986). Similar definitions of porosity and permeability were also used in many other studies on pressure transient analysis for fractal reservoirs (Beier, 1990a; Beier, 1990b; Acuña *et al.*, 1992a; Acuña *et al.*, 1992b). It is to be noted that these definitions of porosity and permeability are not point values, as traditionally understood, but macroscopic values over a region of size  $r$ . Obviously, in the Euclidean limit of  $d_f = d$  and  $\theta = 0$ , these porosity and permeability values become independent of scale and reduce to the corresponding point values. Equations (4-11) and (4-12) show that the conductivity and storativity of a fractal reservoir are power-law functions of scale with different power-law exponents. Thus, the diffusivity is also scale-dependent (in a power-law fashion) with a non-zero exponent which has been shown to be related to the topology of the fracture network (Chang and Yortsos, 1990; Beier, 1990a; Sahimi and Yortsos, 1990; Beier, 1990b; Acuña *et al.*, 1992a; Acuña *et al.*, 1992b).

### 4.3 Assumptions

The following assumptions are made in deriving the mathematical model considered in the present study:

- a) small pressure-gradients exist throughout the reservoir at all times,
- b) gravitational forces are negligible,
- c) the radial flow takes place through an areal fractal network of fractures with the well penetrating the entire formation thickness,
- d) the porous medium has a uniform thickness,
- e) fluid compressibility is small, and
- f) the non-Newtonian fluid obeys the Ostwald-de Waele power-law relationship.

The scalings for porosity and permeability of the areally heterogeneous reservoir are given by Equations (4-11) and (4-12), respectively. From these equations, with  $r_0 = r_w$  (the wellbore radius) and for  $d = 2$ , the spatial variations of porosity and permeability of a two-dimensional areal fractal network can also be expressed as:

$$\phi(r) = \phi_w(r / r_w)^{-(2-d_f)} \quad (4-13)$$

and

$$k(\cdot) = k_w(r / r_w)^{-d_f(2/d_s-1)} \quad (4-14)$$

Equations (4-13) and (4-14) are similar to Beier's Equations (6) and (7) (Beier, 1990a), respectively. The only difference between these two sets of expressions is that in Equations (4-13) and (4-14), the reference length scale is the wellbore radius instead of the equivalent wellbore radius, as was used by Beier.



Now, from Equation (4-8), the superficial flow velocity for a power-law fluid can be expressed in radial coordinates as:

$$u_r = \left\{ \frac{k(r)}{\mu_{eff}(r)} \frac{\partial p}{\partial r} \right\}^{1/n} \quad (4-15)$$

where  $\mu_{eff}(r)$  can be expressed, by combining Equations (4-7), (4-11) and (4-12), as

$$\mu_{eff}(r) = A \left( \frac{r}{r_w} \right)^{(n-1)(d_f/d_s - d_f + 1)} \quad (4-16)$$

where

$$A = \frac{H}{12} (9 + 3/n)^n \{150 k_w \phi_w\}^{\frac{1-n}{2}} \quad (4-17)$$

It is to be noted that Equation (4-15) is a modified version of the generalized form of Darcy's law as has been considered in some previous studies (e.g., Ikoku and Ramey, 1979; Pascal and Pascal, 1985; Olarewaju, 1992). However, in all these studies the power-law flow is considered to take place through a flow medium (or media) having no spatial variability of its transmissive or storage properties. In the present study, the generalized form of Darcy's law for a fractal object within which a power-law flow is taking place is extended. Additional assumptions made in obtaining a linearized partial differential equation are discussed later in this chapter.

#### 4.4 *Some comments about the use of Equation (4-15)*

Yortsos (1991) extended results presented in the physics literature to a study of non-Newtonian power-law flow in percolation systems. The theory of percolation, originally

proposed more than thirty years ago and thus named because of an analogy with the process of a fluid percolating through a solid, continues to be one of the important tools for physicists in the study of the geometric and transport properties of porous media (Sahimi and Yortsos, 1990; Yortsos, 1991; Balberg *et al.*, 1991; Berkowitz and Balberg, 1993). The theory has been developed extensively in the field of statistical physics and has been applied in a variety of problems including the conceptualization of geometrical properties and transport phenomena observed in disordered flow media (Sahimi and Yortsos, 1990; Yortsos, 1991; Balberg *et al.*, 1991; Berkowitz and Balberg, 1993). Percolation theory provides "universal" scaling laws which determine the physical and geometrical characteristics of a system (Balberg *et al.*, 1991; Berkowitz and Balberg, 1993). These laws are generally expressed in power-law forms of the type (Balberg *et al.*, 1991)

$$A \propto (v - v_c)^x \quad (4-18)$$

where  $A$  is a geometrical or physically observable quantity,  $v$  is the fractional volume of the conducting phase and  $v_c$  is the critical (threshold) value for the onset of percolation (i.e., of system connectivity) and  $x$  is the exponent for quantity  $A$  and can be determined from theory and/or computer simulation and/or experiment. Scaling laws of the type shown above hold for  $v$  relatively close to  $v_c$  (typically, for  $v \leq 2v_c$  (Berkowitz and Balberg, 1993)). For the universal scaling laws such as Equation (4-18), the exponent  $x$  is dependent only on the system dimensionality,  $d$ .

Making use of a scaling law similar to Equation (4-18), Sahimi and Yortsos (1990) demonstrated the following scaling relationship, with length, of effective hydraulic conductivity of a percolation system for Newtonian flows:

$$K \propto L^{-\kappa/\nu} \quad (4-19)$$

where  $\kappa \approx 2$  (Sahimi and Yortsos, 1990) and  $\nu \approx 0.88$  (Sahimi and Yortsos, 1990) ( $\nu \approx 0.854$  in the study of Berkowitz and Balberg, 1993) for a 3-D system. It should be noted that in the study of Sahimi and Yortsos (1990),  $\mu$  was used instead of  $\kappa$  as the conductivity scaling exponent. For a non-Newtonian power-law flow in a percolation system, the conductivity scaling has been shown to possess the form (Yortsos, 1991)

$$K \propto L^{-t(n)/\nu} \quad (4-20)$$

where  $t(n)$ , although not precisely known, may be defined approximately for 3-D percolation clusters as (Yortsos, 1991)

$$t(n) \approx 1.76 + 0.24/n \quad (4-21)$$

To the best of our knowledge, an equivalent expression for  $t(n)$  for 2-D systems is not currently available. For an areal flow system, as is considered in the present study, the use of a proper flow equation would require the availability of a suitable approximating form for  $t(n)$  so that the conductivity scaling given by Equation (4-20) may be used.

In the present study, use has been made of Equation (4-15) to describe the flow velocity of a power-law fluid in an arbitrary fractal medium. From Equations (4-14) through (4-16), the scaling for non-Newtonian power-law flow in a fractal has been found to be

$$u_r \propto \left( \frac{r}{r_w} \right)^{(d_f - 1 - d_f/d_s) + (1/n)(1 - d_f/d_s)} \left( \frac{\partial p}{\partial r} \right)^{1/n} \quad (4-22)$$

It should be noted that at this point, to our knowledge, rigorous theoretical and/or experimental results for power-law flow in fractal objects have not been presented in the literature, and hence, the validity of the scaling presented by Equation (4-22) is questionable. However, the present study deals only with areal flow networks, and because of the lack of

available scaling exponents for power-law flow in 2-D percolation systems, use could not be made of a hydraulic conductivity scaling law similar to that considered in the study of Yortsos (1991). The rationale for proceeding in our present analysis with Equation (4-22) also lies in the fact that this equation arises from a straightforward coupling, as it were, of the flow equations used in studies dealing with non-Newtonian power-law flow in homogeneous systems (i.e., Ikoku and Ramey (1979)) and those dealing with Newtonian flow in fractal systems (e.g., Beier (1990a)). And, as will be shown later, the resulting partial differential equation and its solutions consequently are direct generalizations of those presented in the aforementioned studies, and they also reduce to the classical pressure-transient models in the limit of  $n = 1$  and  $d_f = d_s = 2$ .

#### 4.5 Partial Differential Equation

The continuity equation for radial flow in a porous medium may be written as

$$\frac{1}{r} \frac{\partial}{\partial r} (r \rho u_r) = \frac{\partial}{\partial t} (\phi \rho) \quad (4-23)$$

For isothermal fluid flow and assuming constant fluid compressibility, the density of the fluid at any pressure,  $p$ , can be expressed as

$$\rho = \rho_0 e^{c(p-p_0)} \quad (4-24)$$

where  $\rho_0$  is the density at a given pressure,  $p_0$ . From Equation (4-24), one obtains

$$\frac{\partial \rho}{\partial r} = c \rho \frac{\partial p}{\partial r} \quad (4-25)$$

and

$$\frac{\partial \rho}{\partial t} = c \rho \frac{\partial p}{\partial t} \quad (4-26)$$

Also, we have

$$\frac{\partial \phi}{\partial t} = c_f \phi \frac{\partial p}{\partial t} \quad (4-27)$$

where  $c_f$  is the effective pore space compressibility. Introducing Equations (4-15), (4-25), (4-26) and (4-27) into Equation (4-23), one gets, after simplification

$$\frac{1}{r} \frac{\partial}{\partial r} \left[ r \left\{ \frac{k(r)}{\mu_{eff}^{1/n}(r)} \frac{\partial p}{\partial r} \right\}^{1/n} \right] + c \left\{ \frac{k(r)}{\mu_{eff}^{1/n}(r)} \right\}^{1/n} \left( \frac{\partial p}{\partial r} \right)^{\frac{1+n}{n}} = \phi(r) c_t \frac{\partial p}{\partial t} \quad (4-28)$$

Multiplying both sides of Equation (4-28) by  $\left( k(r) \frac{\partial p}{\partial r} \right)^{\frac{n-1}{n}}$ , it is possible to obtain, after further simplification

$$\begin{aligned} & \frac{1}{r \mu_{eff}^{1/n}(r)} \left\{ k(r) \frac{\partial p}{\partial r} \right\} + k(r) \frac{\partial p}{\partial r} \frac{d}{dr} \mu_{eff}^{-1/n}(r) + \frac{1}{n \mu_{eff}^{1/n}(r)} \frac{\partial}{\partial r} \left\{ k(r) \frac{\partial p}{\partial r} \right\} \\ & + c \frac{k(r)}{\mu_{eff}^{1/n}(r)} \left( \frac{\partial p}{\partial r} \right)^2 = \phi(r) c_t \left\{ k(r) \frac{\partial p}{\partial r} \right\}^{\frac{n-1}{n}} \frac{\partial p}{\partial t} \end{aligned} \quad (4-29)$$

If constant and small fluid compressibility and small pressure gradients are assumed, the gradient-squared term may be considered negligible and Equation (4-29) reduces to

$$\begin{aligned} & \frac{1}{n} \frac{\partial}{\partial r} \left[ k(r) \frac{\partial p}{\partial r} \right] + \left[ d_f + \frac{1}{n} + \frac{d_f}{n d_s} - \frac{d_f}{d_s} - \frac{d_f}{n} \right] \frac{k(r)}{r} \frac{\partial p}{\partial r} \\ & = \phi(r) c_t \mu_{eff}^{1/n}(r) \left\{ k(r) \frac{\partial p}{\partial r} \right\}^{\frac{n-1}{n}} \frac{\partial p}{\partial t} \end{aligned} \quad (4-30)$$

Equation (4-30) is a nonlinear partial differential equation and represents the governing equation for the radial flow of a non-Newtonian power-law fluid through an areally heterogeneous porous medium with a fractal structure.

For a Newtonian fluid,  $n=1$  and  $\mu_{eff} = H = \mu$ , and for this case, Equation (4-30) reduces to

$$\frac{1}{r} \frac{\partial}{\partial r} \left[ rk(r) \frac{\partial p}{\partial r} \right] = \phi(r) c_i \mu \frac{\partial p}{\partial t} \quad (4-31)$$

which is the diffusion equation for radial flow of a slightly compressible Newtonian fluid through a heterogeneous reservoir (e.g., Equation (5) of Beier, 1990a). Again, by setting  $d_f = d_s = 2$  (so that,  $k(r) = k$ ,  $\phi(r) = \phi$  and  $\mu_{eff}(r) = \mu$ ), Equation (4-30) becomes

$$\frac{\partial^2 p}{\partial r^2} + \frac{n}{r} \frac{\partial p}{\partial r} = n \phi c_i \left( \frac{\mu_{eff}}{k} \right)^{1/n} \left( \frac{\partial p}{\partial r} \right)^{\frac{n-1}{n}} \frac{\partial p}{\partial t} \quad (4-32)$$

which is the diffusion equation for radial flow of a non-Newtonian power-law fluid through a homogeneous porous medium (similar to Equation (A-9) of Ikoku and Ramey, 1979).

Equation (4-30) is linearized by making an approximation suggested by Ikoku (1978) and Ikoku and Ramey (1979). From Equation (4-15), one has

$$\left( \frac{\partial p}{\partial r} \right)^{1/n} = \left\{ \frac{\mu_{eff}(r)}{k(r)} \right\}^{1/n} u(r, t) \quad (4-33)$$

$$= \left\{ \frac{\mu_{eff}(r)}{k(r)} \right\}^{1/n} \frac{q}{2\pi r h} \quad (4-34)$$

where  $q$  is the production (or injection) rate. Substituting Equation (4-34) into Equation (4-30)

$$\begin{aligned} & \frac{1}{n} \frac{\partial}{\partial r} \left[ k(r) \frac{\partial p}{\partial r} \right] + \left[ d_f + \frac{1}{n} + \frac{d_f}{nd_s} - \frac{d_f}{d_s} - \frac{d_f}{n} \right] \frac{k(r)}{r} \frac{\partial p}{\partial r} \\ & = \phi(r) c_t \mu_{eff}(r) \left\{ \frac{q}{2\pi r h} \right\}^{n-1} \frac{\partial p}{\partial t} \end{aligned} \quad (4-35)$$

The approximation, given by Equation (4-34), has allowed us to linearize Equation (4-30) so that proper (albeit approximate) analytical solutions can be obtained. This approximation is equivalent to assuming that the flow rate at any radial distance from the wellbore is a constant. For non-Newtonian power-law flow in a homogeneous porous medium, Ikoku (1978) and Ikoku and Ramey (1979, 1982) have shown that the analytical solution obtained by making such an approximation compared fairly well with a more rigorous numerical solution when  $n$  is between 0.5 and 1. In the present study, it has been observed that for power-law flow through fractal reservoirs, such an approximation results in errors that are not large for many values of  $d_s$  and  $n$ . A detailed discussion of this aspect of the analytical model will be presented in a later chapter.

Now, introducing Equations (4-13), (4-14) and (4-16) into (4-35) and simplifying, one obtains

$$\frac{\partial^2 p}{\partial r^2} + \left[ d_f + \frac{1}{n} - \frac{d_f}{nd_s} - \frac{d_f}{d_s} \right] \frac{n}{r} \frac{\partial p}{\partial r} = \frac{G}{r^{n-1}} \left\{ \frac{r}{r_w} \right\}^{\{(d_f/d_s)(n+1) - d_f(n-1) + n - 3\}} \frac{\partial p}{\partial t} \quad (4-36)$$

where

$$G = \frac{nA\phi_w c_t}{k_w} \left( \frac{q}{2\pi h} \right)^{n-1} \quad (4-37)$$

#### 4.6 Dimensionless Variables

The dimensionless groups are defined in the following manner:

$$p_D = \frac{(p_i - p) k_w r_w^{n-1} d_f / d_s}{A (q / 2\pi h)^n} \quad (4-38)$$

$$r_D = \frac{r}{r_w} \quad (4-39)$$

$$t_D = \frac{(d_f / d_s)^2 t}{G r_w^{3-n}} \quad (4-40)$$

It should be noted that the dimensionless groups defined in Equations (4-38) through (4-40) are quite similar to the corresponding groups defined by Beier (1990a). In fact, for  $n = 1$  (so that  $A = H = \mu$ , and  $G = \mu \phi_w c_f / k_w$ ), the two sets of groups are identical. Moreover, for  $d_f = d_s = 2$  (so that  $A = \mu_{eff}$ ), Equations (4-38) through (4-40) reduce to the corresponding dimensionless variables, defined by Ikoku (1978) and Ikoku and Ramey (1979, 1980, 1982) for the flow of a power-law fluid through a homogeneous porous medium.

From Equations (4-38) through (4-40), it can be shown that

$$\frac{\partial p}{\partial r} = - \frac{A (q / 2\pi h)^n}{k_w r_w^n (d_f / d_s)} \frac{\partial p_D}{\partial r_D} \quad (4-41)$$

$$\frac{\partial p}{\partial t} = - \frac{A (q / 2\pi h)^n (d_f / d_s)}{G k_w r_w^2} \frac{\partial p_D}{\partial t_D} \quad (4-42)$$

$$\frac{\partial^2 p}{\partial r^2} = - \frac{A (q / 2\pi h)^n}{k_w r_w^{n+1} (d_f / d_s)} \frac{\partial^2 p_D}{\partial r_D^2} \quad (4-43)$$



Substituting Equations (4-41) through (4-43) into Equation (4-36) and simplifying, one gets

$$\frac{\partial^2 p_D}{\partial r_D^2} + \left[ d_f + \frac{1}{n} - \frac{d_f}{nd_s} - \frac{d_f}{d_s} \right] \frac{n}{r_D} \frac{\partial p_D}{\partial r_D} = (d_f / d_s)^2 r_D^{\{(d_f / d_s)(n+1) - d_f(n-1) - 2\}} \frac{\partial p_D}{\partial t_D} \quad (4-44)$$

Equation (4-44) is the dimensionless form of the linearized partial differential equation for the flow of a power-law fluid through a fractal reservoir. For a homogeneous porous medium ( $d_f = d_s = 2$ ), Equation (4-44) reduces to the dimensionless linearized partial differential equation (Equation (B-1) of Ikoku and Ramey, 1979) for the flow of a power-law fluid through a reservoir. Also, for  $n = 1$  (Newtonian fluid), Equation (4-44) is the same as Beier's Equation (A-1) (1990a).

## Chapter V

### SOLUTIONS FOR THE INFINITE RESERVOIR CASE

The emphasis in the present chapter will be on discussion of the solution of the linear partial differential equation (Equation (4-44)) for the case of constant production rate from an infinite reservoir. Wellbore storage and skin effects will not be considered in the present analysis. Subsequently, the rate solution of Equation (4-44) for the case of constant wellbore pressure in an infinite system will be discussed briefly.

#### 5.1 Constant Rate Case

##### 5.1.1 Initial Value Problem: Finite Radius Well

The case of production of a power-law fluid at a constant rate from an infinite reservoir into a finite-radius wellbore is considered in this section. The initial value problem becomes (Equation (4-36))

$$\frac{\partial^2 p}{\partial r^2} + \left[ d_f + \frac{1}{n} - \frac{d_f}{nd_s} - \frac{d_f}{d_s} \right] \frac{n}{r} \frac{\partial p}{\partial r} = \frac{G}{r^{n-1}} \left\{ \frac{r}{r_w} \right\}^{\{(d_f/d_s)(n+1) - d_f(n-1) + n - 3\}} \frac{\partial p}{\partial t} \quad (5-1)$$

with the initial condition given by

$$p(r, 0) = p_i, \text{ for all } r \quad (5-2)$$

The inner boundary condition is given by the following (from Equations (4-6) and (4-7)) relationship

$$\left. \frac{\partial p}{\partial r} \right|_{r=r_w} = \frac{A}{k_w} \left( \frac{q}{2\pi r_w h} \right)^n \quad (5-3)$$

The reservoir is infinitely large so that the pressure at any time and at all locations far away from the production well remains essentially constant at the initial pressure,  $p_i$ . Thus, the outer boundary condition is

$$\lim_{r \rightarrow \infty} p(r, t) = p_i, \text{ for all } t \quad (5-4)$$

In terms of dimensionless variables, Equations (5-1) through (5-4) become, respectively

$$\frac{\partial^2 p_D}{\partial r_D^2} + \left[ d_f + \frac{1}{n} - \frac{d_f}{n d_s} - \frac{d_f}{d_s} \right] \frac{n}{r_D} \frac{\partial p_D}{\partial r_D} = (d_f / d_s)^2 r_D^{\{(d_f / d_s)(n+1) - d_f(n-1) - 2\}} \frac{\partial p_D}{\partial t_D} \quad (5-5)$$

$$p_D(r_D, 0) = 0, \text{ for all } r_D \quad (5-6)$$

$$\left. \frac{\partial p_D}{\partial r_D} \right|_{r_D=1} = -\frac{d_f}{d_s}, \text{ for all } t_D \quad (5-7)$$

and

$$\lim_{r_D \rightarrow \infty} p_D(r_D, t_D) = 0, \text{ for all } t_D \quad (5-8)$$

Equation (5-5) is a linear parabolic partial differential equation expressed in terms of dimensionless variables and may be solved by applying the Laplace transformation. Application of the transformation to Equation (5-5) and the initial and boundary conditions yields

$$r_D^2 \frac{d^2 \bar{p}_D}{dr_D^2} + n \left[ d_f + \frac{1}{n} - \frac{d_f}{n d_s} - \frac{d_f}{d_s} \right] r_D \frac{d \bar{p}_D}{dr_D} = (d_f / d_s)^2 r_D^{\{(d_f / d_s)(n+1) - d_f(n-1)\}} \bar{p}_D \quad (5-9)$$

$$\left. \frac{d\bar{p}_D}{dr_D} \right|_{r_D=l} = -\frac{d_f/d_s}{l} \quad (5-10)$$

and

$$\lim_{r_D \rightarrow \infty} \bar{p}_D(r_D, l) = 0 \quad (5-11)$$

with the initial condition having been used in obtaining the transformation of the time-derivative of  $p_D$  in Equation (5-9). By a suitable change of variables, Equation (5-9) can be transformed into a Bessel equation. Let us assume that

$$\bar{p}_D = r_D^\gamma f(\rho) \quad (5-12)$$

where

$$\rho = \alpha r_D^\beta \quad (5-13)$$

and where  $\alpha$ ,  $\beta$  and  $\gamma$  are arbitrary quantities to be determined. From Equations (5-12) and (5-13), it can be shown that

$$\frac{d\bar{p}_D}{dr_D} = \frac{\gamma}{r_D} r_D^\gamma f + \frac{\beta}{r_D} r_D^\gamma \rho f' \quad (5-14)$$

and that

$$\frac{d^2 \bar{p}_D}{dr_D^2} = \frac{\beta^2}{r_D^2} r_D^\gamma \rho^2 f'' + \frac{\beta}{r_D^2} (\beta - 1 + 2\gamma) r_D^\gamma \rho f' + \frac{\gamma(\gamma - 1)}{r_D^2} r_D^\gamma f \quad (5-15)$$

Substituting Equations (5-12) through (5-15) into Equation (5-9), one obtains, after simplification

$$\rho^2 f'' + \left[ \frac{2\gamma + n(d_f - d_f / nd_s - d_f / d_s)}{\beta} \right] \rho f' + \rho f' + \frac{\gamma^2 + n(d_f - d_f / nd_s - d_f / d_s)}{\beta} f - \frac{l}{\beta^2} (d_f / d_s)^2 r_D^{\{(d_f / d_s)(n+1) - d_f(n-1)\}} f = 0 \quad (5-16)$$

It is now possible to choose values of the parameters  $\alpha$ ,  $\beta$  and  $\gamma$  such that Equation (5-16) reduces to a form for which standard solutions are available. Choosing

$$\alpha = \frac{2\sqrt{l}(d_f / d_s)}{(d_f / d_s)(n+1) - d_f(n-1)}, \quad (5-17)$$

$$\beta = \frac{(d_f / d_s)(n+1) - d_f(n-1)}{2} \quad (5-18)$$

and

$$\gamma = \frac{(d_f / d_s)(n+1) - nd_f}{2}, \quad (5-19)$$

it can be shown that Equation (5-16) reduces to

$$\rho^2 f'' + \rho f' - \left[ 1 - \frac{d_s}{n+1 - d_s(n-1)} \right]^2 f - \rho^2 f = 0 \quad (5-20)$$

Equation (5-20) is Bessel's modified differential equation of order

$$v = 1 - \frac{d_s}{n+1 - d_s(n-1)} \quad (5-21)$$

The magnitude of the parameter  $v$  is quite important in the present analysis. As will be shown later, the value of  $v$  represents the large-time slope of the log-log plot of

dimensionless wellbore pressure against dimensionless time for the flow system under consideration.

The general solution to Equation (5-17) is (Abramowitz and Stegun, 1972)

$$f(\rho) = C_1 I_\nu(\rho) + C_2 K_\nu(\rho) \quad (5-22)$$

where  $I_\nu$  and  $K_\nu$  are modified Bessel functions of the first and second kind, respectively, and of order  $\nu$ ; the parameter  $\nu$  can have integral or nonintegral values. By combining Equations (5-11) and (5-22), it can be shown that  $C_1 = 0$ . Thus, from Equations (5-12), (5-13) and (5-22), one can write

$$\bar{p}_D(r_D, l) = C_2 r_D^\gamma K_\nu(\alpha r_D^\beta) \quad (5-23)$$

so that

$$\left. \frac{d\bar{p}_D}{dr_D} \right|_{r_D=1} = C_2 [\gamma K_\nu(\alpha) + \alpha \beta K'_\nu(\alpha)] \quad (5-24)$$

Using the following property of the modified Bessel function,  $K_\nu$  (Carslaw and Jaeger, 1959):

$$K'_\nu(\alpha) = -\frac{\nu}{\alpha} K_\nu(\alpha) - K_{1-\nu}(\alpha) \quad (5-25)$$

and noting from Equations (5-18), (5-19) and (5-21) that  $\beta\nu = \gamma$ , Equation (5-24) can be rewritten as

$$\left. \frac{d\bar{p}_D}{dr_D} \right|_{r_D=1} = -C_2 \sqrt{l} \left( \frac{d_f}{d_s} \right) K_{1-\nu}(\alpha) \quad (5-26)$$

where

$$1 - \nu = \frac{d_s}{n + 1 - d_s(n - 1)} \quad (5-27)$$

The constant  $C_2$  can be determined by comparing Equation (5-26) with the inner boundary condition (Equation (5-10)) and is given by

$$C_2 = \frac{1}{l^{3/2} K_{1-\nu}(\alpha)} \quad (5-28)$$

Thus, from Equations (5-23) and (5-28), one can write the solution for Equation (5-9) as

$$\bar{P}_D(r_D, l) = \frac{r_D^\gamma K_\nu(\alpha r_D^\beta)}{l^{3/2} K_{1-\nu}(\alpha)} \quad (5-29)$$

where  $\nu$  is defined by Equation (5-21), and  $\alpha$ ,  $\beta$  and  $\gamma$  are given by Equations (5-17), (5-18) and (5-19), respectively. Equation (5-29) is the Laplace transform of the general solution for the transient pressure distribution during the constant rate flow of a power-law fluid in an infinite reservoir showing fractal behaviour.

The general solution at the wellbore ( $r_D = 1$ ) is given by

$$\begin{aligned} \bar{P}_{wD}(l) &= \frac{K_\nu(\alpha)}{l^{3/2} K_{1-\nu}(\alpha)} \\ &= \frac{K_\nu \left\{ \frac{2\sqrt{l}}{n + 1 - d_s(n - 1)} \right\}}{l^{3/2} K_{1-\nu} \left\{ \frac{2\sqrt{l}}{n + 1 - d_s(n - 1)} \right\}} \end{aligned} \quad (5-30)$$

Beier (1990a) concluded that the dimensionless wellbore pressure during the production of a Newtonian fluid from a fractal reservoir depends on  $d_s$  and is independent of  $d_f$  because of the way the dimensionless variables were defined in his study. From Equation (5-30) it can be seen that the dimensionless wellbore pressure during the production of a power-law fluid from a fractal reservoir depends on  $d_s$  and  $n$  and is independent of  $d_f$ . Part of the dependence on  $d_f$  has been absorbed in the definition of the dimensionless groups. The linearization approximation is also responsible for the dimensionless wellbore pressure solution being independent of  $d_f$ .

For zero wellbore storage and Newtonian flow ( $n = 1$ ), Equation (5-30) reduces to Equation (A-13) derived in Beier's study (1990a). Also, for  $d_f = d_s = 2$ , Equation (5-30) exhibits the wellbore pressure response during the flow of a power-law fluid through an infinite homogeneous porous medium (Equation (B-13) of Ikoku and Ramey, 1979). Equation (5-30) may be evaluated directly by numerical inversion. However, it is also possible to find approximate analytical inversions, as will be shown later in this chapter.

### 5.1.2 Limiting Solutions for Early and Late Times

It is possible to derive the early- and late-time approximating forms of Equation (5-30). The limiting form for small times will be presented first. For early times, one has  $l \rightarrow \infty$ , when the modified Bessel function,  $K_\nu(z)$ , can be approximated as (Abramowitz and Stegun, 1972)

$$K_\nu(z) \approx \sqrt{\frac{\pi}{2z}} e^{-z} \quad (5-31)$$



where  $z \left( = \frac{2\sqrt{l}}{n+1-d_s(n-1)} \right) \rightarrow \infty$ . Substituting Equation (5-31) into Equation (5-30) and simplifying, it follows that for  $l \rightarrow \infty$ , Equation (5-30) can be approximated as

$$\bar{p}_{wD}(l) = l^{-3/2} \quad (5-32)$$

Inverting Equation (5-32) analytically (Abramowitz and Stegun, 1972), it can be shown that, at early times, the dimensionless wellbore pressure can be expressed as

$$p_{wD}(t_D) = 2 \sqrt{\frac{t_D}{\pi}} \quad (5-33)$$

Equation (5-33) also represents the early-time pressure solution for a finite-radius well in a homogeneous formation (Streletsova, 1988). This early-time pressure response, when plotted against time on logarithmic coordinates, exhibits a straight line with a slope of 1/2.

Similarly, one can also consider the dimensionless wellbore pressure response (given by Equation (5-30)) at large times. An expression for the modified Bessel function,  $K_\nu(z)$ , can be written as (Abramowitz and Stegun, 1972)

$$\begin{aligned} K_\nu(z) &= \frac{\pi}{2} \frac{I_{-\nu}(z) - I_\nu(z)}{\sin(\nu\pi)} \\ &= \frac{\Gamma(\nu)\Gamma(1-\nu)}{2} [I_{-\nu}(z) - I_\nu(z)] \end{aligned} \quad (5-34)$$

where  $\Gamma(a)$  is Gamma function and where (Ikoku, 1978)

$$I_\nu(z) = \sum_{i=0}^{\infty} \frac{1}{i! \Gamma(i+\nu+1)} \left(\frac{z}{2}\right)^{2i+\nu} \quad (5-35)$$

and

$$I_{-v}(z) = \sum_{i=0}^{\infty} \frac{I}{i! \Gamma(i-v+1)} \left(\frac{z}{2}\right)^{2i-v} \quad (5-36)$$

Thus, from Equations (5-34) through (5-36), one gets

$$\begin{aligned} K_v(z) &= \frac{\Gamma(v) \Gamma(1-v)}{2} \left(\frac{z}{2}\right)^{-v} \left\{ \frac{I}{\Gamma(1-v)} + \frac{(z/2)^2}{\Gamma(2-v)} + \dots \right\} - \\ &\left(\frac{z}{2}\right)^{2v} \left\{ \frac{I}{\Gamma(1+v)} + \frac{(z/2)^2}{\Gamma(2+v)} + \dots \right\} \end{aligned} \quad (5-37)$$

For large times, such that  $l$  (and hence,  $z$ ) is very small, Equation (5-37) can be approximated by neglecting  $z^2$  and higher powers of  $z$  within the winged brackets to obtain

$$\begin{aligned} K_v(z) &\approx \frac{\Gamma(v) \Gamma(1-v)}{2} \left(\frac{z}{2}\right)^{-v} \left\{ \frac{I}{\Gamma(1-v)} - \left(\frac{z}{2}\right)^{2v} \frac{I}{\Gamma(1+v)} \right\} \\ &= \frac{\Gamma(v)}{2} \left(\frac{z}{2}\right)^{-v} \left\{ I - \left(\frac{z}{2}\right)^{2v} \frac{\Gamma(1-v)}{\Gamma(1+v)} \right\} \end{aligned} \quad (5-38)$$

From Equation (5-38), it is possible write

$$\begin{aligned} \frac{K_v(z)}{K_{1-v}(z)} &\approx \frac{\Gamma(v)}{\Gamma(1-v)} \left(\frac{z}{2}\right)^{1-2v} \left[ \frac{I - \frac{\Gamma(1-v)}{v\Gamma(v)} \left(\frac{z}{2}\right)^{2v}}{I - \frac{\Gamma(v)}{(1-v)\Gamma(1-v)} \left(\frac{z}{2}\right)^{2(1-v)}} \right] \\ &= \frac{\Gamma(v)}{\Gamma(1-v)} \left(\frac{z}{2}\right)^{1-2v} \left[ I - \frac{\Gamma(1-v)}{v\Gamma(v)} \left(\frac{z}{2}\right)^{2v} + \frac{\Gamma(v)}{(1-v)\Gamma(1-v)} \left(\frac{z}{2}\right)^{2(1-v)} \right. \\ &\quad \left. - \frac{I}{v\Gamma(1-v)} \left(\frac{z}{2}\right)^2 + \left\{ \frac{\Gamma(v)}{(1-v)\Gamma(1-v)} \right\}^2 \left(\frac{z}{2}\right)^{4(1-v)} - \dots \right] \end{aligned} \quad (5-39)$$

Neglecting  $z^2$  and higher powers of  $z$  within the square brackets, Equation (5-39) reduces, for small magnitudes of  $\nu$ , to

$$\frac{K_\nu(z)}{K_{1-\nu}(z)} \approx \frac{\Gamma(\nu)}{\Gamma(1-\nu)} \left(\frac{z}{2}\right)^{1-2\nu} - \frac{z}{2\nu} + \frac{1}{(1-\nu)} \left\{ \frac{\Gamma(\nu)}{\Gamma(1-\nu)} \right\}^2 \left(\frac{z}{2}\right)^{3-4\nu} - \dots \quad (5-40)$$

Applying Equation (5-40) to Equation (5-30), one gets the large-time approximation of the wellbore pressure solution, in Laplace space, as

$$\begin{aligned} \bar{p}_{wD}(l) \approx & \frac{1}{l^{3/2}} \frac{\Gamma\left\{1 - \frac{d_s}{n+1-d_s(n-1)}\right\}}{\Gamma\left\{\frac{d_s}{n+1-d_s(n-1)}\right\}} \left\{ \frac{\sqrt{l}}{n+1-d_s(n-1)} \right\}^{\frac{(n+1)(d_s-1)}{n+1-d_s(n-1)}} \\ & + \frac{n+1-d_s(n-1)}{l^{3/2} d_s} \left[ \frac{\Gamma\left\{1 - \frac{d_s}{n+1-d_s(n-1)}\right\}}{\Gamma\left\{\frac{d_s}{n+1-d_s(n-1)}\right\}} \right]^2 \left\{ \frac{\sqrt{l}}{n+1-d_s(n-1)} \right\}^{\frac{3d_s+nd_s-n-1}{n+1-d_s(n-1)}} \\ & - \frac{1}{l(n+1-nd_s)} - \dots \end{aligned} \quad (5-41)$$

Inverting Equation (5-41) term by term using Laplace transform tables (Abramowitz and Stegun, 1972), one gets

$$\begin{aligned} p_{wD} = & \frac{\Gamma\left\{1 - \frac{d_s}{n+1-d_s(n-1)}\right\}}{\Gamma\left\{\frac{d_s}{n+1-d_s(n-1)}\right\}} \cdot \left\{ \frac{1}{n+1-d_s(n-1)} \right\}^{\frac{(n+1)(d_s-1)}{n+1-d_s(n-1)}} \\ & \frac{\frac{n+1-nd_s}{n+1-d_s(n-1)}}{t_D} \left\{ \frac{2(n+1)-d_s(2n-1)}{n+1-d_s(n-1)} \right\} - \frac{1}{(n+1-nd_s)} + \frac{n+1-d_s(n-1)}{d_s} \end{aligned}$$

$$\begin{aligned}
& \left[ \frac{\Gamma \left\{ 1 - \frac{d_s}{n+1-d_s(n-1)} \right\}}{\Gamma \left\{ \frac{d_s}{n+1-d_s(n-1)} \right\}} \right]^2 \cdot \left\{ \frac{l}{n+1-d_s(n-1)} \right\}^{\frac{3d_s+nd_s-n-1}{n+1-d_s(n-1)}} \cdot \frac{(n+1)(1-d_s)}{n+1-d_s(n-1)} \cdot t_D \\
& \cdot \frac{l}{\Gamma \left\{ \frac{2(n+1-d_s n)}{n+1-d_s(n-1)} \right\}} - \dots
\end{aligned} \tag{5-42}$$

At sufficiently large times, one can obtain an approximate expression for  $p_{wD}$ , from Equation (5-42), as follows:

$$\begin{aligned}
p_{wD} &= \frac{n+1-d_s(n-1)}{\Gamma \left\{ \frac{d_s}{n+1-d_s(n-1)} \right\}} \cdot \left\{ \frac{l}{n+1-d_s(n-1)} \right\}^{\frac{(n+1)(d_s-1)}{n+1-d_s(n-1)}} \\
& \cdot \frac{\frac{n+1-nd_s}{t_D^{\frac{n+1-d_s}{n+1-d_s(n-1)}}}}{(n+1-nd_s)} - \frac{l}{(n+1-nd_s)}
\end{aligned} \tag{5-43}$$

Equation (5-43) may be compared with dimensionless wellbore pressure values obtained by numerical inversion of Equation (5-30).

Equation (5-43) shows that for practical purposes (i.e., at relatively large times) a Cartesian graph of  $p_{wD}$  against  $t_D^{\frac{n+1-nd_s}{n+1-(n-1)d_s}}$  will yield a straight line with a slope,  $m$ , given by:

$$m = \frac{n+1-d_s(n-1)}{\Gamma \left\{ \frac{d_s}{n+1-d_s(n-1)} \right\}} \cdot \left\{ \frac{l}{n+1-d_s(n-1)} \right\}^{\frac{(n+1)(d_s-1)}{n+1-d_s(n-1)}} \cdot \frac{l}{n+1-nd_s} \tag{5-44}$$

and an intercept, at  $t_D = 0$ , of  $-l/(n+1-nd_s)$ .

Another late-time ( $l \rightarrow 0$ ) approximating form of Equation (5-30) may be derived. When  $z \rightarrow 0$ , the modified Bessel function,  $K_\nu(z)$ , can be approximated as (Abramowitz and Stegun, 1972)

$$K_\nu(z) \approx \frac{1}{2} \Gamma(\nu) \left( \frac{z}{2} \right)^{-\nu} \quad (5-45)$$

Using Equation (5-45), Equation (5-30) can be reduced to the following form:

$$\bar{p}_{wD}(l) = \frac{\Gamma \left\{ 1 - \frac{d_s}{n+1-d_s(n-1)} \right\}}{\Gamma \left\{ \frac{d_s}{n+1-d_s(n-1)} \right\}} \cdot \left\{ \frac{l}{n+1-d_s(n-1)} \right\}^{\frac{(n+1)(d_s-1)}{n+1-d_s(n-1)}} \cdot l^{\frac{1}{2} \left\{ \frac{(n+1)(d_s-1)}{n+1-d_s(n-1)} - 3 \right\}} \quad (5-46)$$

Inverting Equation (5-46) by using Laplace transform tables (Abramowitz and Stegun, 1972), one obtains, after simplifying,

$$p_{wD}(t_D) \approx \frac{n+1-d_s(n-1)}{\Gamma \left\{ \frac{d_s}{n+1-d_s(n-1)} \right\}} \cdot \left\{ \frac{l}{n+1-d_s(n-1)} \right\}^{\frac{(n+1)(d_s-1)}{n+1-d_s(n-1)}} \cdot \frac{\frac{(n+1-nd_s)}{n+1-d_s(n-1)} t_D}{n+1-nd_s} \quad (5-47)$$

Equation (5-47) is the same as Equation (5-43), except that the last term,  $\frac{l}{n+1-nd_s}$ , is omitted from the former equation. Equation (5-47) would apply, therefore, at very large times and for positive values of the exponent of dimensionless time. It can be noted that the exponent of  $t_D$  in Equations (5-43) and (5-47) is given by the parameter  $\nu$  (see Equation (5-21)). Thus, for positive values of  $\nu$  and at large times, a log-log straight line plot of  $p_{wD}$  versus  $t_D$  would exhibit a slope of  $\nu$ . For a pseudoplastic fluid ( $0 < n < 1$ ) and  $d_s \leq 2$ ,  $\nu$

would always be positive. However, for a dilatant fluid ( $1 < n < 2$ ), in order for  $v$  to be positive, it is necessary that  $d_f \leq 1.5$ .

It is obvious that for  $n = 1$  (Newtonian fluid), a large-time plot of the pressure transient, given by Equation (5-47), on logarithmic coordinates would yield a straight line with a slope of  $1 - d_s/2$ , from which the value of  $d_s$  can be obtained. A similar conclusion was also made by Chang and Yortsos (1990) and Beier (1990a). It has also been shown that at large times an identical behaviour would be exhibited by a line-source well in a fractal reservoir (Acuña *et al.*, 1990a, 1990b). Equation (5-47) also shows that for a homogeneous reservoir ( $d_f = d_s = 2$ ) and for a pseudoplastic fluid, a large-time log-log plot of  $p_{wD}$  versus  $t_D$  would be characterized by a straight line with a slope of  $(1-n)/(3-n)$ , as has been observed earlier by Ikoku and Ramey (1978).

### 5.1.3 Pressure Solutions for Line-Source Wellbore Case

It is possible to obtain transient solutions for dimensionless pressure not only in Laplace space but also in real space for the case of a line-source (sink) wellbore in an infinite fractal reservoir. In every respect, other than the inner boundary condition, this case is mathematically the same as the finite-wellbore case. For the infinitesimal-source case, the inner boundary condition may be described in dimensionless terms, from Equation (4-15), as

$$r_D^{nd_f + 1 - (d_f/d_s)(n+1)} \left. \frac{\partial p_D}{\partial r_D} \right|_{r_D \rightarrow 0} = -d_f / d_s \quad (5-48)$$

Now, for the infinite outer boundary condition, the solution to Equation (5-9) is given by Equation (5-23) which includes the constant  $C_2$  to be determined from the inner boundary condition. From Equation (5-23), it can be shown that

$$r_D^{nd_f+1-(d_f/d_s)(n+1)} \left. \frac{d\bar{p}_D}{dr_D} \right|_{r_D \rightarrow 0} = -C_2 \left[ r_D^{d_f/2} \alpha \beta K_{1-\nu}(\alpha r_D^\beta) \right]_{r_D \rightarrow 0} \quad (5-49)$$

Using the following relationship (Barker, 1988)

$$\lim_{z \rightarrow 0} z^\nu K_\nu(z) = 2^{\nu-1} \Gamma(\nu), \text{ for } \nu > 0 \quad (5-50)$$

and combining it with Equation (5-48) expressed in Laplace space, one can obtain an expression for  $C_2$  from Equation (5-49). The resulting expression for dimensionless pressure is given by

$$\bar{p}_D(r_D, l) = \frac{d_f}{d_s} \frac{r_D^\gamma}{\beta \Gamma(1-\nu)} \left( \frac{2}{\alpha} \right)^\nu \frac{K_\nu(\alpha r_D^\beta)}{l}, \nu < 1 \quad (5-51)$$

where  $\alpha$ ,  $\beta$ ,  $\gamma$  and  $\nu$  are given by Equations (5-17), (5-18), (5-19) and (5-21), respectively. Equation (5-51) defines the pressure response (in Laplace space) of an infinite fractal reservoir due to a constant rate of production from it by a line-source well. Equation (5-51) can be inverted to the real plane analytically; this analytical expression can be written as follows

$$p_D(r_D, t_D) = \frac{a r_D^{2\gamma}}{\Gamma(1-\nu)} \Gamma \left\{ -\nu, \frac{a^2 r_D^{2\beta}}{t_D} \right\} \quad (5-52)$$

where the incomplete Gamma function is defined as

$$\Gamma\{b, x\} = \int_x^\infty e^{-u} u^{b-1} du \quad (5-53)$$

and the parameter  $a = d_f/2\beta d_s$ . At the wellbore, Equation (5-52) reduces to

$$p_{wD}(t_D) = \frac{a}{\Gamma(1-\nu)} \Gamma\left\{-\nu, \frac{a^2}{t_D}\right\} \quad (5-54)$$

It can be seen from Equation (5-54) that the wellbore pressure response at a given time depends only on  $n$  and  $d_f$ , as in the finite-wellbore case. The incomplete Gamma function can be expressed as follows (Barker, 1988)

$$\Gamma\{b, x\} = \Gamma(b) - \sum_{i=0}^{\infty} \frac{(-1)^i x^{b+i}}{i! (b+i)} \quad (5-55)$$

For small values of the argument  $a^2/t_D$ , which occur after a short time, one may use only the first two terms of the expanded form of the incomplete Gamma function (Acuña *et al.*, 1992b) and thus, from Equations (5-54) and (5-55), it can be shown that

$$p_{wD} \approx \frac{a^{1-2\nu}}{\nu \Gamma(1-\nu)} t_D^\nu + \frac{1}{nd_f - (n+1)} \quad (5-56)$$

Equation (5-56) is the large-time approximation for the line-source wellbore pressure response. A similar equation has been derived also for the case of  $n = 1$  by Acuña *et al.* (1992b). It is interesting to note that Equation (5-56) is, in fact, identical to the large-time approximation for the finite-wellbore pressure solution (given by Equation (5-43)).

For  $n = 1$  and  $d_f = d_s = 2$ , Equation (5-52) reduces to the following form

$$p_D(r_D, t_D) = \frac{1}{2} E_1\left(\frac{r_D^2}{4t_D}\right) \quad (5-57)$$

where the exponential integral (Theis well function) is given by

$$E_1(x) = \int_x^{\infty} \frac{e^{-u}}{u} du \quad (5-58)$$



#### 5.1.4 Skin Factor

From Equations (4-38), (4-40) and (5-43), one can write

$$\begin{aligned}\Delta p &= p_i - p|_{r_w} \\ &= \frac{1}{C_p(n+1-nd_s)} \left[ \frac{\left\{ (d_f/d_s)(n+1) - d_f(n-1) \right\}^{2\nu} t^\nu}{(Gr_w^{3-n})^\nu \Gamma(1-\nu)} - 1 \right]\end{aligned}\quad (5-59)$$

where

$$C_p = \frac{r_w^{n-1} k_w (d_f/d_s)}{A(q/2\pi h)^n} \quad (5-60)$$

and  $G$  is given by Equation (4-37).

The van Everdingen and Hurst skin factor is defined as a dimensionless constant,  $s$ , which relates the pressure drop in the skin to the dimensionless rate of flow. The skin pressure drop can be defined (Ikoku, 1978) as

$$\Delta p_s = \frac{s}{C_p} \quad (5-61)$$

Combining Equations (5-59) and (5-61), the total pressure drop can be expressed as

$$\begin{aligned}\Delta p &= p_i - p_{wf} \\ &= \frac{1}{C_p} \left[ \frac{\left\{ (d_f/d_s)(n+1) - d_f(n-1) \right\}^{2\nu} t^\nu}{(n+1-nd_s)(Gr_w^{3-n})^\nu \Gamma(1-\nu)} - \frac{1}{(n+1-nd_s)} + s \right]\end{aligned}\quad (5-62)$$

At  $t = 0$ ,  $\Delta p = \Delta p_0$  and the skin factor can be calculated from the above equation as

$$s = \Delta p_o C_p + \frac{l}{n+1-nd_s} \quad (5-63)$$

It is to be noted that, for a fractal reservoir, the value of the skin factor obtained (by using Equation (5-63)) would also include any near-wellbore manifestations of deviations from the fractal distributions of the reservoir properties.

#### 5.1.5 Radius of Investigation

Under steady-state conditions, Equation (5-5) reduces to

$$\frac{d^2 p_D}{dr_D^2} + \left[ d_f + \frac{l}{n} - \frac{d_f}{nd_s} - \frac{d_f}{d_s} \right] \frac{n}{r_D} \frac{dp_D}{dr_D} = 0 \quad (5-64)$$

Integrating Equation (5-64) once with respect to  $r_D$ , one obtains

$$r_D \left( d_f + \frac{l}{n} - \frac{d_f}{nd_s} - \frac{d_f}{d_s} \right) \frac{dp_D}{dr_D} = A_1 \quad (5-65)$$

where  $A_1$  is a constant to be determined. The boundary conditions are

$$\left. \frac{dp_D}{dr_D} \right|_{r_D=1} = - \frac{d_f}{d_s} \quad (5-66)$$

and

$$p_D = 0 @ r_D = r_{Di} \quad (5-67)$$

where  $r_{Di} = r_{inv}/r_w$ . From Equations (5-65) and (5-66), it can be shown that

$$A_1 = - \frac{d_f}{d_s} \quad (5-68)$$

Introducing Equation (5-68) into Equation (5-65) and integrating once more with respect to  $r_D$ , one obtains

$$p_D = A_2 - \frac{r_D^{(d_f/d_s)(n+1)-nd_f}}{n+1-nd_s} \quad (5-69)$$

where  $A_2$  is a constant to be determined. Using the second boundary condition (Equation (5-67)) and Equation (5-69), one can determine  $A_2$  to be

$$A_2 = \frac{r_{Di}^{(d_f/d_s)(n+1)-nd_f}}{n+1-nd_s} \quad (5-70)$$

Combining Equations (5-69) and (5-70), the dimensionless wellbore pressure can be expressed as

$$p_{wD} = \frac{1}{n+1-nd_s} \left[ r_{Di}^{(d_f/d_s)(n+1)-nd_f} - 1 \right] \quad (5-71)$$

Comparing Equation (5-71) with Equation (5-43), one obtains

$$r_{Di}^{(d_f/d_s)(n+1)-nd_f} = \frac{\{n+1-d_s(n-1)\}^{2\nu} t_D^\nu}{\Gamma(1-\nu)} \quad (5-72)$$

from which the value of the radius of investigation at a given time can be calculated.

For  $d_f = d_s = 2$ , Equation (5-72) reduces to

$$r_{Di} = (3-n)^{2/(3-n)} t_D^{1/(3-n)} \left\{ \Gamma\left(\frac{2}{3-n}\right) \right\}^{1/(n-1)} \quad (5-73)$$

so that

$$r_{inv} = \left\{ \frac{(3-n)^2 t}{G} \right\}^{1/(3-n)} \left\{ \Gamma\left(\frac{2}{3-n}\right) \right\}^{1/(n-1)} \quad (5-74)$$

where  $G$  is defined by Equation (4-37). Equation (5-74) is the expression for the radius of investigation derived by Ikoku and Ramey (1979) for power-law flow in a homogeneous porous medium. Moreover, for  $n = 1$ , Equation (5-74) becomes

$$r_{inv} = 2 \sqrt{\frac{k_w t}{\phi_w H c_t}} \quad (5-75)$$

which is the radius of investigation of a constant-rate test during the flow of a Newtonian fluid of viscosity  $H$  through a homogeneous porous medium of permeability  $k_w$  and porosity  $\phi_w$ .

## 5.2 Constant Pressure Case

### 5.2.1 Initial Value Problem

The linear partial differential equation governing the transient flow of a non-Newtonian power-law fluid through a fractal reservoir is governed by Equation (5-1) expressed in terms of dimensional quantities. The initial and outer boundary (infinite) conditions are given by Equations (5-2) and (5-4), respectively. For a constant-pressure inner boundary, the inner boundary condition is expressed as

$$p(r = r_w, t) = p_w \quad (5-76)$$

The dimensionless radius and time are defined by Equations (4-39) and (4-40), respectively. For the constant-pressure inner boundary condition, the dimensionless pressure is defined as

$$p_D = \frac{p_i - p}{p_i - p_w} \quad (5-77)$$

It can be shown easily that using this new definition of dimensionless pressure and Equations (4-39) and (4-40), Equation (5-1) can be rewritten in dimensionless form as Equation (5-5). In order to solve Equation (5-5), one applies the Laplace transformation not only to the equation but also to the relevant boundary conditions. For the constant-pressure wellbore case, the inner boundary condition can be expressed in Laplace space as

$$\bar{p}_D (r_D = 1, l) = \frac{1}{l} \quad (5-78)$$

As has been shown for the constant-rate case, the equation for dimensionless pressure (in Laplace space) after applying the initial and the outer boundary conditions is of the form given by Equation (5-23). Finally, by using the inner boundary condition, the pressure solution is obtained as

$$\bar{p}_D (r_D, l) = \frac{r_D^\gamma K_\nu(\alpha r_D^\beta)}{l K_\nu(\alpha)} \quad (5-79)$$

Let us define, for the constant-pressure inner boundary case, the dimensionless rate in a manner similar to that of Poon and Kisman (1992); that is

$$q_D = \frac{A r_w}{k_w (p_i - p_w) d_f / d_s} \left( \frac{q}{2\pi h r_w} \right)^\eta \quad (5-80)$$

where the dimensionless rate is related to the pressure gradient at the wellbore as

$$q_D(d_f / d_s) = - \left. \frac{\partial p_D}{\partial r_D} \right|_{r_D=1} \quad (5-81)$$

Taking the Laplace transform of Equation (5-81) and using Equation (5-79), the following expression for the dimensionless rate is obtained

$$\bar{q}_D = \frac{1}{\sqrt{l}} \frac{K_{l-\nu}(\alpha)}{K_\nu(\alpha)} \quad (5-82)$$

Defining the cumulative production (over a given time  $t_D$ ) as

$$Q_D = \int_0^{t_D} q_D dt_D \quad (5-83)$$

and taking its Laplace transform, one gets, from Equations (5-82) and (5-83), the following expression for the cumulative production in Laplace space

$$\bar{Q}_D = \frac{1}{l\sqrt{l}} \frac{K_{l-\nu}(\alpha)}{K_\nu(\alpha)} \quad (5-84)$$

### 5.2.2 Limiting Solutions for Early and Late Times

At early times ( $l \rightarrow \infty$ ), the approximation of the modified Bessel function,  $K_\nu(z)$ , is given by Equation (5-31). Substituting Equation (5-31) into Equation (5-82) and simplifying, it follows that for  $l \rightarrow \infty$ , Equation (5-82) can be approximated in the real plane as

$$q_D = \frac{1}{\sqrt{\pi t_D}} \quad (5-85)$$

Equation (5-85) represents the early-time approximation of the dimensionless production rate. Similarly, from Equations (5-31) and (5-84), the early-time approximate form of the cumulative production (in real space) can be obtained as

$$Q_D = 2\sqrt{\frac{t_D}{\pi}} \quad (5-86)$$

The late-time ( $l \rightarrow 0$ ) approximating forms of Equations (5-82) and (5-84) may also be derived. Using the approximation of the modified Bessel function,  $K_\nu(z)$ , when  $z \rightarrow 0$ , as given by Equation (5-45), one can obtain the late-time limiting forms of dimensionless production rate and cumulative production, respectively, as

$$q_D = \left( \frac{l-v}{d_s} \right)^{2\nu-1} \frac{t_D^{-\nu}}{\Gamma(\nu)} \quad (5-87)$$

and

$$Q_D = \left( \frac{l-v}{d_s} \right)^{2\nu-1} \frac{t_D^{1-\nu}}{(1-\nu) \Gamma(\nu)} \quad (5-88)$$

## Chapter VI

### NUMERICAL PRESSURE SOLUTION OF THE NONLINEAR EQUATION GOVERNING POWER-LAW FLOW THROUGH FRACTAL POROUS MEDIA

In Chapter IV, a nonlinear partial differential equation (Equation (4-30)), governing the radial flow of a power-law fluid through a fractal network of fractures embedded into a two-dimensional medium, was derived. A "linearizing approximation" reduced this equation to a linear but approximate form (Equation (4-36)) and an analytical solution of the latter equation was subsequently obtained. The approximation is equivalent to assuming that the flow rate is time-independent at each radial location. Such an assumption is nearly correct in an expanding/contracting region close to the wellbore, but is not correct near the radius of investigation (Ikoku, 1978). This chapter presents a finite-difference scheme to solve the nonlinear partial differential equation for the flow of non-Newtonian power-law fluids through fractal reservoirs.

#### 6.1 Dimensionless Nonlinear Equation

The dimensional form of the nonlinear equation is given by Equation (4-30). Making use of the definitions of the dimensionless variables (given by Equations (4-38) through (4-40)), and by using the following logarithmic transformation,

$$x = \ln(r_D), \quad (6-1)$$

Equation (4-30) may be written in dimensionless form as

$$\frac{\partial^2 p_D}{\partial x^2} + A_1 \frac{\partial p_D}{\partial x} = A_2 e^{A_3 x} \left( -\frac{\partial p_D}{\partial x} \right)^{\frac{n-1}{n}} \frac{\partial p_D}{\partial t_D} \quad (6-2)$$



where

$$A_1 = n (d_f - A_3) \quad (6-3)$$

$$A_2 = (d_f / d_s)^{\frac{n+1}{n}} \quad (6-4)$$

and

$$A_3 = (d_f / d_s)^{\left(\frac{n+1}{n}\right)} \quad (6-5)$$

The initial condition and the inner (constant rate) and outer boundary (infinite reservoir) conditions are given, in terms of variables  $r_D$  and  $t_D$ , by Equations (5-6), (5-7) and (5-8), respectively. These equations can be rewritten, using Equation (6-1), respectively, as

$$p_D(x, 0) = 0 \quad (6-6)$$

$$\left. \frac{\partial p_D}{\partial x} \right|_{x=0} = -\frac{d_f}{d_s} \quad (6-7)$$

and

$$\lim_{x \rightarrow \infty} p_D(x, t_D) = 0 \quad (6-8)$$

The numerical solution of the problem posed by Equations (6-2) and (6-6) through (6-8) is now inspected.

## 6.2 Douglas-Jones Predictor-Corrector Method

Ikoku (1978) and Ikoku and Ramey (1982) used the Douglas-Jones predictor-corrector method to obtain numerical solutions of the nonlinear partial differential equation governing the transient flow of a power-law fluid in a homogeneous reservoir. In this study,

use is made of the same method to solve Equations (6-2) through (6-8). Each of the finite-difference equations advances the solution by one-half of the time increment. In the predictor, the unknowns occur at the  $(j+1/2)$ th time level and the equations are linear. In the corrector, the unknowns occur at the  $(j+1)$ th time level and the equations are again linear. The predictor followed by the corrector is unconditionally stable; moreover, the systems of equations are of the tridiagonal form, and are easy to solve. The Douglas-Jones predictor-corrector method is second-order accurate, whereas the computing effort is doubled at each step.

In order to solve a nonlinear partial differential equation of the form

$$\frac{\partial^2 p}{\partial x^2} = f(x, t, p, \frac{\partial p}{\partial x}) + g(x, t, p, \frac{\partial p}{\partial t}) \quad (6-9)$$

use is made of the predictor (to advance the solution from the  $j$ th to the  $j+1/2$ th time level) given by

$$\begin{aligned} \frac{p_{i-1}^{j+1/2} - 2p_i^{j+1/2} + p_{i+1}^{j+1/2}}{(\Delta x)^2} &= f\left(x_i, t_{j+1/2}, p_i^j, \frac{p_{i+1}^j - p_{i-1}^j}{2\Delta x}\right) \left(\frac{p_i^{j+1/2} - p_i^j}{\Delta t / 2}\right) \\ &+ g\left(x_i, t_{j+1/2}, p_i^j, \frac{p_{i+1}^j - p_{i-1}^j}{2\Delta x}\right) \end{aligned} \quad (6-10)$$

and the corrector (to advance the solution from the  $j+1/2$ th to the  $j+1$ th time level) given by

$$\begin{aligned} \frac{\frac{1}{2}(p_{i-1}^{j+1} - 2p_i^{j+1} + p_{i+1}^{j+1}) + \frac{1}{2}(p_{i-1}^j - 2p_i^j + p_{i+1}^j)}{(\Delta x)^2} &= f\left(x_i, t_{j+1/2}, p_i^{j+1/2}, \frac{p_{i+1}^{j+1/2} - p_{i-1}^{j+1/2}}{2\Delta x}\right) \\ &\cdot \frac{p_i^{j+1} - p_i^j}{\Delta t} + g\left(x_i, t_{j+1/2}, p_i^{j+1/2}, \frac{p_{i+1}^{j+1/2} - p_{i-1}^{j+1/2}}{2\Delta x}\right) \end{aligned} \quad (6-11)$$

Applying the predictor-corrector method to Equation (6-2), one obtains the predictor

$$\frac{p_{i-1}^{j+1/2} - 2p_i^{j+1/2} + p_{i+1}^{j+1/2}}{(\Delta x)^2} = A_2 e^{A_3(i-1)\Delta x} \left( \frac{p_{i-1}^j - p_{i+1}^j}{2\Delta x} \right)^{\frac{n-1}{n}} \left( \frac{p_i^{j+1/2} - p_i^j}{\Delta t / 2} \right) + A_1 \left( \frac{p_{i-1}^j - p_{i+1}^j}{2\Delta x} \right) \quad (6-12)$$

and the corrector

$$\frac{\frac{1}{2}(p_{i-1}^{j+1} - 2p_i^{j+1} + p_{i+1}^{j+1}) + \frac{1}{2}(p_{i-1}^j - 2p_i^j + p_{i+1}^j)}{(\Delta x)^2} = A_1 \left( \frac{p_{i-1}^{j+1/2} - p_{i+1}^{j+1/2}}{2\Delta x} \right) + A_2 e^{A_3(i-1)\Delta x} \left( \frac{p_{i-1}^{j+1/2} - p_{i+1}^{j+1/2}}{2\Delta x} \right)^{\frac{n-1}{n}} \left( \frac{p_i^{j+1} - p_i^j}{\Delta t} \right) \quad (6-13)$$

where  $i = 1, 2, 3, \dots, N+1$  and  $j = 0, 1, 2, 3, \dots$ , where  $N$  is the number of equal space-intervals (or space-increments) into which the system is divided.

The initial and boundary conditions are given as follows:

$$\text{Initial condition: } p_i = 0 \text{ @ } j = 0 \quad (6-14)$$

$$\text{Inner boundary condition (predictor): } \frac{p_2^{j+1/2} - p_0^{j+1/2}}{2\Delta x} = -\frac{d_f}{d_s} \quad (6-15)$$

$$\text{Inner boundary condition (corrector): } \frac{p_2^{j+1} - p_0^{j+1}}{2\Delta x} = -\frac{d_f}{d_s} \quad (6-16)$$

$$\text{Outer boundary condition: } p_i \rightarrow 0 \text{ as } i \rightarrow \infty, \text{ for all } j \quad (6-17)$$

The expressions for the predictor and corrector will now be written for the various grid points into which the system is divided. By defining

$$\alpha = \frac{2(\Delta x)^2}{\Delta t} \quad (6-18)$$

where  $\Delta x$  is the space increment, the predictor (Equation (6-12)) can be expressed in the following manner:

$$\begin{aligned} - \left[ 2 + A_2 (d_f / d_s)^{\frac{n-1}{n}} \alpha \right] p_i^{j+1/2} + 2 p_2^{j+1/2} &= A_1 (\Delta x)^2 (d_f / d_s) \\ &- A_2 (d_f / d_s)^{\frac{n-1}{n}} \alpha p_i^j - 2 \Delta x (d_f / d_s), \text{ for } i = 1 \end{aligned} \quad (6-19)$$

$$\begin{aligned} p_{i-1}^{j+1/2} - \left[ 2 + A_2 e^{A_3(i-1)\Delta x} \left( \frac{p_{i-1}^j - p_{i+1}^j}{2\Delta x} \right)^{\frac{n-1}{n}} \alpha \right] p_i^{j+1/2} + p_{i+1}^{j+1/2} &= (\Delta x)^2 A_1 \left( \frac{p_{i-1}^j - p_{i+1}^j}{2\Delta x} \right) \\ &- A_2 e^{A_3(i-1)\Delta x} \left( \frac{p_{i-1}^j - p_{i+1}^j}{2\Delta x} \right)^{\frac{n-1}{n}} \alpha p_i^j, \text{ for } 2 \leq i \leq N-1 \end{aligned} \quad (6-20)$$

$$\begin{aligned} p_{N-1}^{j+1/2} - \left[ 2 + A_2 e^{A_3(N-1)\Delta x} \left( \frac{p_{N-1}^j - p_{N+1}^j}{2\Delta x} \right)^{\frac{n-1}{n}} \alpha \right] p_N^{j+1/2} + p_{N+1}^{j+1/2} &= (\Delta x)^2 A_1 \left( \frac{p_{N-1}^j - p_{N+1}^j}{2\Delta x} \right) \\ &- A_2 e^{A_3(N-1)\Delta x} \left( \frac{p_{N-1}^j - p_{N+1}^j}{2\Delta x} \right)^{\frac{n-1}{n}} \alpha p_N^j - p_{N+1}^{j+1/2}, \text{ for } i = N \end{aligned} \quad (6-21)$$

Equations (6-19) through (6-21) represent a system of  $N$  equations in  $N$  unknowns (pressures), with the coefficients of the unknowns forming a tridiagonal matrix. The system

of equations can be solved by using the Thomas algorithm. The corrector (Equation (6-13)) may be written in the following manner

$$\begin{aligned}
& - \left[ 2 + A_2 \left( d_f / d_s \right)^{\frac{n-1}{n}} \alpha \right] p_i^{j+1} + 2p_2^{j+1} = \left[ 2 - A_2 \left( d_f / d_s \right)^{\frac{n-1}{n}} \alpha \right] p_i^j - 2p_2^j \\
& + 2A_1(\Delta x)^2 \left( d_f / d_s \right) - 4\Delta x \left( d_f / d_s \right), \text{ for } i = 1
\end{aligned} \tag{6-22}$$

$$\begin{aligned}
& p_{i-1}^{j+1} - \left[ 2 + A_2 e^{A_3(i-1)\Delta x} \left( \frac{p_{i-1}^{j+1/2} - p_{i+1}^{j+1/2}}{2\Delta x} \right)^{\frac{n-1}{n}} \alpha \right] p_i^{j+1} + p_{i+1}^{j+1} = A_1 \Delta x \left( p_{i-1}^{j+1/2} - p_{i+1}^{j+1/2} \right) \\
& - (p_{i-1}^j + p_{i+1}^j) + \left[ 2 - A_2 e^{A_3(i-1)\Delta x} \left( \frac{p_{i-1}^{j+1/2} - p_{i+1}^{j+1/2}}{2\Delta x} \right)^{\frac{n-1}{n}} \alpha \right] p_i^j, \text{ for } 2 \leq i \leq N-1
\end{aligned} \tag{6-23}$$

$$\begin{aligned}
& p_{N-1}^{j+1} - \left[ 2 + A_2 e^{A_3(N-1)\Delta x} \left( \frac{p_{N-1}^{j+1/2} - p_{N+1}^{j+1/2}}{2\Delta x} \right)^{\frac{n-1}{n}} \alpha \right] p_N^{j+1} = A_1 \Delta x \left( p_{N-1}^{j+1/2} - p_{N+1}^{j+1/2} \right) - p_{N+1}^{j+1} \\
& - (p_{N-1}^j + p_{N+1}^j) + \left[ 2 - A_2 e^{A_3(N-1)\Delta x} \left( \frac{p_{N-1}^{j+1/2} - p_{N+1}^{j+1/2}}{2\Delta x} \right)^{\frac{n-1}{n}} \alpha \right] p_N^j, \text{ for } i = N
\end{aligned} \tag{6-24}$$

Here also, Equations (6-22) through (6-24) form an  $N \times N$  tridiagonal system of equations which can be solved by means of the Thomas algorithm.

## Chapter VII

### ANALYTICAL SOLUTIONS FOR POWER-LAW FLOW THROUGH A FINITE-SIZED FRACTAL RESERVOIR

In this chapter, analytical solutions of the partial differential equation (Equation (4-44)), that governs the transient flow of a non-Newtonian power-law fluid through a fractal reservoir, will be presented for a finite circular reservoir case. Both closed and constant-pressure outer boundary conditions will be considered. Moreover, the solutions will be presented for both constant-rate and constant-pressure inner boundary conditions.

#### *7.1 Constant-Rate Inner Boundary, Closed Outer Boundary*

The approximate (linearized) partial differential equation governing the radial flow of a non-Newtonian power-law fluid in a fractal reservoir is given by (Equation (4-36))

$$\frac{\partial^2 p}{\partial r^2} + \left[ d_f + \frac{1}{n} - \frac{d_f}{nd_s} - \frac{d_f}{d_s} \right] \frac{n}{r} \frac{\partial p}{\partial r} = \frac{G}{r^{n-1}} \left\{ \frac{r}{r_w} \right\}^{\{(d_f/d_s)(n+1) - d_f(n-1) + n - 3\}} \frac{\partial p}{\partial t} \quad (7-1)$$

with the initial condition given by

$$p(r, 0) = p_i, \text{ for all } r \quad (7-2)$$

For the constant-rate case, the inner boundary condition may be expressed as

$$\left. \frac{\partial p}{\partial r} \right|_{r=r_w} = \frac{A}{k_w} \left( \frac{q}{2\pi r_w h} \right)^n \quad (7-3)$$

and for a closed (zero-flux outer boundary) reservoir, the outer boundary condition may be written as

$$\left. \frac{\partial p}{\partial r} \right|_{r=r_e} = 0 \quad (7-4)$$

where  $r_e$  is the radius of the outer boundary of the circular reservoir.

Before solving Equation (7-1), it is written in terms of dimensionless variables. Defining the dimensionless variables as follows

$$p_D = \frac{(p_i - p) k_w r_w^{n-1} d_f / d_s}{A (q / 2\pi h)^n} \quad (7-5)$$

$$r_D = \frac{r}{r_w} \quad (7-6)$$

and

$$t_D = \frac{(d_f / d_s)^2 t}{G r_w^{3-n}} \quad (7-7)$$

Equations (7-1) through (7-4) may be written, respectively, as

$$\frac{\partial^2 p_D}{\partial r_D^2} + \left[ d_f + \frac{1}{n} - \frac{d_f}{n d_s} - \frac{d_f}{d_s} \right] \frac{n}{r_D} \frac{\partial p_D}{\partial r_D} = (d_f / d_s)^2 r_D^{\{(d_f / d_s)(n+1) - d_f(n-1) - 2\}} \frac{\partial p_D}{\partial t_D} \quad (7-8)$$

$$p_D(r_D, 0) = 0, \text{ for all } r_D \quad (7-9)$$

$$\left. \frac{\partial p_D}{\partial r_D} \right|_{r_D=1} = -\frac{d_f}{d_s}, \text{ for all } t_D \quad (7-10)$$

and

$$\left. \frac{\partial p_D}{\partial r_D} \right|_{r_D = r_{eD}} = 0, \text{ for all } t_D \quad (7-11)$$

where

$$r_{eD} = \frac{r_e}{r_w} \quad (7-12)$$

Equation (7-8) may be solved, as in the infinite reservoir case, by applying the Laplace transformation. Application of the transformation to Equation (7-8) and the initial and boundary conditions yields

$$r_D^2 \frac{d^2 \bar{p}_D}{dr_D^2} + n \left[ d_f + \frac{1}{n} - \frac{d_f}{nd_s} - \frac{d_f}{d_s} \right] r_D \frac{d\bar{p}_D}{dr_D} = (d_f / d_s)^2 r_D^{\{(d_f / d_s)(n+1) - d_f(n-1)\}} \bar{p}_D \quad (7-13)$$

$$\left. \frac{d\bar{p}_D}{dr_D} \right|_{r_D = l} = - \frac{d_f / d_s}{l} \quad (7-14)$$

and

$$\left. \frac{d\bar{p}_D}{dr_D} \right|_{r_D = r_{eD}} = 0 \quad (7-15)$$

In order to solve Equation (7-13), it needs to be transformed into a Bessel equation by using a suitable change of variables (as has been shown in Chapter V). Following exactly the same procedure as outlined in Chapter V, it can be shown that the general solution to Equation (7-13) may be expressed as



$$\bar{p}_D(r_D, l) = r_D^\gamma [C_1 I_\nu(\alpha r_D^\beta) + C_2 K_\nu(\alpha r_D^\beta)] \quad (7-16)$$

where

$$\nu = 1 - \frac{d_s}{n+1-d_s(n-1)} \quad (7-17)$$

$$\alpha = \frac{2\sqrt{l}(d_f / d_s)}{(d_f / d_s)(n+1) - d_f(n-1)}, \quad (7-18)$$

$$\beta = \frac{(d_f / d_s)(n+1) - d_f(n-1)}{2} \quad (7-19)$$

and

$$\gamma = \frac{(d_f / d_s)(n+1) - nd_f}{2}, \quad (7-20)$$

and where  $C_1$  and  $C_2$  are constants to be determined from the two boundary conditions (Equations (7-14) and (7-15)).

Differentiating Equation (7-16) with respect to  $r_D$  and using the following recurrence relations (Carslaw and Jaeger, 1959),

$$K'_\nu(z) = -\frac{\nu}{z} K_\nu(z) - K_{1-\nu}(z) \quad (7-21)$$

and

$$I'_\nu(z) = -\frac{\nu}{z} I_\nu(z) + I_{\nu-1}(z), \quad (7-22)$$

where  $z = \alpha r_D^\beta$ , one gets

$$\frac{d\bar{p}_D}{dr_D} = \alpha \beta r_D^{\gamma+\beta-1} [C_1 I_{\nu-1}(\alpha r_D^\beta) - C_2 K_{1-\nu}(\alpha r_D^\beta)] \quad (7-23)$$

Applying the inner and outer boundary conditions to Equation (7-23), one obtains

$$C_1 = \frac{K_{1-\nu}(\alpha r_{eD}^\beta)}{l^{3/2} \{K_{1-\nu}(\alpha) I_{\nu-1}(\alpha r_{eD}^\beta) - K_{1-\nu}(\alpha r_{eD}^\beta) I_{\nu-1}(\alpha)\}} \quad (7-24)$$

and

$$C_2 = \frac{I_{\nu-1}(\alpha r_{eD}^\beta)}{l^{3/2} \{K_{1-\nu}(\alpha) I_{\nu-1}(\alpha r_{eD}^\beta) - K_{1-\nu}(\alpha r_{eD}^\beta) I_{\nu-1}(\alpha)\}} \quad (7-25)$$

Substituting for  $C_1$  and  $C_2$  in Equation (7-16), the pressure solution is obtained as

$$\bar{p}_D(r_D, l) = \frac{r_D^\gamma \{I_{\nu-1}(\alpha r_{eD}^\beta) K_\nu(\alpha r_D^\beta) + I_\nu(\alpha r_D^\beta) K_{1-\nu}(\alpha r_{eD}^\beta)\}}{l^{3/2} \{K_{1-\nu}(\alpha) I_{\nu-1}(\alpha r_{eD}^\beta) - K_{1-\nu}(\alpha r_{eD}^\beta) I_{\nu-1}(\alpha)\}} \quad (7-26)$$

where  $\nu$ ,  $\alpha$ ,  $\beta$  and  $\gamma$  are given by Equations (7-17), (7-18), (7-19) and (7-20), respectively. Equation (7-26) is the general solution (in Laplace space) for the transient pressure behaviour in a circular closed fractal reservoir with a centrally located well producing a power-law fluid at a constant rate. Equation (7-26) reduces to the following form at the wellbore ( $r_D = 1$ )

$$\bar{p}_{wD}(l) = \frac{I_{\nu-1}(\alpha r_{eD}^\beta) K_\nu(\alpha) + I_\nu(\alpha) K_{1-\nu}(\alpha r_{eD}^\beta)}{l^{3/2} \{K_{1-\nu}(\alpha) I_{\nu-1}(\alpha r_{eD}^\beta) - K_{1-\nu}(\alpha r_{eD}^\beta) I_{\nu-1}(\alpha)\}} \quad (7-27)$$

For  $d_f = d_s = 2$ , Equation (7-27) exhibits the wellbore pressure response during the flow of a power-law fluid through a closed (circular) homogeneous reservoir (Equation (6-16) of Ikoku (1978)).

## 7.2 Constant-Rate Inner Boundary, Constant-Pressure Outer Boundary

This case represents the situation where radial flow takes place in a circular fractal reservoir, the outer boundary of which is essentially at a constant pressure due to either natural or artificial pressure maintenance at that location. Here also, as in the previous case, the objective is to obtain the transient pressure solution of Equation (7-1) with the initial and inner boundary conditions being expressed by Equations (7-2) and (7-3), respectively. In this case, however, the outer boundary condition is different from that in the previous case and may be written as

$$p(r = r_e, t) = p_i \quad (7-28)$$

In a manner similar to that used in the previous case, one can rewrite the governing equation (Equation (7-1)) in dimensionless form (where the dimensionless variables are defined by Equations (7-5) through (7-7)) and then express the resulting equation and the boundary conditions in Laplace space. The Laplace transform of the governing equation in dimensionless form is given by Equation (7-13); the Laplace transform of the inner boundary condition is given by Equation (7-14). The Laplace transform of the dimensionless form of the outer boundary condition is expressed as

$$\bar{p}_D(r_D, l) = 0 \quad (7-29)$$

Equation (7-13) has the following general solution

$$\bar{p}_D(r_D, l) = r_D^\gamma [C_1 I_\nu(\alpha r_D^\beta) + C_2 K_\nu(\alpha r_D^\beta)] \quad (7-30)$$

where the parameters  $\nu$ ,  $\alpha$ ,  $\beta$  and  $\gamma$  are given by Equations (7-17), (7-18), (7-19) and (7-20), respectively, and  $C_1$  and  $C_2$  are constants to be determined from the boundary conditions. Differentiating Equation (7-30) and using the recurrence relations given by Equations (7-21) and (7-22), one obtains

$$\frac{d\bar{p}_D}{dr_D} = \alpha\beta r_D^{\gamma+\beta-1} [C_1 I_{\nu-1}(\alpha r_D^\beta) - C_2 K_{1-\nu}(\alpha r_D^\beta)] \quad (7-31)$$

Using the inner and outer boundary conditions, given by Equations (7-14) and (7-29), respectively, the constants  $C_1$  and  $C_2$  can be determined; substituting for  $C_1$  and  $C_2$  in Equation (7-30), the pressure solution can be expressed as

$$\bar{p}_D(r_D, l) = \frac{r_D^\gamma \{I_\nu(\alpha r_D^\beta) K_\nu(\alpha r_D^\beta) - I_\nu(\alpha r_D^\beta) K_\nu(\alpha r_D^\beta)\}}{l^{3/2} \{K_{1-\nu}(\alpha) I_\nu(\alpha r_D^\beta) + K_\nu(\alpha r_D^\beta) I_{\nu-1}(\alpha)\}} \quad (7-32)$$

Equation (7-32) is the Laplace transform of the general solution for the transient pressure behaviour for the case of constant rate of flow of a power-law fluid in a circular fractal reservoir with a constant pressure outer boundary. At the wellbore ( $r_D = 1$ ), Equation (7-32) reduces to the following form

$$\bar{p}_{wD}(l) = \frac{I_\nu(\alpha r_D^\beta) K_\nu(\alpha) - I_\nu(\alpha) K_\nu(\alpha r_D^\beta)}{l^{3/2} \{K_{1-\nu}(\alpha) I_\nu(\alpha r_D^\beta) + K_\nu(\alpha r_D^\beta) I_{\nu-1}(\alpha)\}} \quad (7-33)$$

For  $d_f = d_s = 2$ , Equation (7-33) reduces to Equation (6-28) of Ikoku (1978) for a homogeneous reservoir.

### 7.3 Constant-Pressure Inner Boundary, Closed Outer Boundary

The linearized partial differential equation governing the transient flow of a power-law fluid in a fractal reservoir is expressed by Equation (7-1). Before solving Equation (7-1) for a variety of boundary conditions, it is expressed in terms of dimensionless variables. For the constant-pressure inner boundary condition, the dimensionless pressure may be defined as follows

$$p_D(r_D, t_D) = \frac{p_i - p(r, t)}{p_i - p_w} \quad (7-34)$$

where  $p_w$  is the constant wellbore pressure. The dimensionless radius and time are expressed, as in the previous cases, by Equations (7-6) and (7-7), respectively. It can be shown that, by using these definitions of dimensionless variables, Equation (7-1) can be expressed in dimensionless form as Equation (7-8). Assuming that initially the pressure throughout the reservoir is uniform (such that @  $t_D = 0, p_D = 0$  at all  $r_D$ ), Equation (7-8) can be rewritten, using the Laplace transform, as Equation (7-13), which can be transformed into a modified Bessel equation and solved in a straightforward manner. The general solution to Equation (7-13), as has been shown earlier, is of the form

$$\bar{p}_D(r_D, l) = r_D^\gamma [C_1 I_\nu(\alpha r_D^\beta) + C_2 K_\nu(\alpha r_D^\beta)] \quad (7-35)$$

where the parameters  $\nu$ ,  $\alpha$ ,  $\beta$  and  $\gamma$  are given by Equations (7-17), (7-18), (7-19) and (7-20), respectively, and  $C_1$  and  $C_2$  are constants to be determined from the inner and outer boundary conditions.

For a flow situation corresponding to this case, the inner and outer boundary conditions are expressed, respectively, as

$$p(r = r_w, t) = p_w \quad (7-36)$$

and

$$\left. \frac{\partial p}{\partial r} \right|_{r=r_e} = 0 \quad (7-37)$$

where  $r_e$  is the radius of the outer boundary of the circular reservoir. Rewriting Equations (7-36) and (7-37) in terms of dimensionless variables, and then using the Laplace transform, the inner and outer boundary conditions are expressed as

$$\bar{p}_D(r_D = 1, l) = \frac{1}{l} \quad (7-38)$$

and

$$\left. \frac{d\bar{p}_D}{dr_D} \right|_{r_D=r_{eD}} = 0 \quad (7-39)$$

where  $r_{eD}$  is the dimensionless radius of the outer boundary of the reservoir (given by Equation (7-12)).

Using Equations (7-35), (7-38) and (7-39), the constants  $C_1$  and  $C_2$  can be determined as follows

$$C_1 = \frac{K_{1-\nu}(\alpha r_{eD}^\beta)}{l \{ K_\nu(\alpha) I_{\nu-1}(\alpha r_{eD}^\beta) + K_{1-\nu}(\alpha r_{eD}^\beta) I_\nu(\alpha) \}} \quad (7-40)$$

$$C_2 = \frac{I_{\nu-1}(\alpha r_{eD}^\beta)}{l \{ K_\nu(\alpha) I_{\nu-1}(\alpha r_{eD}^\beta) + K_{1-\nu}(\alpha r_{eD}^\beta) I_\nu(\alpha) \}} \quad (7-41)$$

and thus, the pressure solution becomes

$$\bar{p}_D(r_D, l) = \frac{r_D^\gamma \{I_{\nu-1}(\alpha r_{eD}^\beta) K_\nu(\alpha r_D^\beta) + K_{1-\nu}(\alpha r_{eD}^\beta) I_\nu(\alpha r_D^\beta)\}}{l \{K_\nu(\alpha) I_{\nu-1}(\alpha r_{eD}^\beta) + K_{1-\nu}(\alpha r_{eD}^\beta) I_\nu(\alpha)\}} \quad (7-42)$$

Defining the transient dimensionless rate as

$$q_D = \frac{A r_w}{k_w (p_i - p_w) d_f / d_s} \left( \frac{q}{2\pi h r_w} \right)^n, \quad (7-43)$$

where the dimensionless rate is related to the pressure gradient at the wellbore as

$$q_D(d_f / d_s) = - \left. \frac{\partial p_D}{\partial r_D} \right|_{r_D=1} \quad (7-44)$$

and taking the Laplace transforms of Equation (7-44) and using Equation (7-42), one obtains the following expression for the dimensionless rate in Laplace space

$$\bar{q}_D(l) = \frac{I_{\nu-1}(\alpha r_{eD}^\beta) K_{1-\nu}(\alpha) - K_{1-\nu}(\alpha r_{eD}^\beta) I_{\nu-1}(\alpha)}{\sqrt{l} \{K_\nu(\alpha) I_{\nu-1}(\alpha r_{eD}^\beta) + K_{1-\nu}(\alpha r_{eD}^\beta) I_\nu(\alpha)\}} \quad (7-45)$$

Defining the cumulative production (over a given time  $t_D$ ) as

$$Q_D = \int_0^{t_D} q_D dt_D \quad (7-46)$$

and taking its Laplace transform, the cumulative production solution in Laplace space can be expressed as

$$\bar{Q}_D(l) = \frac{I_{\nu-1}(\alpha r_{eD}^\beta) K_{1-\nu}(\alpha) - K_{1-\nu}(\alpha r_{eD}^\beta) I_{\nu-1}(\alpha)}{l^{3/2} \{K_\nu(\alpha) I_{\nu-1}(\alpha r_{eD}^\beta) + K_{1-\nu}(\alpha r_{eD}^\beta) I_\nu(\alpha)\}} \quad (7-47)$$

#### 7.4 Constant-Pressure Inner Boundary, Constant-Pressure Outer Boundary

In this case, the inner and outer boundary conditions are defined by Equations (7-38) and (7-29), respectively, with the dimensionless pressure being defined by Equation (7-34). Using the two boundary conditions, the two unknown constants in Equation (7-35) can be determined and the dimensionless pressure solution expressed as

$$\bar{p}_D(r_D, l) = \frac{r_D^\gamma \{I_\nu(\alpha r_D^\beta) K_\nu(\alpha r_{eD}^\beta) - K_\nu(\alpha r_D^\beta) I_\nu(\alpha r_{eD}^\beta)\}}{l \{K_\nu(\alpha r_{eD}^\beta) I_\nu(\alpha) - K_\nu(\alpha) I_\nu(\alpha r_{eD}^\beta)\}} \quad (7-48)$$

and thus, the dimensionless rate and cumulative production solutions for this case are

$$\bar{q}_D(l) = \frac{I_{\nu-1}(\alpha) K_\nu(\alpha r_{eD}^\beta) + K_{1-\nu}(\alpha) I_\nu(\alpha r_{eD}^\beta)}{\sqrt{l} \{K_\nu(\alpha) I_\nu(\alpha r_{eD}^\beta) - K_\nu(\alpha r_{eD}^\beta) I_\nu(\alpha)\}} \quad (7-49)$$

and

$$\bar{Q}_D(l) = \frac{I_{\nu-1}(\alpha) K_\nu(\alpha r_{eD}^\beta) + K_{1-\nu}(\alpha) I_\nu(\alpha r_{eD}^\beta)}{l^{3/2} \{K_\nu(\alpha) I_\nu(\alpha r_{eD}^\beta) - K_\nu(\alpha r_{eD}^\beta) I_\nu(\alpha)\}}, \quad (7-50)$$

respectively, where the dimensionless rate and cumulative production are defined by Equations (7-43) and (7-46), respectively.



## Chapter VIII

### ANALYTICAL SOLUTIONS FOR POWER-LAW FLOW THROUGH A TWO-ZONE COMPOSITE RESERVOIR

In the realm of hydrocarbon reservoir engineering and well testing, the study of composite reservoirs is of great importance because of the wide range of reservoir configurations they represent. The composite reservoir model has been used to describe and study the behaviour of damaged/stimulated reservoirs, reservoirs undergoing waterflooding, in situ combustion, and so forth. In a (two-zone) composite reservoir model, the reservoir system is generally considered to include a circular inner region with rock and fluid properties significantly different from those in the outer region. It is usual in these modelling efforts to assume that the radial extent of the inner zone and the flow properties (such as permeability) of the two zones are adequately described by the parameters of the composite model.

In this section, an infinite reservoir with a physical radial discontinuity in the rock system is considered. The zone nearest to the wellbore is a fractal reservoir (with spatial distributions of porosity and permeability); the outer zone is infinite in extent, is homogeneous. The major contribution of the material presented in this section is the development of analytical transient pressure and rate solutions during the flow of a non-Newtonian power-law fluid in such a reservoir system. The characteristics of the solutions, presented in the form of dimensionless pressure and pressure-derivative curves, will be discussed in a subsequent chapter.

#### 8.1 *Mathematical Formulation*

The reservoir system under consideration is illustrated schematically in Figure 8-1,

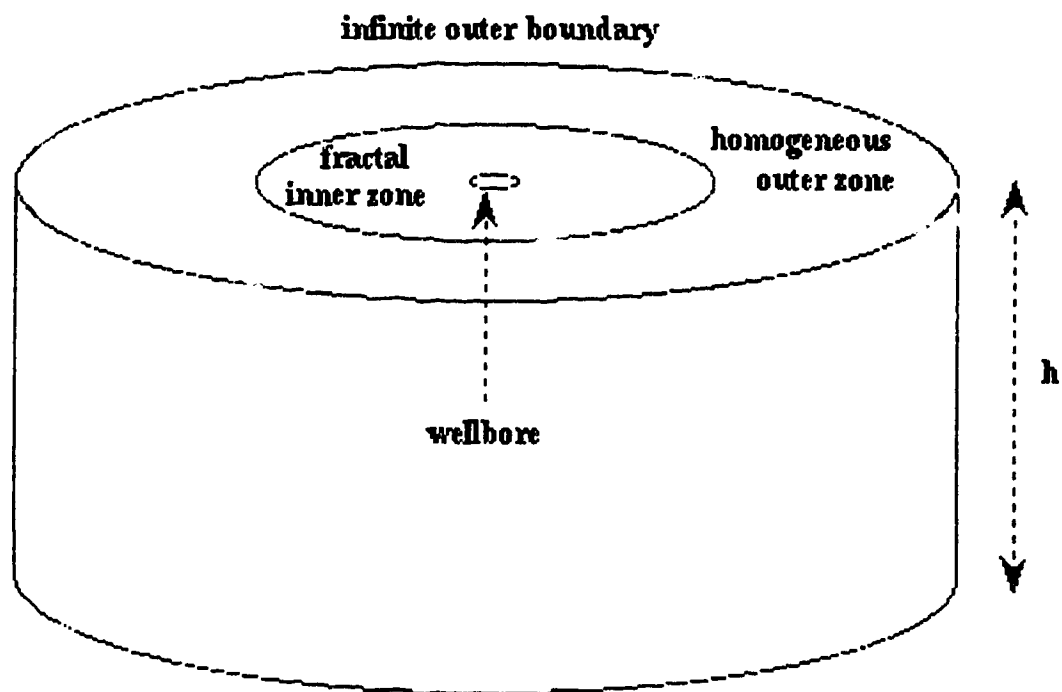


**Figure 8-1: Schematic Representation of a Two-Zone Composite Reservoir**

which exhibits a reservoir system composed of two concentric zones. The inner zone is composed of a fractal zone; that is, the inner zone consists of a fractal network of fractures embedded into a homogeneous matrix with the former dominating the flow, or, equivalently, the entire inner region is fractal. The inner zone surrounds the well to a radius  $r_1$  and there is a sharp radial discontinuity between the inner and outer zones. The outer zone is homogeneous, has a permeability  $k'$  and a porosity  $\phi'$  and is infinite in extent. The wellbore of radius  $r_w$  is located at the centre of the reservoir system.

The transient flow behaviour of a single-phase, slightly compressible, power-law fluid in the reservoir system described above and shown in Figure 8-1 is considered. The transient cylindrical flow in the composite system is modelled by the following system of partial differential equations:

Inner zone

$$\frac{\partial^2 p_1}{\partial r^2} + \left[ d_f + \frac{1}{n} - \frac{d_f}{nd_s} - \frac{d_f}{d_s} \right] \frac{n}{r} \frac{\partial p_1}{\partial r} = \frac{G}{r^{n-1}} \left\{ \frac{r}{r_w} \right\}^{\{(d_f/d_s)(n+1) - d_f(n-1) + n - 3\}} \frac{\partial p_1}{\partial t},$$

for  $r_w \leq r \leq r_1$  (8-1)

Outer zone

$$\frac{\partial^2 p_2}{\partial r^2} + \frac{n}{r} \frac{\partial p_2}{\partial r} = \frac{G'}{r^{n-1}} \frac{\partial p_2}{\partial t}, \text{ for } r > r_1 \quad (8-2)$$

where  $G$  is given by Equation (4-37). Also,

$$G' = \frac{n\phi'c'_i}{k'} \left[ \frac{H}{12} (9 + 3/n)^n (150k'\phi')^{\frac{1-n}{2}} \right] \left( \frac{q}{2\pi h} \right)^{n-1} \quad (8-3)$$

and  $p_1$  and  $p_2$  are the pressures in the inner and outer zones, respectively. Transforming Equations (8-1) and (8-2) into dimensionless form yields

$$\frac{\partial^2 p_{D1}}{\partial r_D^2} + \left[ d_f + \frac{1}{n} - \frac{d_f}{n d_s} - \frac{d_f}{d_s} \right] \frac{n}{r_D} \frac{\partial p_{D1}}{\partial r_D} = (d_f / d_s)^2 r_D^{\{(d_f / d_s)(n+1) - d_f(n-1) - 2\}} \frac{\partial p_{D1}}{\partial t_D},$$

for  $1 \leq r_D \leq a$  (8-4)

$$\frac{\partial^2 p_{D2}}{\partial r_D^2} + \frac{n}{r_D} \frac{\partial p_{D2}}{\partial r_D} = (d_f / d_s)^2 \sigma_1 r_D^{1-n} \frac{\partial p_{D2}}{\partial t_D}, \quad \text{for } r_D > a$$

(8-5)

where

$$a = \frac{r_l}{r_w} \quad (8-6)$$

and

$$\sigma_1 = \frac{\phi' c_i / k'}{\phi_w c_i / k_w} \left( \frac{\phi' k'}{\phi_w k_w} \right)^{-\frac{n}{n-1}} \quad (8-7)$$

The dimensionless variables are defined as follows

$$p_D = \frac{(p_i - p) k_w r_w^{n-1} d_f / d_s}{A (q / 2\pi h)^n} \quad (8-8)$$

$$r_D = \frac{r}{r_w} \quad (8-9)$$

$$t_D = \frac{(d_f / d_s)^2 t}{G r_w^{3-n}} \quad (8-10)$$

### 8.1.1 Constant Rate Case

Equations (8-4) and (8-5) are first solved for a constant rate inner boundary condition and an infinite outer boundary condition. The various boundary conditions for the flow situation considered in this case are described below.

Inner boundary condition:

This condition is for a finite-sized wellbore producing at a constant rate such that

$$\left. \frac{\partial p_{D1}}{\partial r_D} \right|_{r_D=1} = -\frac{d_f}{d_s}, \text{ for all } t_D \quad (8-11)$$

Interface boundary conditions:

Two interface boundary conditions will be considered. The first condition is used to impose pressure continuity at the interface between the two zones:

$$p_{D1}(a, t_D) = p_{D2}(a, t_D) \quad (8-12)$$

The second condition imposes rate continuity at the interface such that the flow rate from the outer zone across the interface equals the flow rate into the inner zone:

$$\frac{\partial p_{D1}}{\partial r_D} = \sigma_2 \frac{\partial p_{D2}}{\partial r_D} @ r_D = a \quad (8-13)$$

where

$$\sigma_2 = \frac{k'}{k_w} \left( \frac{\phi_w k_w}{\phi' k'} \right)^{\frac{1-n}{2}} a^{(n+1)(d_f/d_s) - n d_f + n - 1} \quad (8-14)$$

Outer boundary condition:

For an infinite outer boundary condition, one has

$$p_{D2} \rightarrow 0 \text{ as } r_D \rightarrow \infty \quad (8-15)$$

The system of partial differential equations and the associated boundary conditions, as shown above, is solved using the Laplace transformation.

Applying the Laplace transformation to Equations (3-4) and (8-5) yields

$$r_D^2 \frac{d^2 \bar{p}_{D1}}{dr_D^2} + n \left[ d_f + \frac{1}{n} - \frac{d_f}{nd_s} - \frac{d_f}{d_s} \right] r_D \frac{d \bar{p}_{D1}}{dr_D} = (d_f / d_s)^2 r_D^{\{(d_f / d_s)(n+1) - d_f(n-1)\} / l} \bar{p}_{D1} \quad (8-16)$$

$$r_D^2 \frac{d^2 \bar{p}_{D2}}{dr_D^2} + nr_D \frac{d \bar{p}_{D2}}{dr_D} = (d_f / d_s)^2 \sigma_l r_D^{3-n} l \bar{p}_{D2} \quad (8-17)$$

It is to be noted that in transforming Equations (8-4) and (8-5) into Equations (8-16) and (8-17), respectively, use has been made of the initial condition (i.e., @  $t_D = 0$ ,  $p_D = 0$ ). The boundary conditions become, in Laplace space,

$$\left. \frac{d \bar{p}_{D1}}{dr_D} \right|_{r_D=l} = - \frac{d_f / d_s}{l} \text{ (inner boundary condition)} \quad (8-18)$$

$$\bar{p}_{D1}(a, l) = \bar{p}_{D2}(a, l) \text{ (pressure continuity at interface)} \quad (8-19)$$

$$\frac{d \bar{p}_{D1}}{dr_D} = \sigma_2 \frac{d \bar{p}_{D2}}{dr_D} @ r_D = a \text{ (rate continuity at interface)} \quad (8-20)$$

and

$$\bar{p}_{D2} \rightarrow 0 \text{ as } r_D \rightarrow \infty \quad (8-21)$$

As has been demonstrated in Chapter V, the solution of Equation (8-16) is of the form

$$\bar{p}_{D1}(r_D, l) = r_D^\gamma [C_1 I_\nu(\alpha r_D^\beta) + C_2 K_\nu(\alpha r_D^\beta)] \quad (8-22)$$

where  $\nu$ ,  $\alpha$ ,  $\beta$  and  $\gamma$  are given by Equations (5-21), (5-17), (5-18) and (5-19), respectively.

In a similar fashion, it can be assumed that the solution of Equation (8-17) is of the form

$$\bar{p}_{D2} = r_D^{\gamma'} g(\rho') \quad (8-23)$$

where

$$\rho' = \alpha' r_D^{\beta'} \quad (8-24)$$

Following an approach identical to the one outlined in Chapter V, it is possible to obtain, by substituting Equations (8-23) and (8-24) into Equation (8-17), the following equation in  $\rho'$

$$\rho'^2 g'' + \rho' g' - \left[ \frac{1-n}{3-n} \right]^2 g - \rho'^2 g = 0 \quad (8-25)$$

In arriving at Equation (8-25) it was necessary to choose

$$\alpha' = \frac{2\sqrt{\sigma_l l}}{3-n} (d_f / d_s) \quad (8-26)$$

$$\beta' = \frac{3-n}{2} \quad (8-27)$$

and

$$\gamma' = \frac{l-n}{2} \quad (8-28)$$

Equation (8-25) is in the form of the modified Bessel equation and, hence, the solution to Equation (8-17) is

$$\bar{p}_{D2}(r_D, l) = r_D^{\gamma'} [C_3 I_{\nu'}(\alpha' r_D^{\beta'}) + C_4 K_{\nu'}(\alpha' r_D^{\beta'})] \quad (8-29)$$

where

$$\nu' = \frac{l-n}{3-n} \quad (8-30)$$

By applying the outer boundary condition (Equation (8-21)) to Equation (8-29), it is easily seen that  $C_3 = 0$  and thus, Equation (8-29) reduces to

$$\bar{p}_{D2}(r_D, l) = C_4 r_D^{\gamma'} K_{\nu'}(\alpha' r_D^{\beta'}) \quad (8-31)$$

From Equations (8-18) and (8-22), the constants  $C_1$  and  $C_2$  can be shown to be related as

$$C_1 I_{\nu-\nu'}(\alpha) - C_2 K_{\nu-\nu'}(\alpha) = -l^{-3/2} \quad (8-32)$$

Substituting Equations (8-22) and (8-31) into the pressure continuity relationship (Equation (8-19)) yields

$$C_1 I_{\nu}(\alpha a^{\beta}) + C_2 K_{\nu}(\alpha a^{\beta}) = C_4 a^{\gamma'-\gamma} K_{\nu'}(\alpha' a^{\beta'}) \quad (8-33)$$

Finally, by applying Equations (8-22) and (8-31) in the rate continuity relationship (Equation (8-20)), one obtains

$$C_1 I_{\nu-\nu'}(\alpha a^{\beta}) - C_2 K_{\nu-\nu'}(\alpha a^{\beta}) = -C_4 (\sigma_2 \sqrt{\sigma_1}) a^{\gamma'+\beta'-\gamma-\beta} K_{\nu-\nu'}(\alpha' a^{\beta'}) \quad (8-34)$$



Solving Equations (8-32) through (8-34) simultaneously, the three unknowns  $C_1$ ,  $C_2$  and  $C_4$  can be determined. The constants  $C_1$  and  $C_2$  are found to be

$$C_1 = \frac{\lambda K_v(\alpha' a^{\beta'}) K_{I-v}(\alpha a^\beta) - K_v(\alpha a^\beta) K_{I-v}(\alpha' a^{\beta'})}{\Delta} \quad (8-35)$$

and

$$C_2 = \frac{\lambda K_v(\alpha' a^{\beta'}) I_{v-1}(\alpha a^\beta) + I_v(\alpha a^\beta) K_{I-v}(\alpha' a^{\beta'})}{\Delta}, \quad (8-36)$$

respectively, where

$$\lambda = \frac{a^{\beta-\beta'}}{\sigma_2 \sqrt{\sigma_1}} \quad (8-37)$$

and

$$\begin{aligned} \Delta = l^{3/2} & \left[ \lambda K_v(\alpha' a^{\beta'}) \{ I_{v-1}(\alpha a^\beta) K_{I-v}(\alpha) - I_{v-1}(\alpha) K_{I-v}(\alpha a^\beta) \} \right. \\ & \left. + K_{I-v}(\alpha' a^{\beta'}) \{ I_v(\alpha a^\beta) K_{I-v}(\alpha) + I_{v-1}(\alpha) K_v(\alpha a^\beta) \} \right] \end{aligned} \quad (8-38)$$

Thus, the required pressure solution at the well in the inner zone is given by

$$\bar{p}_{D1}(l, l) = C_1 I_v(\alpha) + C_2 K_v(\alpha) \quad (8-39)$$

where  $C_1$  and  $C_2$  are given by Equations (8-35) and (8-36), respectively. One may write the above equation also in the following fashion

$$\bar{p}_{D1}(l, l) = \frac{a_1 + a_2}{\Delta} \quad (8-40)$$

where

$$a_1 = \{ \lambda K_v(\alpha' a^{\beta'}) K_{I-v}(\alpha a^\beta) - K_v(\alpha a^\beta) K_{I-v}(\alpha' a^{\beta'}) \} I_v(\alpha), \quad (8-41)$$

$$a_2 = \{ \lambda K_v(\alpha' a^{\beta'}) I_{v-1}(\alpha a^\beta) + I_v(\alpha a^\beta) K_{I-v}(\alpha' a^{\beta'}) \} K_v(\alpha) \quad (8-42)$$

and  $\Delta$  is given by Equation (8-38).

### 8.1.2 Constant Pressure Case

It has been demonstrated in the previous section, by using the initial and the outer boundary conditions, that the pressure solutions for the inner and outer zones are given, respectively, by Equations (8-22) and (8-31). For the constant pressure inner boundary condition, defining the dimensionless pressure as

$$p_D = \frac{p_i - p}{p_i - p_w} \quad (8-43)$$

and using the same initial and outer boundary (infinite) conditions as in the previous case, the pressure solutions for the inner and outer zones may again be expressed by Equations (8-22) and (8-31), respectively.

The inner boundary condition in Laplace space is

$$\bar{p}_{D1}|_{r_D=1} = \frac{1}{l} \quad (8-44)$$

Substituting Equation (8-22) into Equation (8-44), one gets

$$C_1 I_v(\alpha) + C_2 K_v(\alpha) = \frac{1}{l} \quad (8-45)$$

Applying Equations (8-22) and (8-31) in the pressure and rate continuity relationships, one obtains, as in the previous case, Equations (8-33) and (8-34). Solving these two equations together with Equation (8-45) simultaneously, it is possible to determine  $C_1$ ,  $C_2$  and  $C_4$ . The constants  $C_1$  and  $C_2$  are determined, respectively, to be

$$C_1 = \frac{\lambda K_v(\alpha' a^{\beta'}) K_{I-v}(\alpha a^\beta) - K_v(\alpha a^\beta) K_{I-v}(\alpha' a^{\beta'})}{l(a_1 + a_2)} \quad (8-46)$$

$$C_2 = \frac{\lambda K_v(\alpha' a^{\beta'}) I_{v-1}(\alpha a^\beta) + I_v(\alpha a^\beta) K_{I-v}(\alpha' a^{\beta'})}{l(a_1 + a_2)} \quad (8-47)$$

where  $a_1$  and  $a_2$  are given by Equations (8-41) and (8-42), respectively. Thus, the pressure solution for the inner zone is

$$\bar{p}_{D1}(r_D, l) = r_D^\gamma [C_1 I_v(\alpha r_D^\beta) + C_2 K_v(\alpha r_D^\beta)] \quad (8-48)$$

where  $C_1$  and  $C_2$  are given by Equations (8-46) and (8-47), respectively.

Defining dimensionless rate and cumulative production, respectively, as

$$q_D = \frac{A r_w}{k_w (p_i - p_w) d_f / d_s} \left( \frac{q}{2\pi h r_w} \right)^n \quad (8-49)$$

and

$$Q_D = \int_0^{t_D} q_D dt_D, \quad (8-50)$$

the dimensionless rate and cumulative production can be evaluated in Laplace space as

$$\bar{q}_D(d_f / d_s) = - \left. \frac{d\bar{p}_{D1}}{dr_D} \right|_{r_D=1} \quad (8-51)$$

and

$$\bar{Q}_D = \frac{\bar{q}_D}{l} \quad (8-52)$$

The expressions for the dimensionless rate and cumulative production can thus be written as

$$\bar{q}_D(l) = \frac{\Delta}{l^3 (a_1 + a_2)} \quad (8-53)$$

and

$$\bar{Q}_D(l) = \frac{\Delta}{l^3 (a_1 + a_2)}, \quad (8-54)$$

respectively, where  $\Delta$ ,  $a_1$  and  $a_2$  are given by Equations (8-38), (8-41) and (8-42), respectively.

## Chapter IX

### PRESSURE TRANSIENTS WITH MATRIX PARTICIPATION IN FLOW: A SPECIAL CASE

The previous chapters dealt with the development of transient pressure and rate solutions for the single-phase flow of a non-Newtonian power-law fluid through infinite and finite fractal flow networks. In the material considered in the previous chapters, the analysis of the pressure transients was performed by assuming that the matrix does not participate in the flow process. In this chapter, a mathematical formulation is presented for the transient flow of a non-Newtonian power-law fluid in a naturally fractured reservoir that consists of a fractal network of fractures embedded into a homogeneous matrix. The conventional Newtonian flow model in a double-porosity system is generalized by allowing the matrix to exchange fluid with the fractal fracture system. Following the Warren and Root approach (Warren and Root, 1963), it is assumed in the present model that flow between the matrix blocks takes place only through the fracture system. Furthermore, the well intersects the fracture system and all the fluid produced at the wellbore moves through the fractures. Analytical solutions are obtained for a special case of the flow situation where a Newtonian fluid travels through infinite and finite fracture/matrix systems; the main reasons for considering this particular case are also discussed.

#### 9.1 Mathematical Formulation

The continuity equation for cylindrical flow in this fracture-matrix system may be written as

$$\frac{1}{r} \frac{\partial}{\partial r}(r \rho_f u_r) = \frac{\partial}{\partial t}(\phi_f \rho_f) + \frac{\partial}{\partial t}(\phi_m \rho_m) \quad (9-1)$$

where the subscripts  $f$  and  $m$  refer to the fracture network and matrix, respectively. The modified Darcy's law for a power-law fluid flowing in the fracture network is

$$u_r = \left\{ \frac{1}{\mu_{eff}(r)} \frac{\partial p_f}{\partial r} \right\}^{1/n} \quad (9-2)$$

Applying Equation (9-2) in Equation (9-1) yields

$$\begin{aligned} & \frac{1}{n} \frac{\partial}{\partial r} \left\{ k_f(r) \frac{\partial p_f}{\partial r} \right\} + k_f(r) \frac{\partial p_f}{\partial r} \left\{ \frac{1}{r} - \frac{1}{n \mu_{eff}(r)} \frac{d \mu_{eff}(r)}{dr} \right\} \\ &= \left\{ \phi_f(r) c_f \frac{\partial p_f}{\partial t} + \phi_m c_m \frac{\partial p_m}{\partial t} \right\} \mu_{eff}^{1/n}(r) \left\{ k_f(r) \frac{\partial p_f}{\partial r} \right\}^{\frac{n-1}{n}} \end{aligned} \quad (9-3)$$

In deriving the above equation, it was assumed that pressure gradients in the fracture network are small at all times. Equation (9-3) can be further simplified, by making use of Equations (4-13), (4-14), (4-16) and (4-34), to

$$\begin{aligned} & \frac{\partial^2 p_f}{\partial r^2} + \left[ d_f + \frac{1}{n} - \frac{d_f}{n d_s} - \frac{d_f}{d_s} \right] \frac{n}{r} \frac{\partial p_f}{\partial r} = \\ & \frac{nA}{k_w} \left( \frac{q}{2\pi r h} \right)^{n-1} \left\{ \phi_w c_f (r/r_w)^{d_f-2} \frac{\partial p_f}{\partial t} + \phi_m c_m \frac{\partial p_m}{\partial t} \right\} \left\{ \frac{r}{r_w} \right\}^{\{(d_f/d_s)/(n+1) - d_f/n + n-1\}} \end{aligned} \quad (9-4)$$

For a Newtonian fluid ( $n = 1$ ) flowing in a naturally fractured reservoir where a homogeneous fracture network is embedded into a homogeneous matrix (such that  $d_f = d_s = 2$ ), Equation (9-4) is reduced to the following form

$$\frac{\partial^2 p_f}{\partial r^2} + \frac{1}{r} \frac{\partial p_f}{\partial r} = \frac{\mu}{k_w} \left\{ \phi_w c_f \frac{\partial p_f}{\partial t} + \phi_m c_m \frac{\partial p_m}{\partial t} \right\} \quad (9-5)$$

Equation (9-5) is the Warren and Root (1963) equation for transient radial flow in a double-porosity system (Sabet, 1991). Warren and Root have shown that, for such a flow medium, a semilog plot of the drawdown data (flowing wellbore pressure versus time) exhibits two parallel straight lines. The earlier line indicates transient radial flow through the fractures before the matrix makes its presence felt; the later straight line develops after an equilibrium is reached between the fracture and the matrix pressures. The transition between these two lines develops as a result of the matrix-to-fracture interporosity crossflow. This transition from early production from the fractures to late production from the total reservoir (matrix and fractures) is affected by the way the matrix and fracture network are assumed to interact. In the Warren and Root model (Warren and Root, 1963), the flow from matrix to fractures is assumed to take place under pseudosteady-state conditions; in other words, the interporosity flow rate is proportional to the pressure difference between matrix and fractures. Such an assumption was also employed by Chang and Yortsos (1990) in their model describing flow in both the fractal object and the matrix. The pseudosteady-state flux assumption will also be used in the present study.

Following the approach of Chang and Yortsos (1990), the expression for the interporosity fluid exchange rate is given by

$$q_{mf} = br^{D'-1} \left\{ \frac{k_m (p_f - p_m)}{\mu_{eff} e r^{D''}} \right\}^{1/\alpha} \quad (9-6)$$

where  $D'$  is the fractal exponent for the perimeter of the fractal object and  $b$  is the corresponding proportionality constant with a dimension of  $[L^{2-D'}]$ , and  $D''$  is the fractal exponent for the average distance between the matrix and the fractal object and  $e$  is the corresponding proportionality constant with a dimension of  $[L^{1-D''}]$ . In the Euclidean limit,  $D' = 2$ ,  $D'' = 0$ ,  $b = 1$  and  $e =$  the characteristic length  $l$  of the Warren and Root model

(Chang and Yortsos, 1990). By applying a mass balance for the fluid contained within the matrix, it can be shown that

$$\frac{\partial}{\partial t}(\rho_m \phi_m) = \frac{\rho_m q_{mf}}{2\pi r h} \quad (9-7)$$

Combining Equations (9-6) and (9-7) and simplifying, one obtains

$$\frac{\partial p_m}{\partial t} = \frac{b r^{D'-2-D''/n}}{e^{1/n} 2\pi h \phi_m c_m} \left\{ \frac{12 k_m (p_f - p_m)}{H(9 + 3/n)^n (150 k_m \phi_m)^{\frac{1-n}{2}}} \right\}^{1/n} \quad (9-8)$$

Equations (9-4) and (9-8) can be combined and solved for various sets of boundary conditions to present and analyze the behaviour of the pressure transients with matrix participation in flow.

## 9.2 Analytical Solutions for a Special Case

Equation (9-4) is an approximate partial differential equation describing the transient flow of a non-Newtonian power-law fluid through a fractal fracture network-matrix system. The suitability of Equation (9-4) in describing such flows is limited mainly because of the use of the approximation, given by Equation (4-29), in deriving it. However, for the Newtonian fluid case ( $n = 1$ ), Equation (9-4) does not suffer from this limitation. It is, therefore, of theoretical and practical value to consider analytical solutions for Equation (9-4) for the case of a Newtonian fluid. For the Newtonian fluid case, Equations (9-4) and (9-8) reduce, respectively, to

$$\frac{\partial^2 p_f}{\partial r^2} + \left[ d_f + 1 - \frac{2d_f}{d_s} \right] \frac{1}{r} \frac{\partial p_f}{\partial r} =$$



$$\frac{\mu}{k_w} \left\{ \phi_w c_f (r / r_w)^{d_f - 2} \frac{\partial p_f}{\partial t} + \phi_m c_m \frac{\partial p_m}{\partial t} \right\} \left\{ \frac{r}{r_w} \right\}^{2d_f / d_s - d_f} \quad (9-9)$$

and

$$\frac{\partial p_m}{\partial t} = - \frac{b k_m}{e \mu 2 \pi h \phi_m c_m} (p_f - p_m) r^{-\sigma} \quad (9-10)$$

where  $\sigma = D'' + 2 - D'$ . The similarity between the above equations and the corresponding equations (for flow in both fractal object and matrix) used in the study of Chang and Yortsos (1990) is obvious; in fact, Equation (9-10) is identical to Equation (25) of Chang and Yortsos for  $d = 2$ . In their study, however, Chang and Yortsos considered numerical solutions to the partial differential equations governing flow in both fractures and matrix; analytical solutions could not be considered because of the presence of spatially variable coefficients. It was found in their study that the system pressure response exhibited early- and late-time linear behaviour in the log-log plot (of dimensionless pressure against dimensionless time). It can be inferred from the results presented in their study that the slope of the early linear segment depends on  $d_s$ , whereas that of the late segment depends on both  $d_f$  and  $d_s$ ; it was, however, mentioned that the difference in the two slopes is small. Chang and Yortsos also studied the effects of the various relevant parameters on the transitional period between the two linear segments and concluded that  $\sigma$  had the least significant effect.

### 9.2.1 Constant Rate Case

Defining dimensionless pressure, time and radius as follows

$$p_{Df,m} = \frac{2 \pi k_w h (d_f / d_s) (p_i - p_{f,m})}{q \mu} \quad (9-11)$$

$$\tau = \frac{\omega k_w (d_f / d_s)^2 t}{\mu \phi_w c_f r_w^2} \quad (9-12)$$

$$r_D = r / r_w \quad (9-13)$$

where

$$\omega = \frac{\phi_w c_f}{\phi_w c_f + \phi_m c_m} \quad (9-14)$$

It is to be noted that the dimensionless time defined here (Equation (9-12)) and that defined in the previous chapters (Equation (4-40)), for  $n = 1$ , are related as  $\tau = \omega t_D$ . Equations (9-9) and (9-10) can be expressed in terms of the dimensionless variables as

$$\frac{\partial^2 p_{Df}}{\partial r_D^2} + \left[ d_f + 1 - \frac{2d_f}{d_s} \right] \frac{1}{r_D} \frac{\partial p_{Df}}{\partial r_D} = \left( \frac{d_f}{d_s} \right)^2 \left\{ \omega r_D^{d_f-2} \frac{\partial p_{Df}}{\partial \tau} + (1 - \omega) \frac{\partial p_{Dm}}{\partial \tau} \right\} r_D^{2d_f/d_s - d_f} \quad (9-15)$$

and

$$\frac{\partial p_{Dm}}{\partial \tau} = \frac{\lambda}{r_D^\sigma} (p_{Df} - p_{Dm}) \quad (9-16)$$

where

$$\lambda = \frac{b k_m r_w^{D'-D''}}{(1 - \omega) 2 \pi h e k_w (d_f / d_s)^2} \quad (9-17)$$

The parameter  $\omega$  represents the ratio of near-wellbore fracture storage to total storage. The interporosity interaction parameter,  $\lambda$ , is proportional to the ratio of matrix permeability to

near wellbore fracture permeability ( $k_m/k_w$ ) and generally has values much smaller than one. Large values of  $\omega$  (say, greater than 0.01) would indicate a significant amount of storage in the fracture system; large values of  $\lambda$  (say, larger than  $10^{-5}$ ) would indicate a relatively large flow conductivity in the matrix.

Before solving the equations describing the transient response of the fracture-matrix system, two assumptions will be made – the system behaviour for  $d_f = 2$ , and for  $\sigma = 0$  will be considered. The effect of the second assumption will be felt only during the transitional period, as has been discussed earlier. This effect, however, will be minor, as the parameters  $\omega$  and  $\lambda$  have been shown to have more significant roles to play during that period (Chang and Yortsos, 1990). The first assumption is extremely significant; it will influence both the transitional period and the late-time behaviour of the system. However, as will be shown in the next chapter, this assumption is intended to help bring out some interesting characteristics of the transient response of the fractured medium.

Incorporating the above-described assumptions, Equations (9-15) and (9-16) can be expressed in Laplace space and then combined to yield

$$\frac{d^2 \bar{p}_{Df}}{dr_D^2} + \left(3 - \frac{4}{d_s}\right) \frac{1}{r_D} \frac{d\bar{p}_{Df}}{dr_D} = \xi r_D^{4/d_s - 2} \bar{p}_{Df} \quad (9-18)$$

where

$$\xi = l(2/d_s)^2 \left( \frac{\omega l + \lambda}{l + \lambda} \right) \quad (9-19)$$

The inner and outer (infinite) boundary conditions are

$$\left. \frac{d\bar{p}_{Df}}{dr_D} \right|_{r_D=1} = - \frac{2}{d_s} \quad (9-20)$$

$$\bar{p}_{Df} \rightarrow 0 \text{ as } r_D \rightarrow \infty \quad (9-21)$$

It is assumed that the pressure solution for the given drawdown problem may be expressed as

$$\bar{p}_{Df} = r_D^\gamma f(\rho), \quad \rho = \alpha r_D^\beta \quad (9-22)$$

Substitution of Equation (9-22) in Equation (9-18) yields

$$\rho^2 f'' + \rho f' - \left[ 1 - \frac{d_s}{2} \right]^2 f - \rho^2 f = 0 \quad (9-23)$$

provided one chooses

$$\alpha = \frac{\sqrt{\xi}}{\beta} = \sqrt{\frac{l(\omega l + \lambda)}{l + \lambda}} \quad (9-24)$$

$$\beta = 2 / d_s \quad (9-25)$$

and

$$\gamma = 2 / d_s - 1 \quad (9-26)$$

The solution to Equation (9-23) is, as has been shown previously in Chapter IV,

$$f(\rho) = C_1 I_\nu(\rho) + C_2 K_\nu(\rho) \quad (9-27)$$

where

$$\nu = 1 - d_s/2 \quad (9-28)$$

Combining Equations (9-22) and (9-27) and applying the outer boundary condition (Equation (9-21)), one gets

$$\bar{P}_{Df}(r_D, l) = C_2 r_D^\gamma K_\nu(\alpha r_D^\beta) \quad (9-29)$$

Applying the inner boundary condition (Equation (9-20)) in Equation (9-28), the constant  $C_2$  is determined to be

$$C_2 = \frac{l}{l^\alpha K_{1-\nu}(\alpha)} \quad (9-30)$$

and thus, the dimensionless wellbore pressure solution in Laplace space is obtained as

$$\bar{P}_{Df}(r_D = 1, l) = \frac{K_\nu(\alpha)}{\alpha l K_{1-\nu}(\alpha)} \quad (9-31)$$

For the case of a closed circular reservoir with a centrally-located well producing at a constant rate, the wellbore pressure solution may be obtained in a similar fashion

$$\bar{P}_{Df}(r_D = 1, l) = \frac{I_{\nu-1}(\alpha r_{eD}^\beta) K_\nu(\alpha) + I_\nu(\alpha) K_{1-\nu}(\alpha r_{eD}^\beta)}{\alpha l \{K_{1-\nu}(\alpha) I_{\nu-1}(\alpha r_{eD}^\beta) - K_{1-\nu}(\alpha r_{eD}^\beta) I_{\nu-1}(\alpha)\}} \quad (9-32)$$

The wellbore pressure solution for a constant pressure outer boundary condition is

$$\bar{P}_{Df}(r_D = 1, l) = \frac{I_\nu(\alpha r_{eD}^\beta) K_\nu(\alpha) - I_\nu(\alpha) K_\nu(\alpha r_{eD}^\beta)}{\alpha l \{K_{1-\nu}(\alpha) I_\nu(\alpha r_{eD}^\beta) + K_\nu(\alpha r_{eD}^\beta) I_{\nu-1}(\alpha)\}} \quad (9-33)$$

It can be shown from Equation (9-24) that as  $\omega \rightarrow 1$ ,  $\alpha \rightarrow \sqrt{l}$  and Equations (9-31) through (9-33) reduce to the corresponding wellbore pressure solutions for flow only in the fractal fracture network for  $n = 1$  and  $d_f = 2$ . This behaviour is expected, since the reservoir

must contain only the fracture system if  $\omega$  is to approach unity. Similarly, Equations (9-31) through (9-33) indicate fracture flow behaviour as  $\lambda \rightarrow \infty$ ; this is also proper because either  $\omega \rightarrow 1$  or  $k_m \rightarrow \infty$  (indicating no impedance to interporosity flow) if  $\lambda$  has to approach infinity.

#### *Limiting Solutions for Early and Late Times*

At early times,  $l \rightarrow \infty$ , so that  $\alpha \rightarrow \sqrt{\omega l}$  and the modified Bessel function,  $K_\nu(z)$ , may be approximated by Equation (5-31). Thus, Equation (9-31) approximates to

$$\bar{P}_{Df}(r_D = 1, l) \approx \frac{K_\nu(\sqrt{\omega l})}{l \sqrt{\omega l} K_{1-\nu}(\sqrt{\omega l})} \quad (9-34)$$

Using Equation (5-31), the early-time limiting wellbore pressure solution in the real plane can then be expressed as

$$p_{Df}(r_D = 1, \tau) = 2\sqrt{\frac{\tau}{\omega\pi}} = 2\sqrt{\frac{t_D}{\pi}} \quad (9-35)$$

where  $\tau$  is given by Equation (9-12) and  $t_D$  by Equation (4-35), for  $n = 1$  and  $d_f = 2$ . Thus, at early times, the wellbore pressure response would be exactly the same as that when only the fracture system participates in the flow process (see Section 5.1.2).

At late times,  $l \rightarrow 0$  ( $\alpha \rightarrow \sqrt{l}$ ), and applying Equation (5-50) in Equation (9-31), the late-time approximation of the Laplace space wellbore pressure solution is

$$\bar{P}_{Df}(r_D = 1, l) \approx \frac{2^{2\nu-1} \Gamma(\nu)}{l \Gamma(1-\nu) \alpha^{2\nu}} \quad (9-36)$$

which can be inverted to

$$p_{Df}(r_D = 1, \tau) = \frac{2^{2\nu-1} \tau^\nu}{\nu \Gamma(1-\nu)} \quad (9-37)$$

It is also of interest to consider the early- and late-time limiting solutions for the special case of  $\omega = 0$ , which applies for negligible storage capacity in the fracture system; this case has been discussed extensively for a homogeneous fracture system by Warren and Root (1963). For this case, at early times, when  $\alpha \rightarrow \sqrt{\lambda}$ , the wellbore pressure solution has a constant value given by

$$p_{Df}(r_D = 1, \tau) = \frac{K_\nu(\sqrt{\lambda})}{\sqrt{\lambda} K_{1-\nu}(\sqrt{\lambda})} \quad (9-38)$$

Thus, a constant early-time wellbore pressure in a "double-porosity" system would indicate an extremely small value of the storage parameter,  $\omega$ . At large times,  $\alpha \rightarrow \sqrt{l}$ , and the wellbore pressure response is given by Equation (9-37).

### 9.2.2 Constant Pressure Case

For the constant pressure inner boundary condition, the dimensionless pressure has been defined previously (Equation (5-77)) as

$$p_{Df, m} = \frac{p_i - p_{f, m}}{p_i - p_w} \quad (9-39)$$

The dimensionless time and radius are given by Equations (9-12) and (9-13), respectively. Equation (9-18) describes the transient flow of a Newtonian fluid in a fractal fracture-homogeneous matrix system with  $d_f = 2$  and  $\sigma = 0$ . The inner boundary condition is

$$\bar{p}_{Df}(r_D = 1, l) = \frac{l}{l} \quad (9-40)$$

and the outer boundary condition (for an infinite system) is given by Equation (9-21). In a manner similar to that shown for the constant rate case, the dimensionless fracture pressure solution for the constant pressure inner and infinite outer boundary conditions may be obtained as

$$\bar{P}_{Df}(r_D, l) = \frac{r_D^\gamma K_\nu(\alpha r_D^\beta)}{l K_\nu(\alpha)} \quad (9-41)$$

Defining the dimensionless rate as

$$q_D = \frac{q \mu d_s}{4 \pi k_w h (p_i - p_w)}, \quad (9-42)$$

it is possible to show that

$$q_D = - \frac{d_s}{2} \left. \frac{\partial p_{Df}}{\partial r_D} \right|_{r_D=1} \quad (9-43)$$

Combining Equation (9-43) with Equation (9-41), the following expression for dimensionless rate is obtained

$$\bar{q}_D = \frac{\alpha K_{1-\nu}(\alpha)}{l K_\nu(\alpha)} \quad (9-44)$$

Finally, by defining the cumulative production as

$$Q_D = \int_0^\tau q_D d\tau, \quad (9-45)$$

it can be demonstrated very simply, by combining Equations (9-44) and (9-45), that



$$\bar{Q}_D = \frac{\alpha K_{1-\nu}(\alpha)}{l^2 K_\nu(\alpha)} \quad (9-46)$$

Similarly, the dimensionless rate and cumulative production solutions for a closed reservoir are obtained as

$$\bar{q}_D(l) = \frac{\alpha \{I_{\nu-1}(\alpha r_{eD}^\beta) K_{1-\nu}(\alpha) - K_{1-\nu}(\alpha r_{eD}^\beta) I_{\nu-1}(\alpha)\}}{l \{K_\nu(\alpha) I_{\nu-1}(\alpha r_{eD}^\beta) + K_{1-\nu}(\alpha r_{eD}^\beta) I_\nu(\alpha)\}} \quad (9-47)$$

and

$$\bar{Q}_D(l) = \frac{\alpha \{I_{\nu-1}(\alpha r_{eD}^\beta) K_{1-\nu}(\alpha) - K_{1-\nu}(\alpha r_{eD}^\beta) I_{\nu-1}(\alpha)\}}{l^2 \{K_\nu(\alpha) I_{\nu-1}(\alpha r_{eD}^\beta) + K_{1-\nu}(\alpha r_{eD}^\beta) I_\nu(\alpha)\}} \quad (9-48)$$

Finally, the solutions for a constant pressure outer boundary situation are given by

$$\bar{q}_D(l) = \frac{\alpha \{I_{\nu-1}(\alpha) K_\nu(\alpha r_{eD}^\beta) + K_{1-\nu}(\alpha) I_\nu(\alpha r_{eD}^\beta)\}}{l \{K_\nu(\alpha) I_\nu(\alpha r_{eD}^\beta) - K_{1-\nu}(\alpha r_{eD}^\beta) I_\nu(\alpha)\}} \quad (9-49)$$

and

$$\bar{Q}_D(l) = \frac{\alpha \{I_{\nu-1}(\alpha) K_\nu(\alpha r_{eD}^\beta) + K_{1-\nu}(\alpha) I_\nu(\alpha r_{eD}^\beta)\}}{l^2 \{K_\nu(\alpha) I_\nu(\alpha r_{eD}^\beta) - K_{1-\nu}(\alpha r_{eD}^\beta) I_\nu(\alpha)\}} \quad (9-50)$$

#### *Limiting Solutions for Early and Late Times*

At early times,  $l \rightarrow \infty$ , so that  $\alpha \rightarrow \sqrt{\omega l}$  and thus, from Equation (9-44),

$$\bar{q}_D \approx \sqrt{\frac{\omega}{l}} \quad (9-51)$$

Equation (9-51) can be inverted analytically to yield

$$q_D(\tau) = \sqrt{\frac{\omega}{\pi\tau}} = \sqrt{\frac{1}{\pi\tau_D}} \quad (9-52)$$

and thus, the cumulative production solution becomes

$$Q_D(t_D) = 2\sqrt{\frac{t_D}{\pi}} \quad (9-53)$$

At late times,  $l \rightarrow 0$  ( $\alpha \rightarrow \sqrt{l}$ ), and thus, from Equation (9-44),

$$\bar{q}_D \approx \frac{\Gamma(1-\nu)}{\Gamma(\nu) 2^{2\nu-1} l^{1-\nu}} \quad (9-54)$$

The late-time dimensionless rate solution, expressed in the real plane, is then

$$q_D(t_D) = \frac{2^{1-2\nu}}{\omega^\nu \Gamma(\nu) t_D^\nu} \quad (9-55)$$

and the cumulative production solution is

$$Q_D(t_D) = \frac{(\omega t_D)^{1-\nu}}{2^{2\nu-1} \Gamma(\nu) (1-\nu)} \quad (9-56)$$

## **Chapter X**

### **RESULTS AND DISCUSSION**

Various models have been presented in the previous chapters to analyze the transient pressure and rate behaviour of power-law fluid flow in reservoirs exhibiting power-law variations of permeability and porosity with distance from the wellbore. In Chapter IV, a partial differential equation was derived for an approximate description of the transient flow of a non-Newtonian power-law fluid in an infinite fractal flow medium. Chapter V presents analytical solutions, in Laplace space, to this equation for both constant-rate and -pressure inner boundary conditions; early- and large-time limiting forms of the analytical solutions have been derived in real space. In Chapter VI, a finite-difference scheme was presented to solve the nonlinear partial differential equation describing the transient flow of a power-law fluid in an infinite fractal reservoir. Chapter VII contains analytical pressure and rate solutions for finite reservoirs; both closed and constant-pressure outer boundary conditions have been considered. Chapter VIII presents analytical pressure and rate solutions for a two-zone composite reservoir, with the inner zone being fractal and the outer homogeneous. Chapter IX demonstrates the development of analytical solutions for a special case of the situation where the transient flow of a Newtonian fluid takes place in a fracture/matrix system, with the fracture network showing anomalous diffusion.

This chapter presents the results obtained from the different models described in the previous chapters (see Figure 10-1) and discusses the effects of the various parameters on these results. The discussion mainly focusses on analysis of results obtained from the transient pressure and rate models for flow in an infinite fractal medium, with particular emphasis on the late-time behaviour of the flow system. Discussion is also presented on the results obtained for flow in a finite system, in a composite system and in an infinite fractal

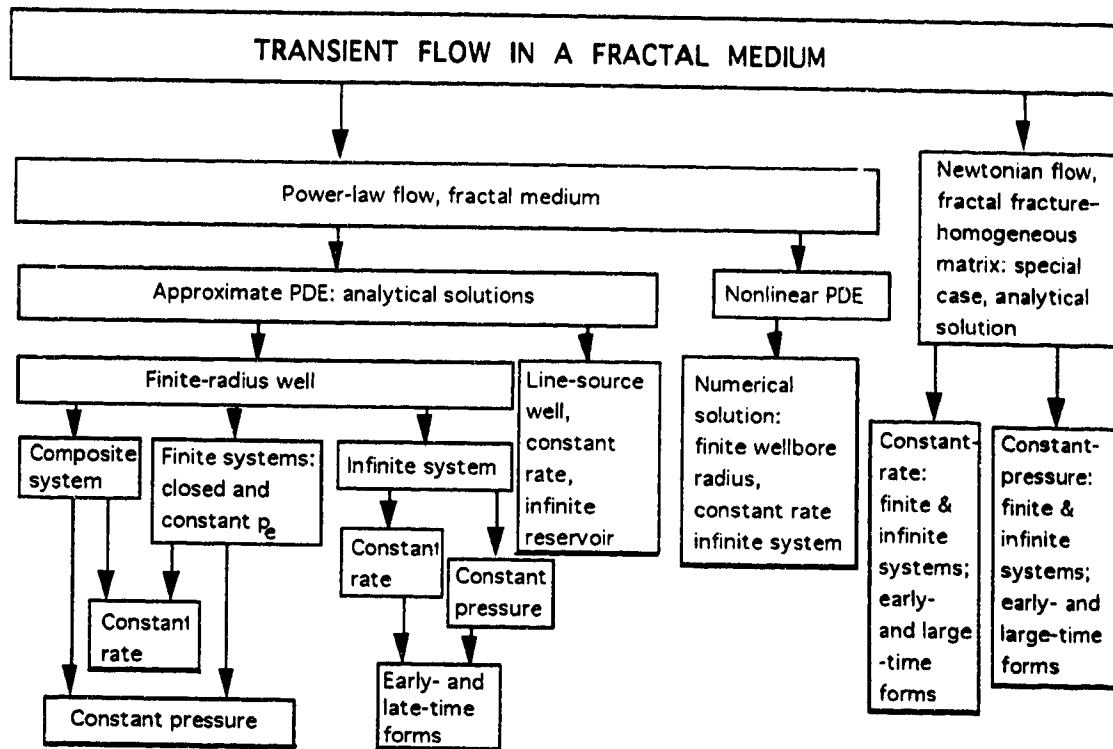


**Figure 10-1: An Organizational Map Depicting the Situations Considered in this Study**

fracture/matrix system.

## 10.1 Transient Flow Through a Fractal Medium

### 10.1.1 Analytical Solutions: Infinite Reservoir

Transient solutions for dimensionless pressure (Equation (5-30)) and rate (Equation (5-82)) for an infinite fractal reservoir can be evaluated readily in real space by using numerical techniques. In this study, the numerical Laplace transform inversion scheme developed by Stehfest (1970) is applied to obtain the dimensionless pressure ( $p_{wD}$ ) and pressure-derivative ( $dp_{wD}/d\ln t_D$ ) solutions for various combinations of  $d_f$  and  $n$ . Some of the results for  $d_f = 2$  and for various values of the flow behaviour index,  $n$ , are shown in Figures 10-2 through 10-4. It can be seen from these figures that with increasing time, the pressure solutions start diverging from each other depending on the relative magnitudes of  $n$ ; the dimensionless pressure at any given time is larger for a smaller value of  $n$ . In fact, Figure 10-2 shows that the dimensionless pressure at a given time during the production (or injection) of a pseudoplastic fluid may be more than an order of magnitude larger than that for a Newtonian fluid. However, it is to be noted from Equation (4-38) that the definition of dimensionless pressure involves flow rate and well radius raised to powers of  $n$  (where  $0 < n < 1$ ) and thus, the actual pressure drop (for production) or increase (for injection) may be lower for a pseudoplastic fluid than for a Newtonian one (Ikoku, 1978; Olarewaju, 1992).

Figure 10-2 shows that at late times and for  $\nu > 0$ , the dimensionless pressure solution exhibits a straight line in the log-log plot; this is expected, as has been demonstrated earlier by Equation (5-47). The slope of this straight line is equal to the parameter  $\nu$ . It is interesting to note, however, that the pressure-derivative plots (see Figure 10-3) exhibit a large-time straight line behaviour for a longer period of time; such a behaviour may be explained by inspecting Equations (5-43) and (5-47). The slope of the linear segment of the pressure-

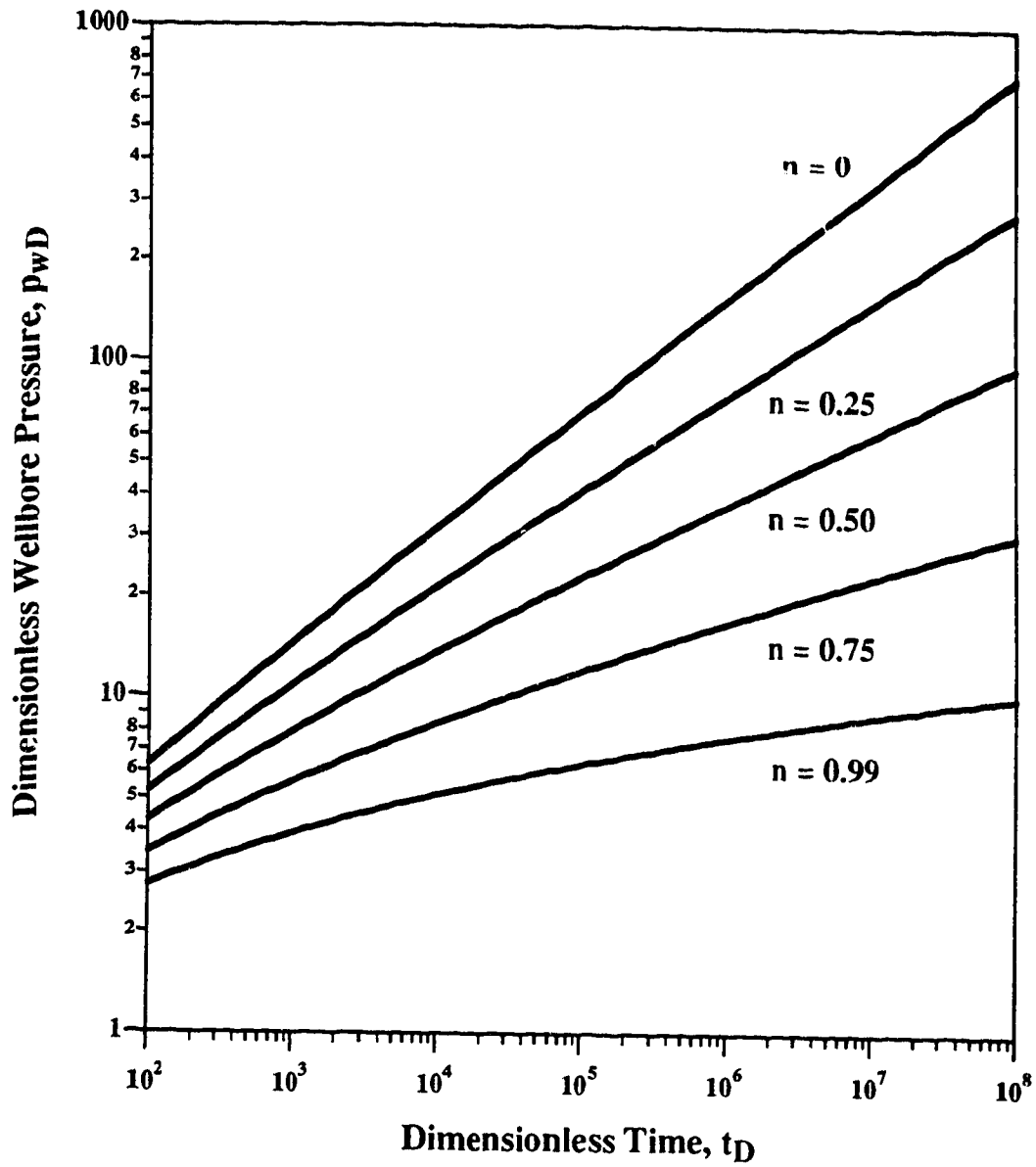


**Figure 10-2: Dimensionless Wellbore Pressure versus Time for an Infinite System; Pseudoplastic Fluids,  $d_s = 2$**

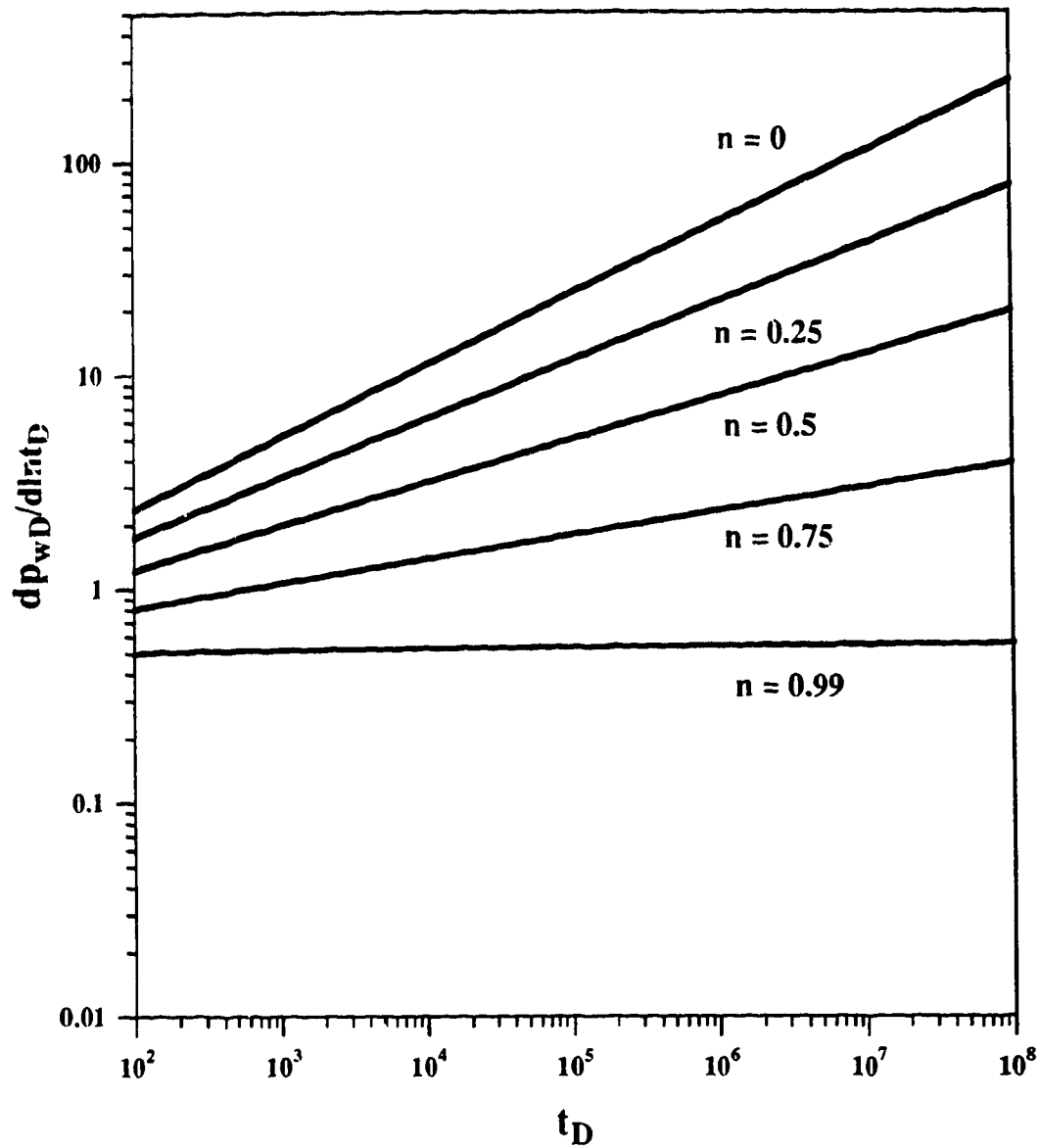


**Figure 10-3: Dimensionless Wellbore Pressure Derivative versus Time for an Infinite System; Pseudoplastic Fluids,  $d_s = 2$**

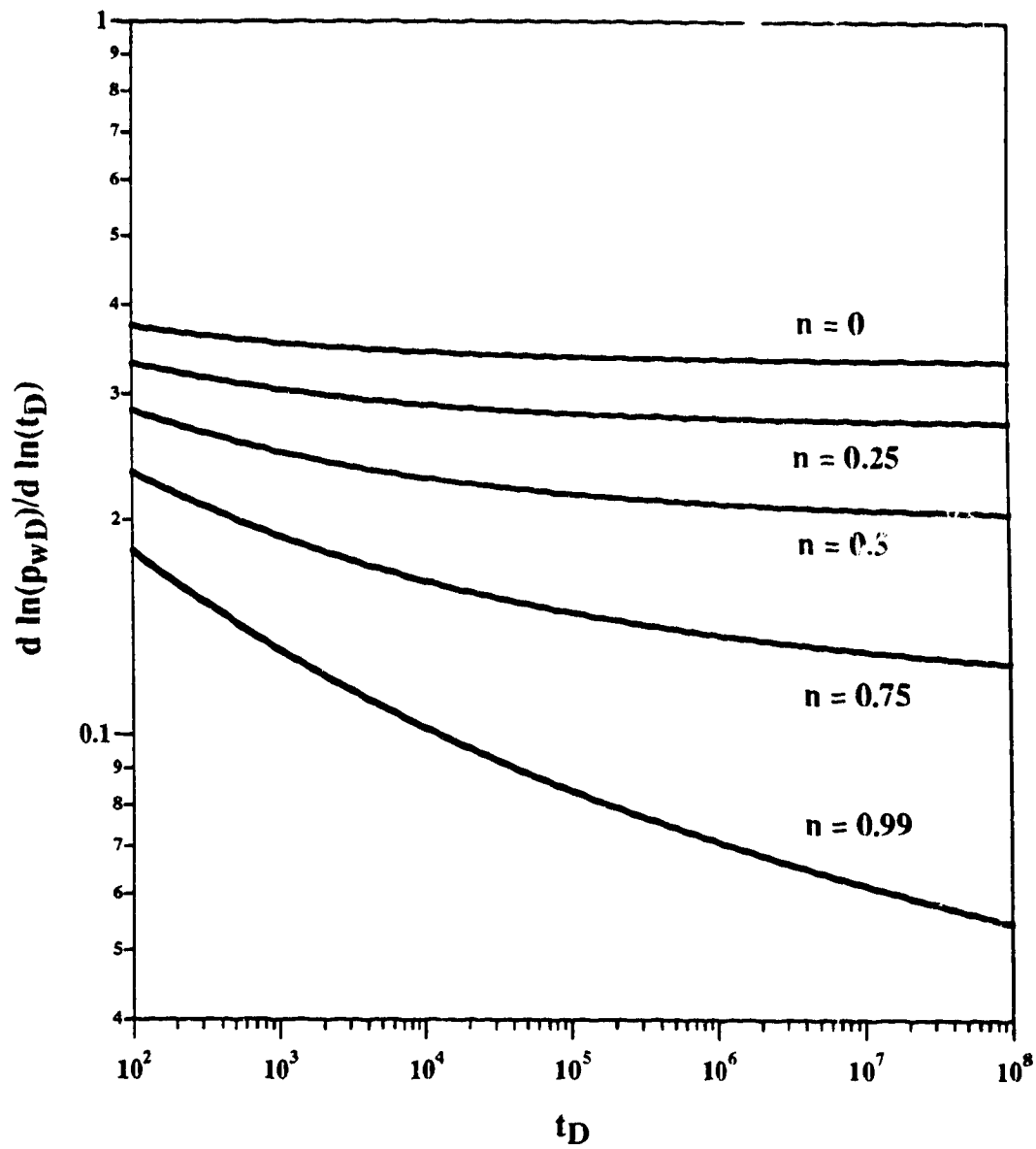


**Figure 10-4: Dimensionless Wellbore Pressure Derivative to Pressure Ratio versus Time for an Infinite System; Pseudoplastic Fluids,  $d_s = 2$**



derivative plots also equals  $v$ . In fact, the late-time value of the wellbore pressure-derivative function equals the product of the wellbore pressure function and the parameter  $v$ . And therefore, a plot of  $d\ln(p_{wD})/d\ln(t_D)$  against  $t_D$  would asymptotically tend to a constant value of  $v$  at late times (see Figure 10-4). An identical observation was also made in the study of Chang and Yortsos (1990) for the case of Newtonian fluid flow in a fractal object.

There are certain advantages in using the pressure derivative group,  $d\ln(p_{wD})/d\ln(t_D)$ , when constructing type curves for various flow situations (Duong, 1989). Duong has shown that by combining the pressure and pressure-derivative functions, a single set of type curves may be constructed by using the pressure/pressure-derivative ratio (*PDR*). By plotting dimensionless *PDR* (vertical axis) versus dimensionless time (horizontal axis), the vertical scales for both type-curve and field data are found to be identical. This alignment of the vertical scale constrains the type-curve match on the vertical axis. In this study, use is made of the dimensionless pressure-derivative/pressure ratio, which also serves the purpose of automatic alignment of one scale of the type curves and field data plots. This can be demonstrated by considering Equations (4-38) and (4-40) which can be rewritten, respectively, as

$$p_{wD} = a(p_i - p_{wf}) = a(\Delta p) \quad (10-1)$$

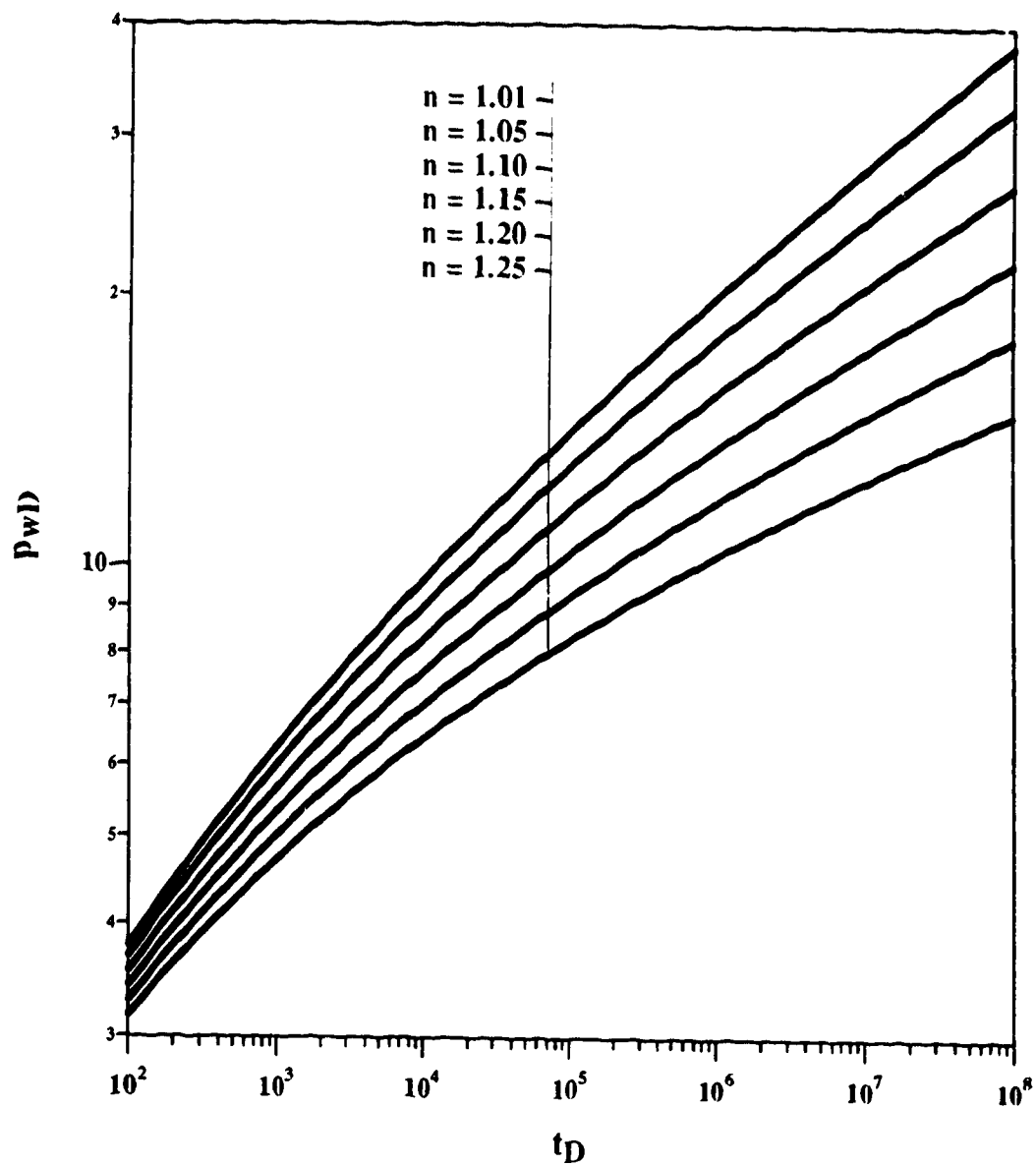
$$t_D = bt \quad (10-2)$$

where  $a$  and  $b$  are constants. The pressure-derivative, then, is given as

$$t_D p'_{wD} = at\Delta p', \quad (10-3)$$

and thus,

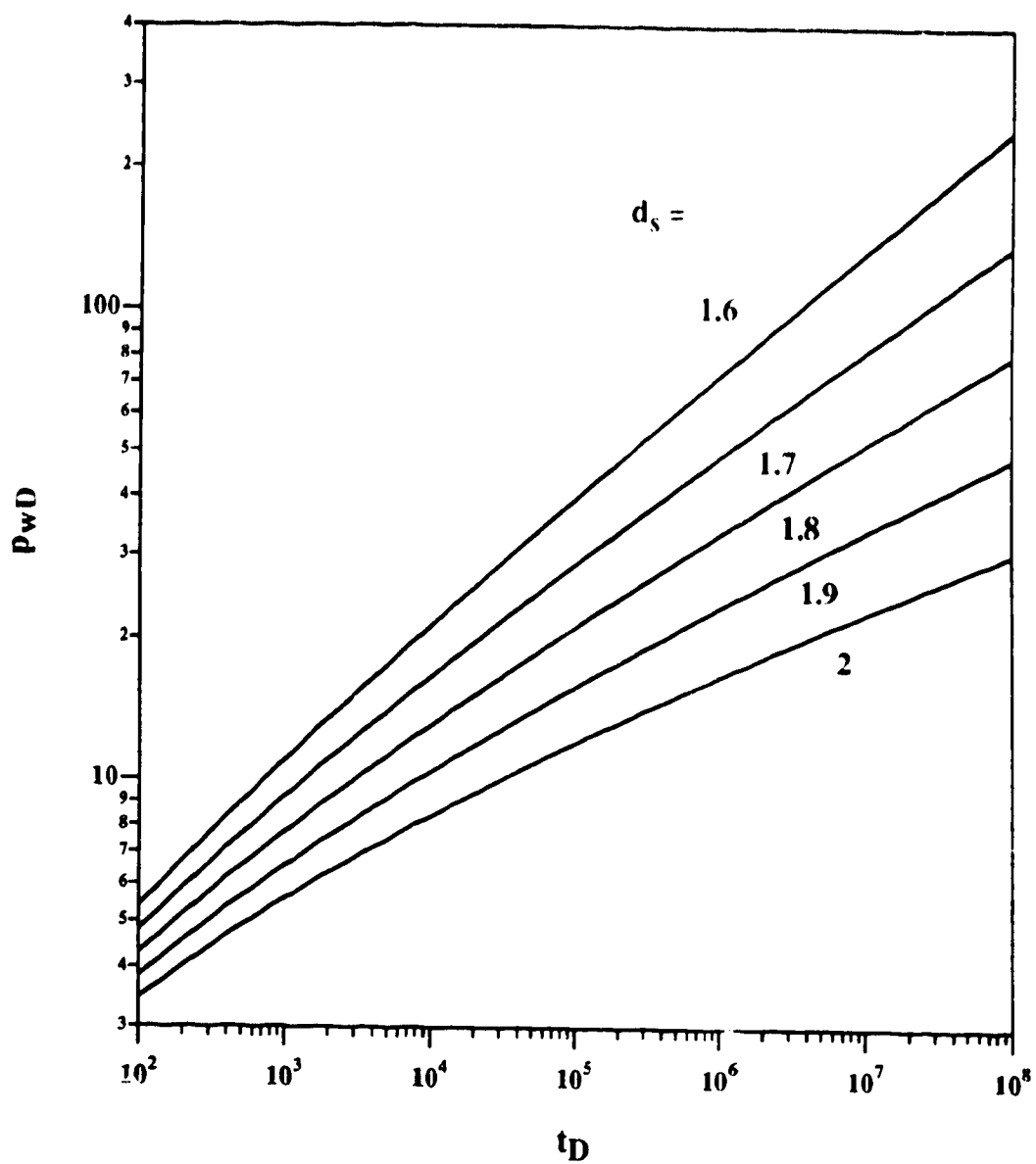
$$\frac{d\ln(p_{wD})}{d\ln(t_D)} = \frac{\Delta p' t}{\Delta p} \quad (10-4)$$



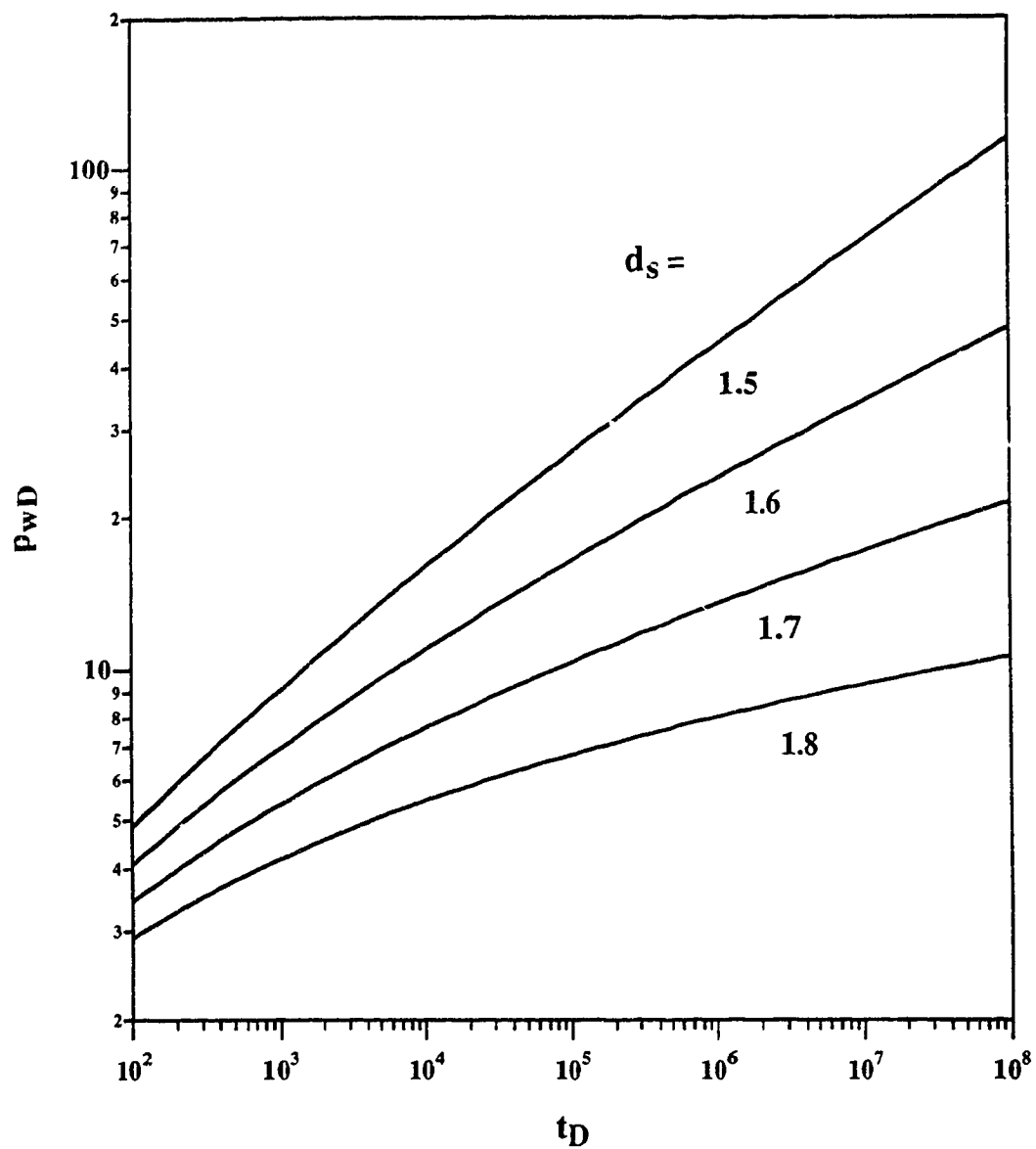
**Figure 10-5: Dimensionless Wellbore Pressure versus Time in an Infinite System; Dilatant Fluid,  $d_s = 1.75$**

Figure 10-5 demonstrates the transient wellbore pressure behaviour for different values of  $n$  (dilatant fluid) and for  $d_s = 1.75$ . Figure 10-5 shows that the dimensionless pressure decreases with increasing values of  $n$ , at any given time. Here also, the late-time linear behaviour in the log-log plot of  $p_{wD}$  versus  $t_D$  is apparent. Figures 10-6 and 10-7 demonstrate the variation of  $p_{wD}$  with time for various values  $d_s$  of and for  $n = 0.75$  and 1.25, respectively. These figures show, as was shown by the previous figures, that with increasing magnitudes of  $v$ , the dimensionless pressure drop at a given time, increases. For example, in Figure 10-6, the lowermost curve corresponds to  $v = 0.111$  and the uppermost curve to  $v = 0.256$ . Similarly, in Figure 10-7, the uppermost and the lowermost curves correspond to  $v = 0.2$  and 0, respectively.

In their groundbreaking study on mathematical modeling of single-phase transient flow of slightly compressible Newtonian fluids in fractal reservoirs, Chang and Yortsos (1990) have noted that with the sole exception of 2D cylindrical flow systems, the asymptotic pressure behaviour exhibited by any pressure-transient response model is of the power-law type  $p_{wD} \sim t_D^v$ . The Warren and Root (1963) type double-porosity system exhibits the well-known asymptotic behaviour given by  $p_{wD} \sim \ln t_D$ . On the other hand, the single-fracture pressure response, both at early (linear flow period) and later (bilinear flow period) times, shows behaviours consistent with the description of  $p_{wD} \sim t_D^v$ . The fractal reservoir model also exhibits such a linear behaviour in the late-time log-log plot of pressure versus time. It has been shown in the present study, as was demonstrated earlier by Ikoku and Ramey (1979), that the power-law description also applies for the case of non-Newtonian power-law fluid flow in a 2D cylindrical flow medium. For Newtonian flow in a fractal reservoir, the exponent  $v$  of the asymptotic pressure-time behaviour is only a function of the spectral dimension,  $d_s$ . For non-Newtonian flow in a homogeneous reservoir, the exponent is only a function of the flow behaviour index,  $n$ . And has been shown earlier, for non-Newtonian flow in a fractal reservoir, the exponent  $v$  depends on both  $n$  and  $d_s$ .



**Figure 10-6: Dimensionless Wellbore Pressure versus Time for an Infinite System with varying  $d_s$ ;  $n = 0.75$**



**Figure 10-7: Dimensionless Wellbore Pressure versus Time for the Flow of a Dilatant Fluid ( $n = 1.25$ ) in a Fractal Reservoir; Infinite System, Varying  $d_s$**

Figure 10-8 presents plots of pressure and pressure-derivative for two different cases of non-Newtonian fluid flow in a fractal medium. The upper pressure curve describes Newtonian flow in a fractal network and is characterized by a value of  $\nu$  of 0.125. The lower pressure curve describes non-Newtonian flow in a homogeneous medium and is defined by  $\nu = 0.111$ . The two lowermost curves in Figure 10-8 are the pressure-derivative plots and at late times, the parallel straight lines of pressure and pressure-derivative are separated by a distance equal to  $\log(1/\nu)$ .

It can be inferred also from Figure 10-8, and from the other results presented so far in this chapter, that the transient pressure behaviour of non-Newtonian flow in a homogeneous medium and that of Newtonian flow in a fractal medium are similar in many ways. Thus, an important question that may arise in the context of the present study is how to separate the individual characteristics of the non-Newtonian fluid and of the fractal medium when the complexities of both are present in the response of the flow system. In other words, how is it possible to determine both  $n$  and  $d_s$  from single-well test results if one can only calculate a value of the parameter  $\nu$  from the late-time pressure-time data? In order to find a possible solution to this question, one has to inspect the late-time behaviour of dimensionless rate for a constant-pressure wellbore condition.

It may be noted from Equations (5-30), (5-82) and (5-84) that the relationships between the constant rate solution ( $p_{wD}$ ) and the constant pressure solutions ( $q_D, Q_D$ ), in Laplace space, are given as

$$\bar{p}_{wD}(l, n, d_s) = \frac{l}{l^2 \bar{q}_D(l, n, d_s)} \quad (10-5)$$

and

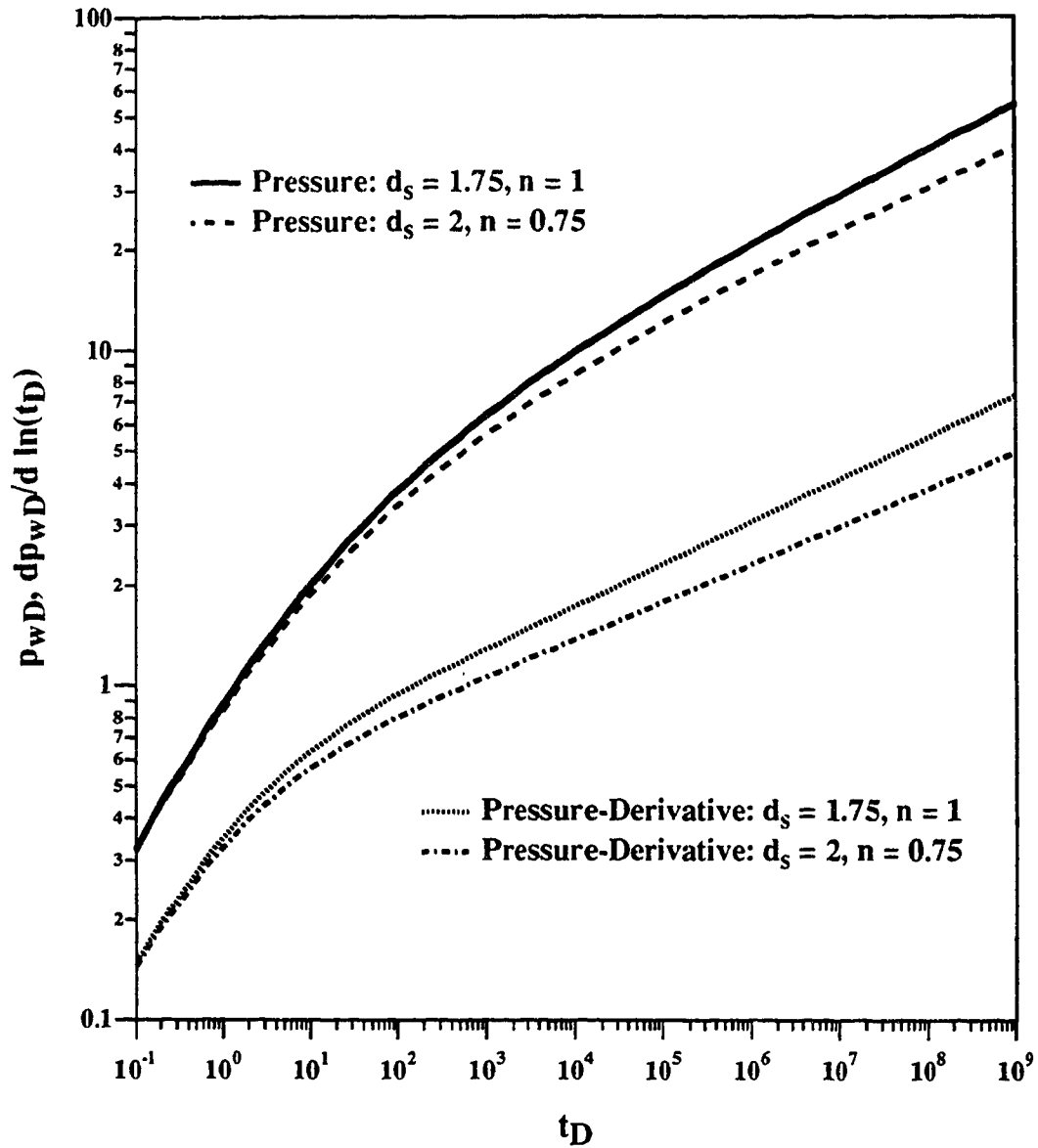


**Figure 10-8: Pressure and Pressure-Derivative Solutions for Two Different Cases**

$$\bar{p}_{wD}(l, n, d_s) = \frac{1}{l^3 \bar{Q}_D(l, n, d_s)} \quad (10-6)$$

It may be interesting to note that, for an infinite outer boundary condition, these relationships would also hold for other flow situations considered in this study (see, for example, Equations (8-40), (8-53) and (8-54) for the case of a composite system; also see Equations (9-31), (9-44) and (9-46) for flow in the fracture/matrix system). Identical observations were made also in the classical study of van Everdingen and Hurst (1949) for the case of transient flow in a homogeneous flow medium.

Figures 10-9 and 10-10 illustrate some transient dimensionless rate solutions. Equation (5-82) defines the dimensionless rate,  $q_D$ , in Laplace space for the transient flow of a non-Newtonian power-law fluid in an infinite fractal medium. Equation (5-82) has been inverted to real space numerically by using the Stehfest algorithm (1970) in order to generate data for Figures 10-9 and 10-10. Figures 10-9 and 10-10 show that at early times the dimensionless rate curves are merged together, as predicted by Equation (5-85). With increasing time, the curves start diverging from each other with the degree of divergence depending on the values of  $n$  and  $d_s$ . The value of dimensionless rate is higher at any given time for smaller magnitudes of  $\nu$ . For example, the uppermost curve in Figure 10-9 corresponds to  $\nu = 0.111$ , and the lowermost one to  $\nu = 0.294$ . Similarly, the uppermost curve in Figure 10-10 corresponds to  $\nu = 0.125$ , and the lowermost curve to  $\nu = 0.263$ . At late times, the rate solutions exhibit linear behaviour in the log-log plot, as predicted by Equation (5-87). Thus, if the late-time rate versus time data is available, then it is possible to calculate the slope of this linear segment. From (5-87), the magnitude of the slope, for a plot of dimensionless rate ( $q_D$ ) versus dimensionless time ( $t_D$ ), is given by  $\nu$ . However, by combining Equations (5-80) and (5-87) it is clear that, a late-time log-log plot of dimensional rate (i.e.,  $q$ ) versus dimensional time ( $t$ ) would be characterized by a straight



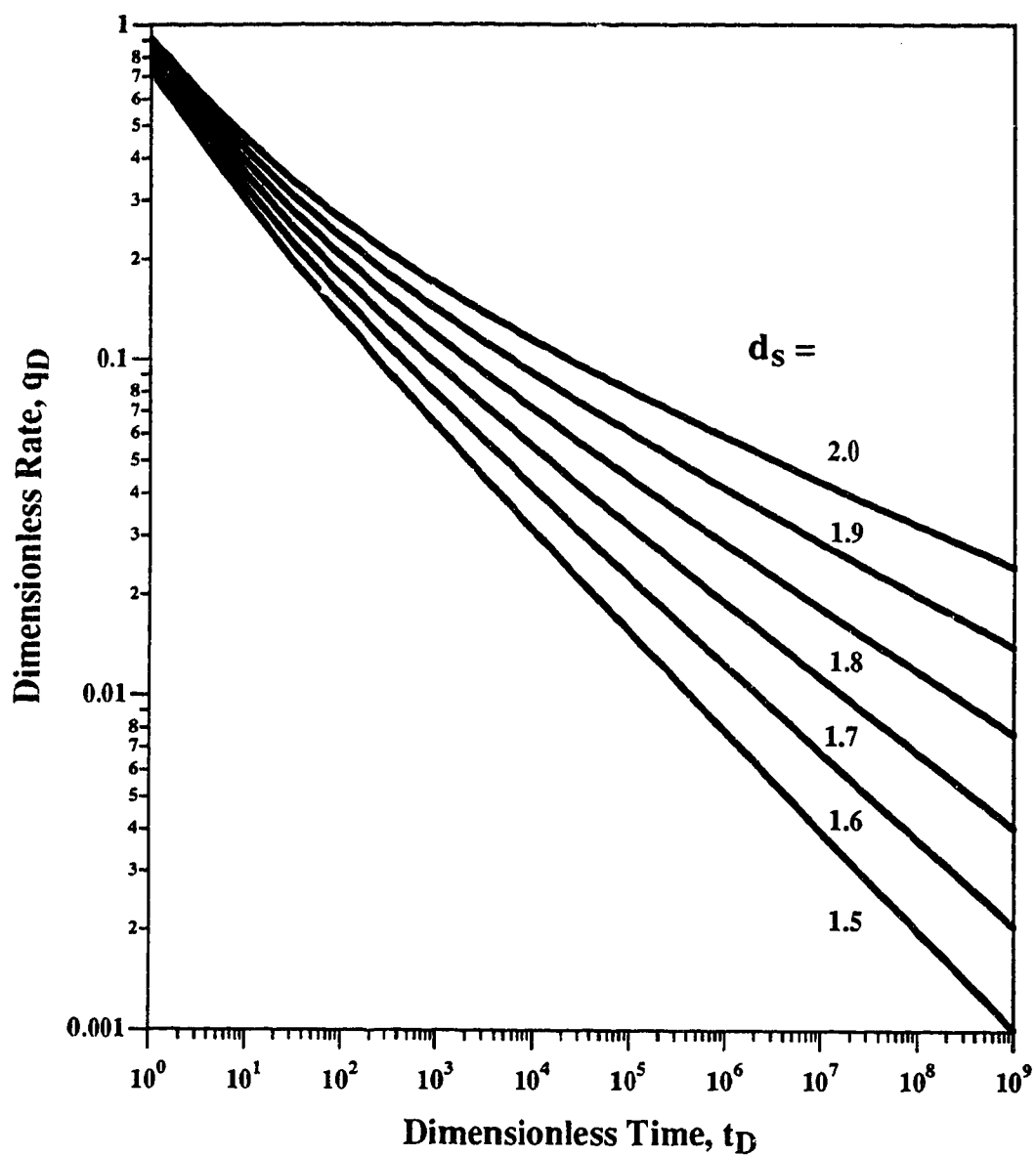


**Figure 10-9: Dimensionless Rate versus Time in an Infinite System;  $n = 0.75$**

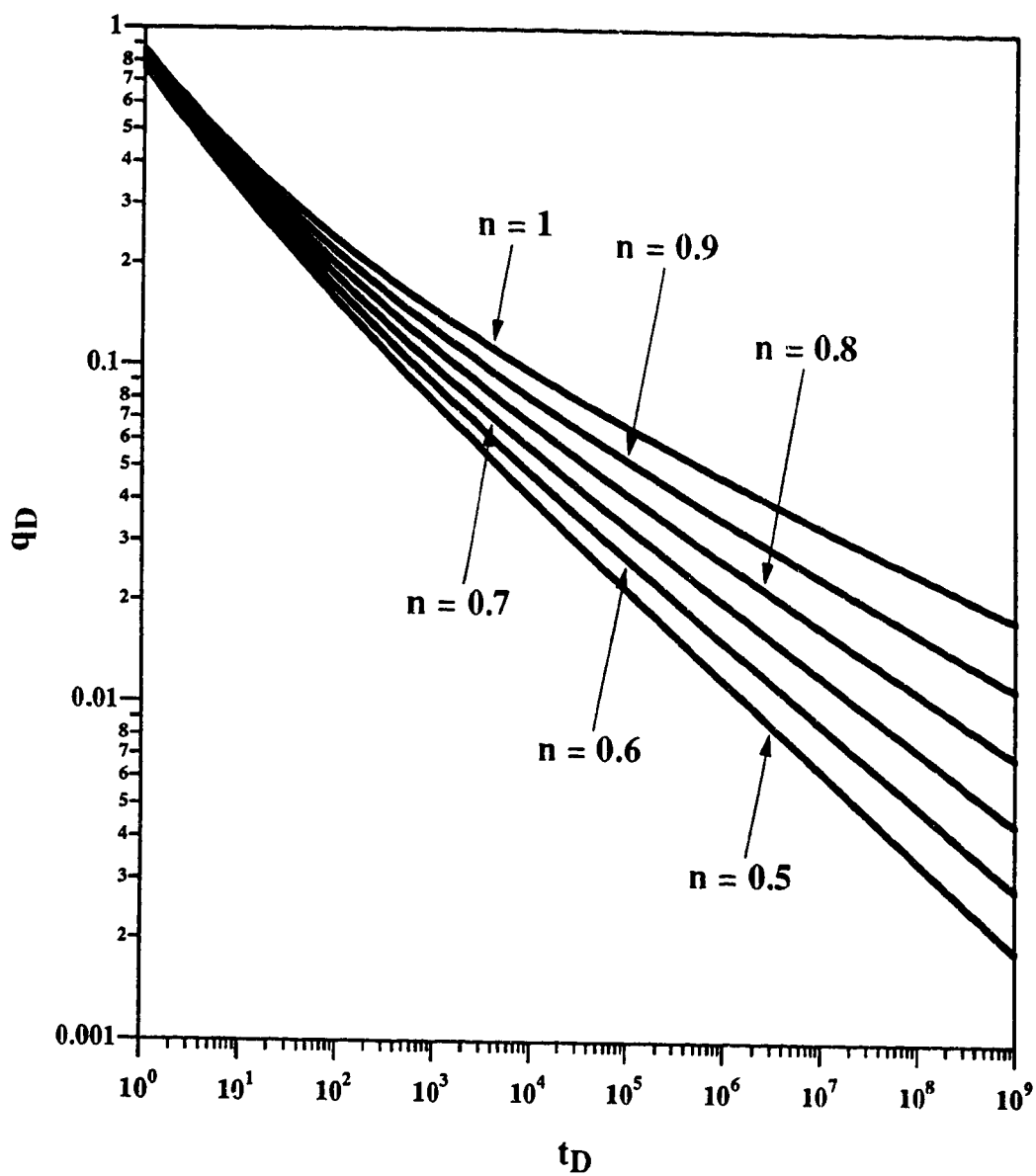


**Figure 10-10: Dimensionless Rate versus Time  
in an Infinite System;  $d_s = 1.75$**

line, the slope of which has a magnitude of  $v/n$ . Thus, it may be possible to calculate the values of both  $n$  and  $d_s$ , provided both late-time rate (in a constant-pressure situation) and pressure (in a constant-rate situation) data are available.

So far in the present chapter, various aspects of the late-time behaviour of transient pressure and rate solutions have been discussed. It has been demonstrated that, at relatively large times, the dimensionless wellbore pressure solution can be approximated by Equation (5-47). However, at fairly short times, the Laplace space wellbore pressure solution (given by Equation (5-30)) can be approximated very well by Equation (5-43), which is expressed in real space. In order to demonstrate the close approximation of Equation (5-30) by Equation (5-43), Figures 10-11 and 10-12, exhibiting comparisons of  $p_{wD}$  values calculated from these two equations, are presented. It is clear that there is good agreement between the two solutions for  $t_D$  greater than 100 and for  $v$  less than or equal to about 0.5. For larger values of  $v$ , the time when the two solutions match increases. It may be noted that a value of  $t_D > 100$  translates to real time of the order of a few minutes. Thus, for all practical purposes, the wellbore pressure solution can be represented by Equation (5-43), so long as the condition  $v \leq 0.5$  is met.

It is also of importance to be able to determine the times at the beginning of the log-log straight lines in the wellbore pressure versus time plots. Various types of correlations have been attempted in order to define the dimensionless time, at which the log-log straight lines appear, as a function of parameter  $v$  only. It has been found in this study that, in order to define a proper correlation of the said type, the dimensionless wellbore pressure and time should be redefined as follows:

$$p^* = p_{wD}(n+1 - nd_s) \quad (10-7)$$

$$t^* = t_D \{n+1 - (n-1)d_s\}^2 \quad (10-8)$$

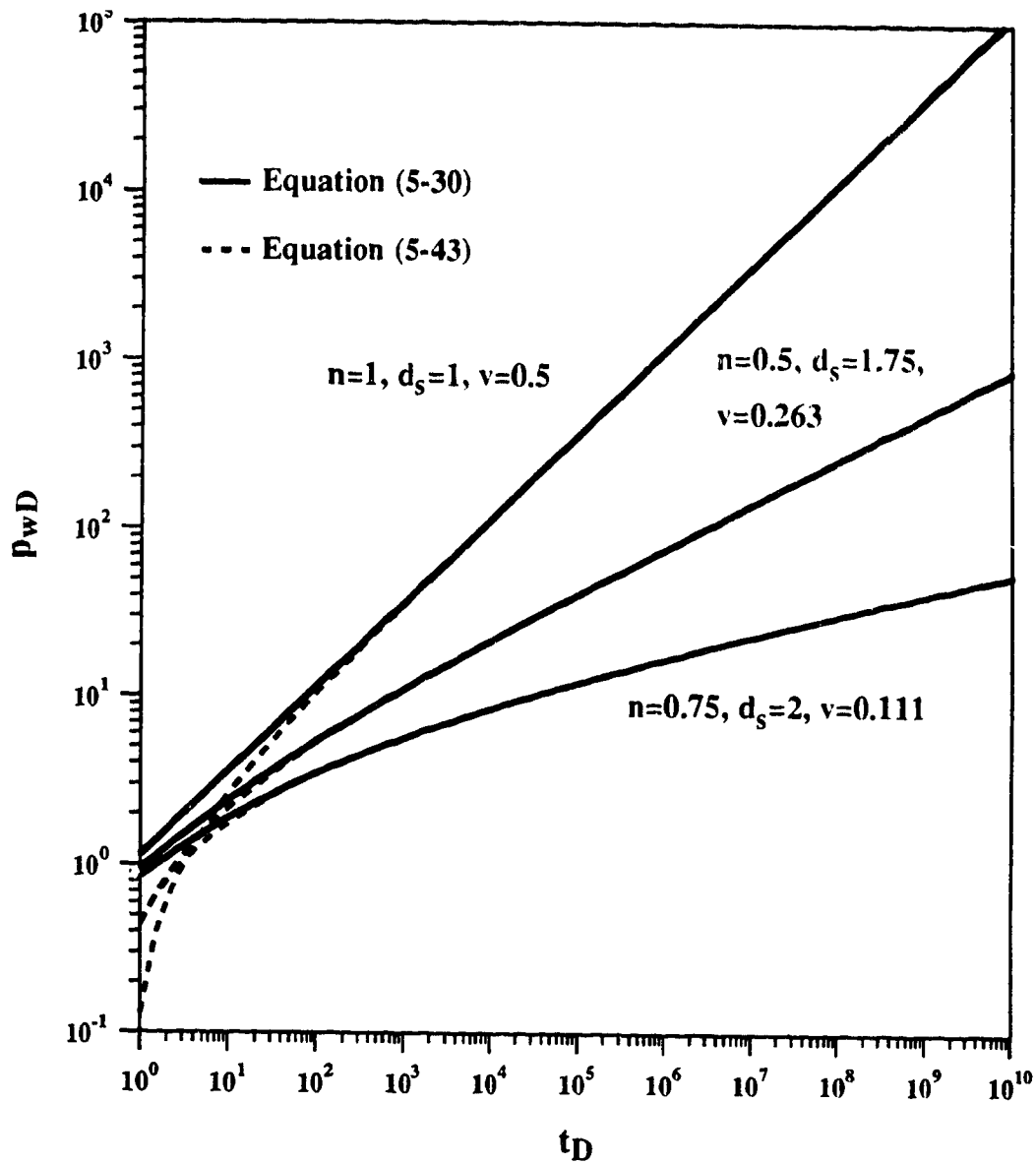


**Figure 10-11: Comparison of Wellbore Pressure Solutions Using Equations (5-30) and (5-43)**

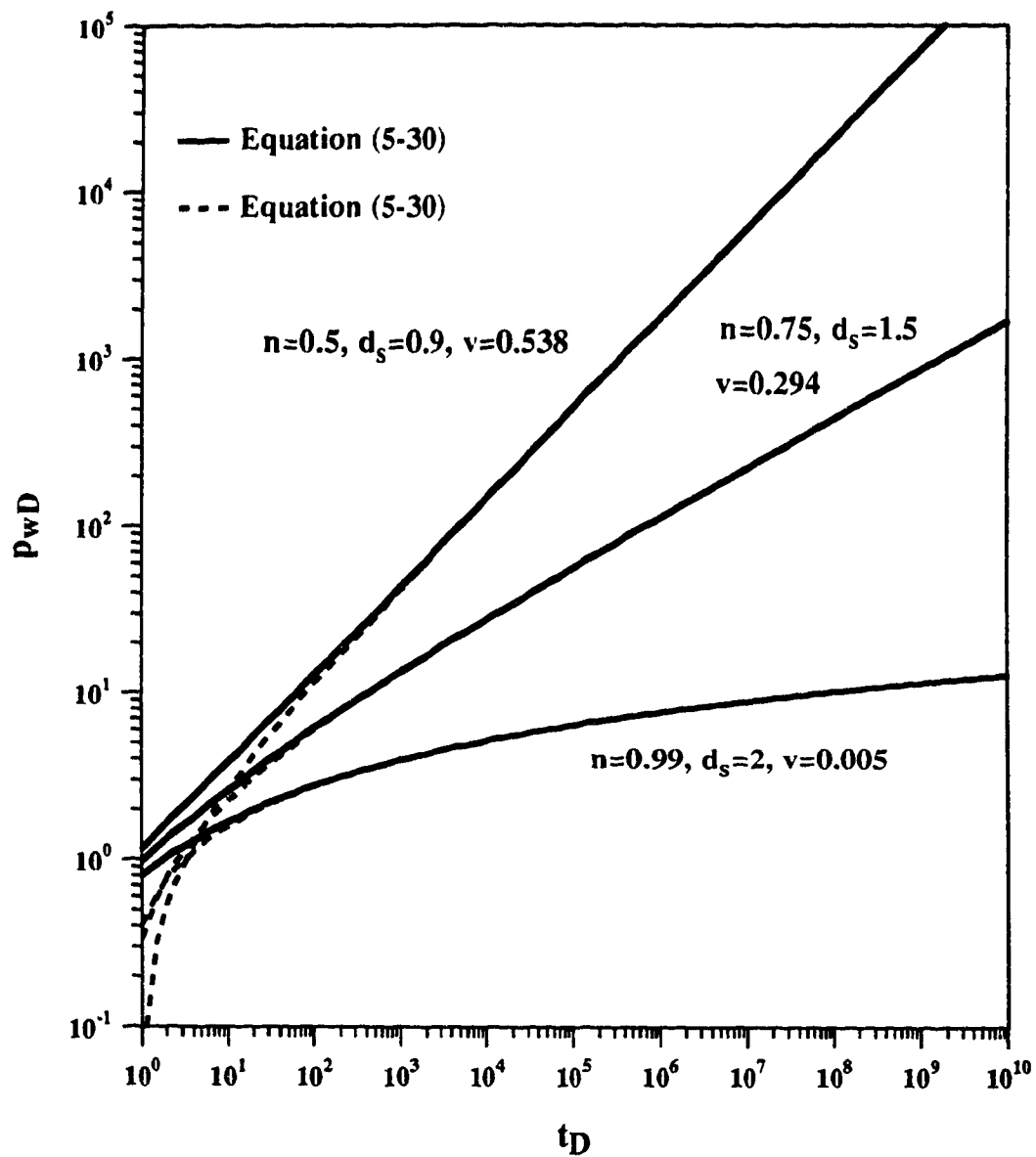


**Figure 10-12: Comparison of Wellbore Pressure Solutions Using Equations (5-30) and (5-43)**

Then the time ( $t^*$ ), at which the pressure solution ( $p^*$ ) is within 2% of the log-log straight line behaviour, may be expressed as a function of parameter  $\nu$ , as shown in Figure 10-13. It should be noted that the correlation exhibited in Figure 10-13 is valid only for pseudoplastic fluids and for  $1 < d_f \leq 2$ . An explanation for why Equations (10-7) and (10-8) should be used in order to obtain the shown correlation may also be given by examining the large-time approximation of the wellbore pressure solution (Equation (5-43)). From Equation (5-43) it is clear that, after relatively short times, the wellbore pressure solution may be expressed as

$$p^* = \frac{t^{*\nu}}{\Gamma(1-\nu)} - 1, \quad (10-9)$$

when the wellbore pressure and time are expressed by Equations (10-7) and (10-8), respectively.

#### 10.1.2 Comparison of Analytical and Numerical Solutions

In Chapter VI, a finite-difference scheme was presented for solution of the nonlinear form of the partial differential equation governing the transient flow of a non-Newtonian power-law fluid in a fractal reservoir. The main reason for attempting a numerical solution of the nonlinear partial differential equation, Equation (6-2), is to explore the consequences of the approximation given by Equation (4-29). This approximation resulted in the analytical solution for dimensionless wellbore pressure solution, given by Equation (5-30). The approximation introduced some incompressibility into the system (Ikoku, 1978; Ikoku and Ramey, 1982) and also removed the dependence of the analytical solution on the fractal dimension,  $d_f$ , which may result in an inaccurate theoretical prediction of the model behaviour. Thus, the effects of this approximation should be analyzed by a direct comparison of the analytical and numerical solutions for transient dimensionless wellbore pressure during the flow of a power-law fluid in a fractal medium.

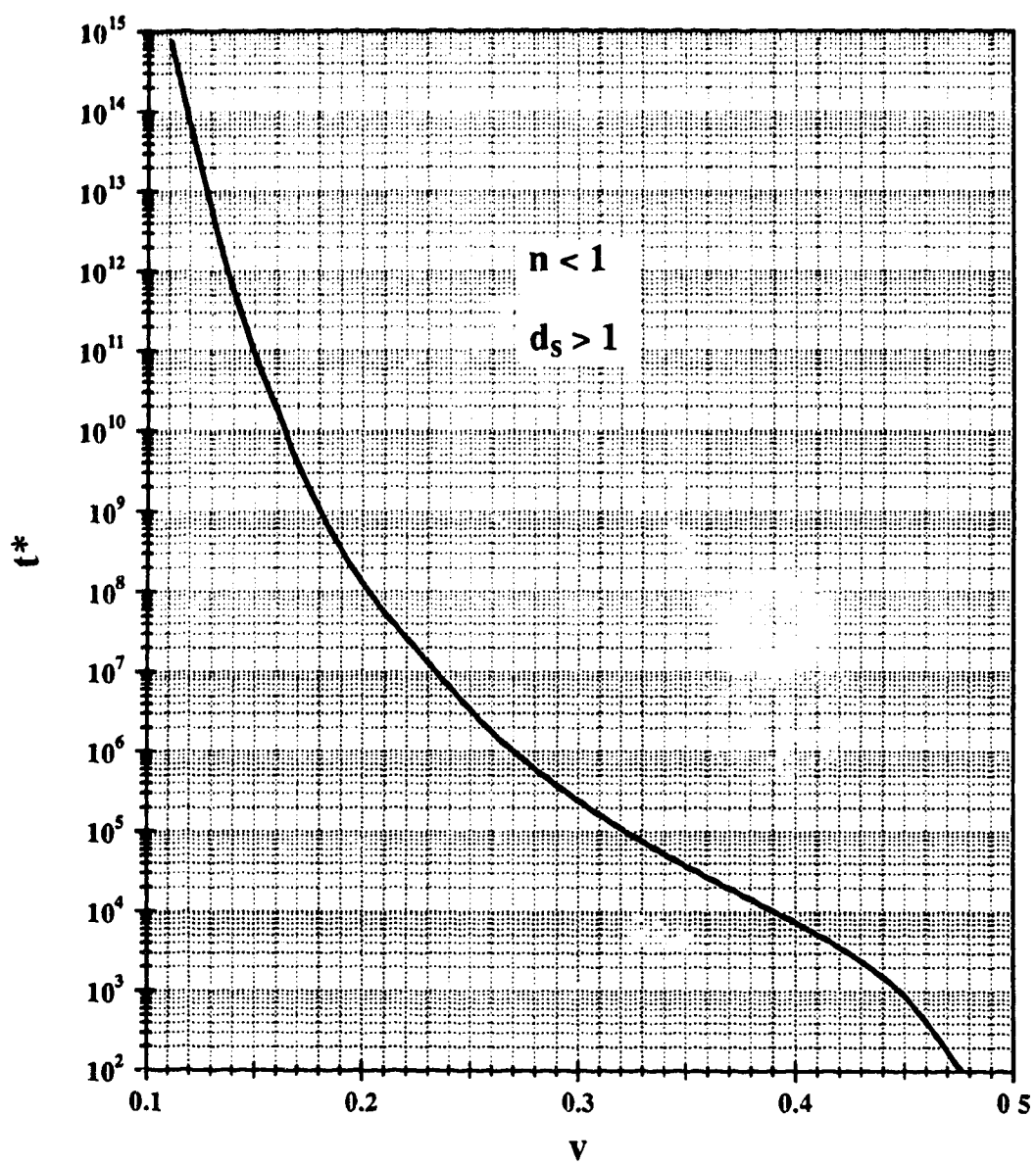
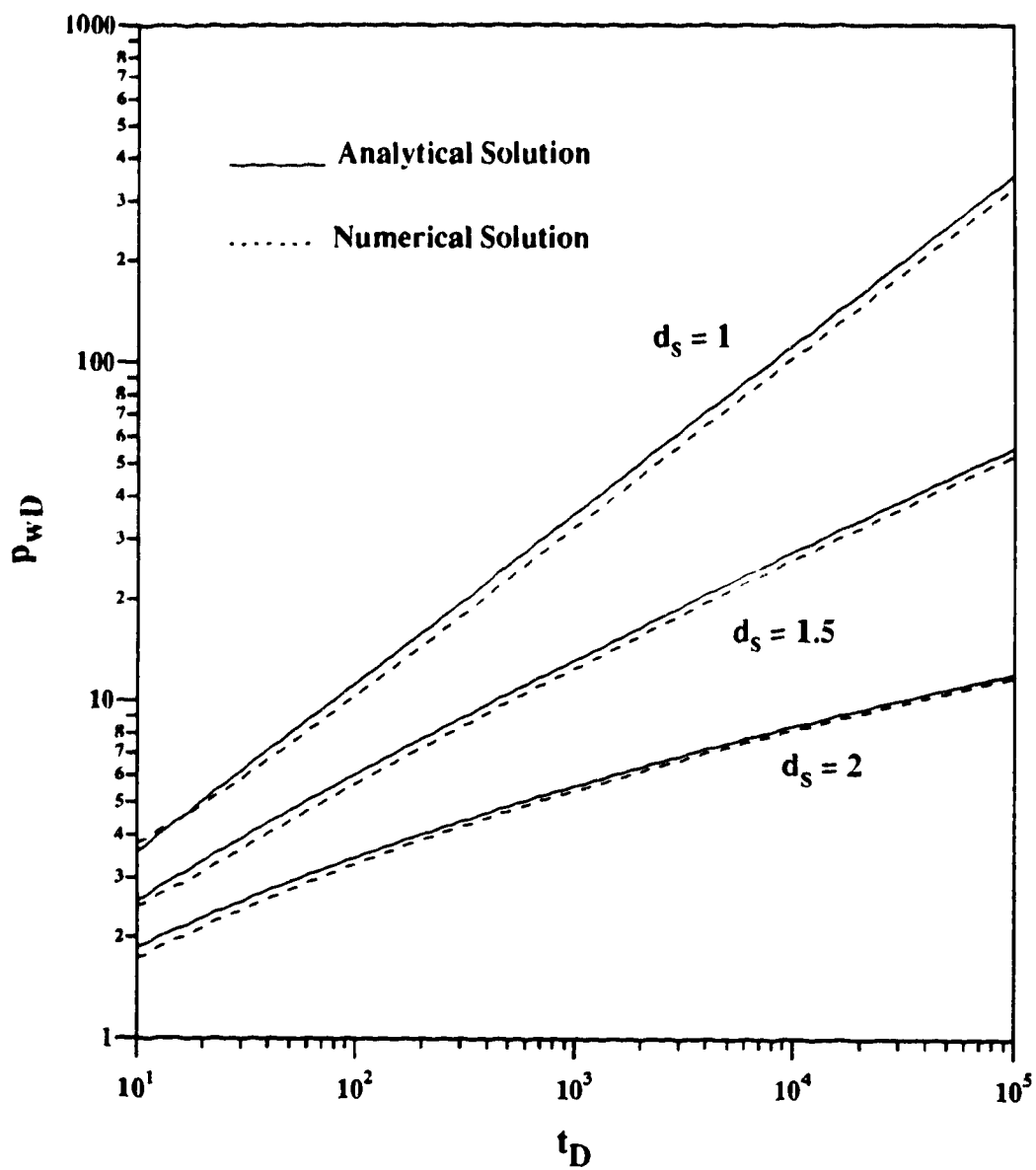


**Figure 10-13: Plot of Dimensionless Time at the Beginning of Log-Log Straight Line Against Parameter  $v$**

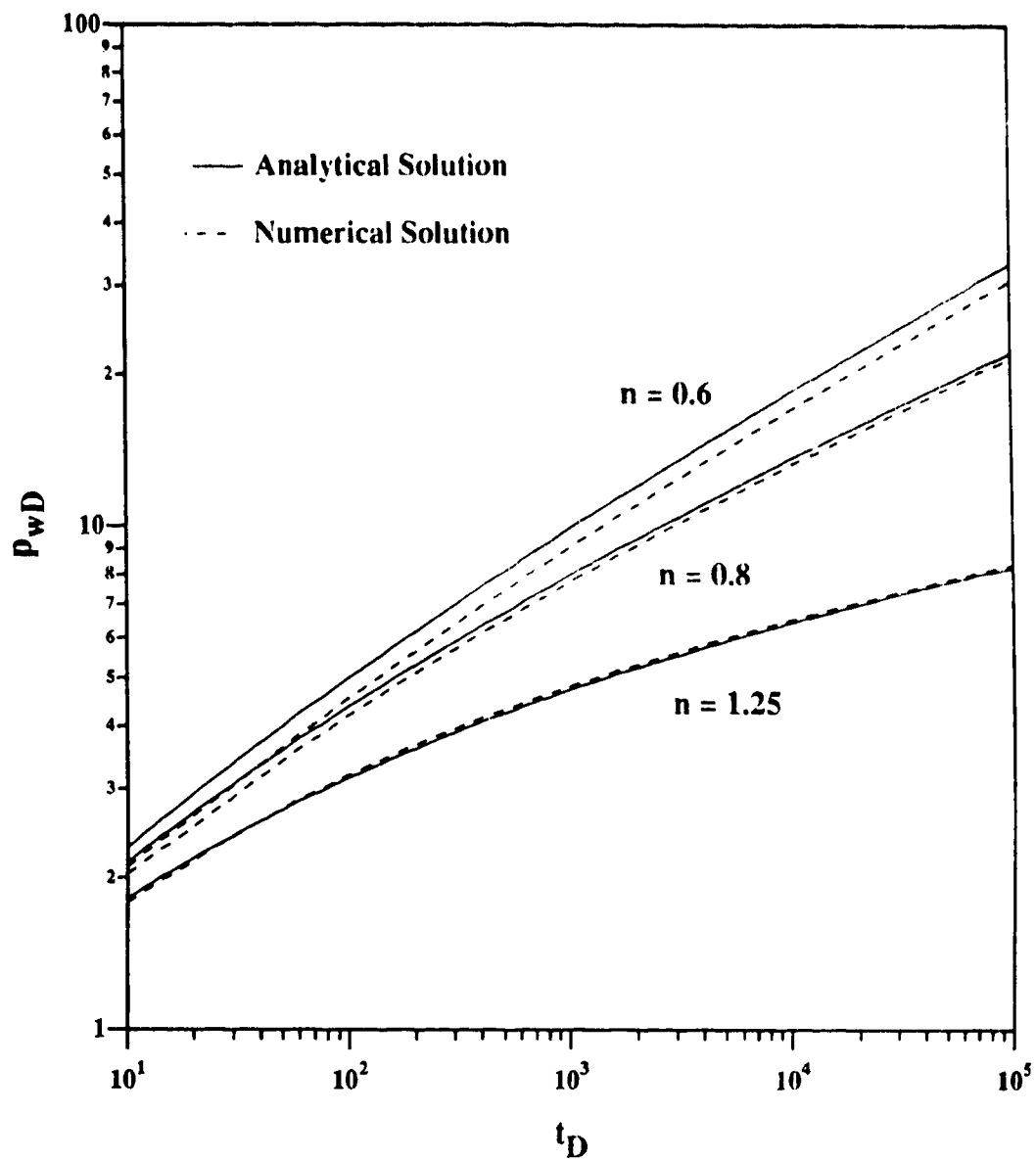
Attempts were made to solve Equation (6-2) for different values of the flow behaviour index,  $n$ , and the spectral dimension,  $d_s$ . The effect of the fractal dimension,  $d_f$ , on the numerical solutions was also studied. Numerical solutions could not be obtained for values of  $n$  smaller than 0.3 and values of  $d_s$  smaller than 1. In fact, the early-time numerical results for  $n$  values of 0.3 and 0.4 were not meaningful. The results presented in this section are based upon the following ranges of values of the parameters:  $0.5 \leq n < 1$ ,  $d_s \geq 1$  and  $1.75 \leq d_f \leq 2$ . For the numerical solutions, the spatial increment was maintained at  $\Delta x = 0.1$  and a time increment of 10 was taken between printed results.

Figure 10-14 presents a comparison of numerical and analytical solutions for  $n = 0.75$ ,  $d_f = 2$  and for three different values of  $d_s$ . The curves (from top to bottom) are characterized by  $d_s = 1, 1.5$  and  $2$ , which correspond to values of  $\nu = 0.5, 0.294$  and  $0.111$ , respectively. It is clear from these curves that, at large times, the difference between the analytical and numerical solutions is small. Moreover, the error in the analytical solution is seen to decrease, at any time, with an increasing magnitude of  $d_s$ . Figure 10-15 demonstrates the temporal variation of the difference between the analytical and numerical solutions with varying  $n$ . The values of  $d_f$  and  $d_s$  are 2 and 1.75, respectively, for all the curves displayed in Figure 10-15. The graphs (from top to bottom) are characterized by  $n = 0.6, 0.8$  and  $1.25$ , which correspond to values of  $\nu$  of 0.239, 0.186 and 0.034, respectively. Here also, as in Figure 10-14, the error in the analytical solution decreases gradually with increasing time. The analytical wellbore pressure solution, given by Equation (5-30) for an infinite system, does not show any dependence on  $d_f$ . In order to study the variation of  $p_{wD}$ , evaluated numerically, with  $d_f$ , Figure 10-16 is presented. The analytical solution for  $n = 0.5$  and  $d_s = 2$  is compared with three different numerical solutions defined also by  $d_f$  values of 2, 1.85 and 1.75. As Figure 10-16 shows, the three different numerical solutions can be distinguished in the log-log plot only upto a dimensionless time of about 50; beyond this





**Figure 10-14: Comparison of Analytical and Numerical Solutions for Dimensionless Wellbore Pressure Variation ( $n = 0.75$ ,  $d_f = 2$ )**



**Figure 10-15: Comparison of Analytical and Numerical Solutions for Dimensionless Wellbore Pressure Variation ( $d_f = 2$ ,  $d_s = 1.75$ )**

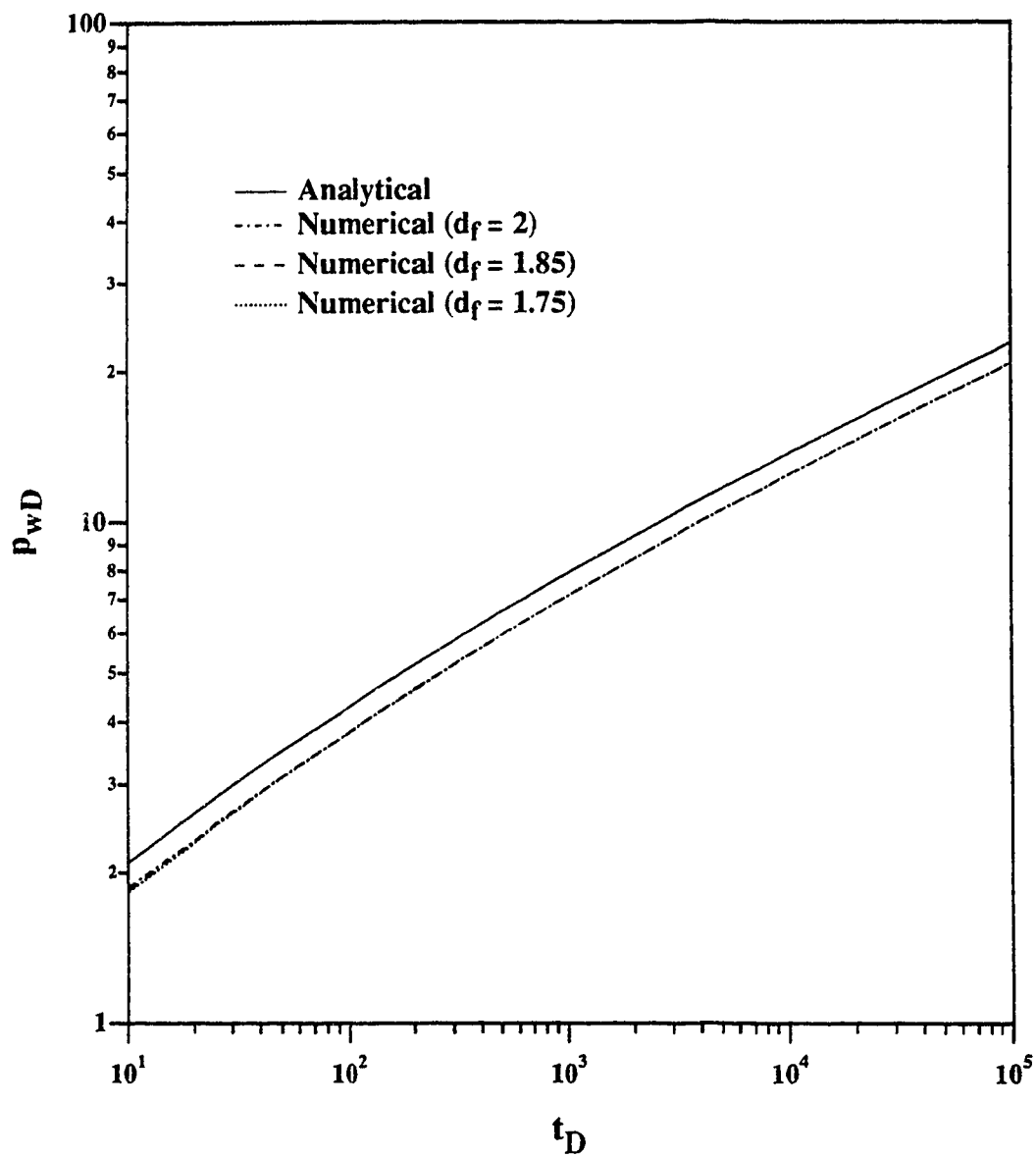


**Figure 10-16: Comparison of Analytical and Numerical Solutions for Dimensionless Wellbore Pressure Variation ( $n = 0.5$ ,  $d_s = 2$ )**

time, the numerical solutions appear as one curve, and the analytical and numerical solutions are more or less parallel to each other. Figure 10-17 presents two different sets of analytical and numerical solutions; as expected, the upper curve corresponds to a higher value of  $\nu$  ( $= 0.263$ ) and the lower one to a smaller value of  $\nu = 0.006$ . Here also, the difference between the analytical and numerical solutions is larger at smaller times and for larger values of  $\nu$ . Figure 10-18 presents another graph describing the effect of  $n$  on the difference between the two solutions. Here, the values of  $n$  were chosen such that they are fairly close to that for a Newtonian fluid; also,  $d_f = d_s = 2$ . Figure 10-18 clearly demonstrates that the difference between the analytical and numerical solutions is practically negligible for  $t_D > 100$  for both sets of solutions.

It may be observed, from Figures 10-14 through 10-18, that after large enough times ( $t_D > 200$ ), the numerical and analytical solutions appear to possess the same shape. Also, the difference between these two solutions generally seems to decrease with increasing times and decreasing magnitudes of the parameter  $\nu$ . The results from these graphs may be summarized by comparing the difference between the numerical and analytical solutions at  $t_D$  values of  $10^2$  and  $10^4$  for all the curves presented in Figures 10-14 through 10-18. Such a comparison is presented in Table 10-1, where the relative difference is defined as the ratio of the magnitude of the difference between the numerical and analytical solutions to the value given by the numerical solution. As Table 10-1 shows, for a pseudoplastic fluid the relative difference is small at large times, provided the magnitude of  $n$  is large (i.e., close to 1, the Newtonian limit). For example, for  $n = 0.5$  and  $d_f = d_s = 2$ , the relative difference is about 10% at  $t_D = 10^4$ . Keeping everything else the same, the relative difference is seen to be 3% for  $n = 0.75$  and  $< 1\%$  for  $n = 0.9$ . Also, for  $n > 1$ , the relative difference is observed to be small at large times, provided the magnitude of  $\nu$  is small. Again, the analytical solution appears to yield good results if  $d_s$  is large, every other parameter being the same. Finally, the large-time relative difference seems to be relatively insensitive to small variations in  $d_f$ , at

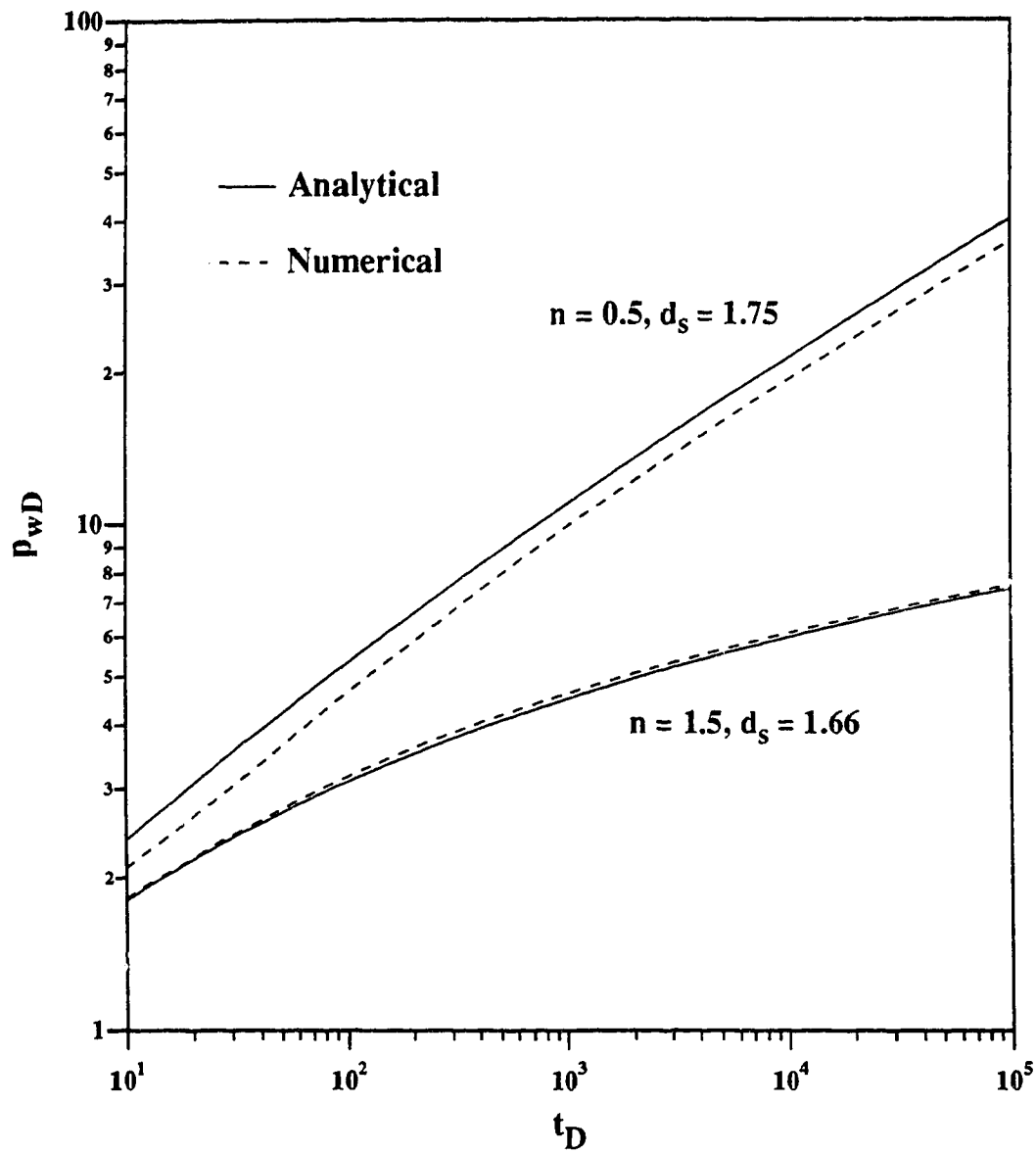


**Figure 10-17: Comparison of Analytical and Numerical Solutions for Dimensionless Wellbore Pressure Variation ( $d_f = 2$ )**

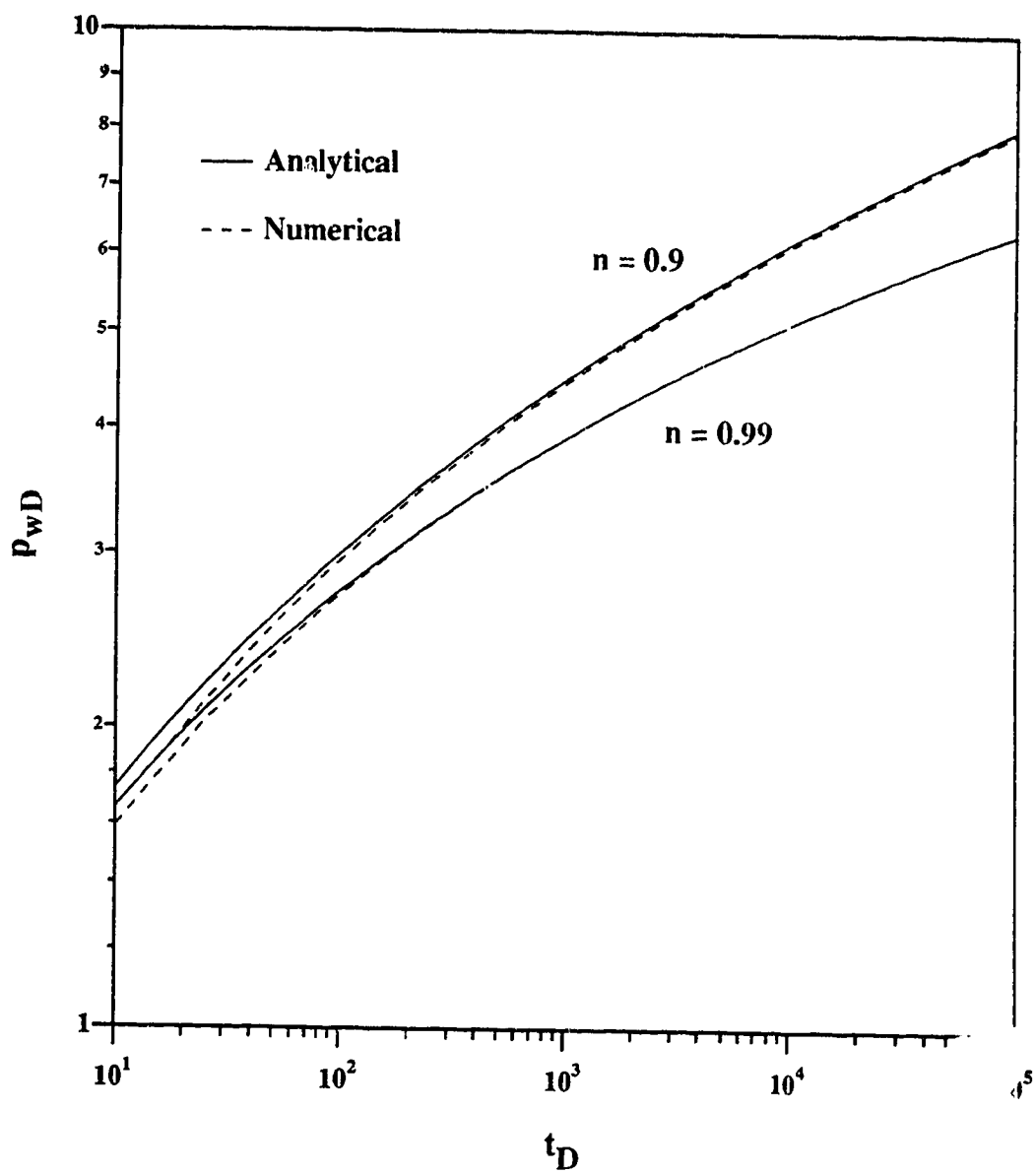


**Figure 10-18: Comparison of Analytical and Numerical Solutions for Dimensionless Wellbore Pressure Variation ( $d_f = d_s = 2$ )**

**Table 10-1: Comparison of Analytical and Numerical Solutions  
at Two Different Dimensionless Times**

n	$d_f$	$d_s$	$v$	Relative Difference, %, @	
				$t_D = 10^2$	$t_D = 10^4$
0.75	2.00	1.00	0.500	9	9
0.75	2.00	1.50	0.294	6	5
0.75	2.00	2.00	0.111	4	3
0.60	2.00	1.75	0.239	10	8
0.80	2.00	1.75	0.186	4	3
1.25	2.00	1.75	0.034	1	1
0.50	2.00	2.00	0.200	12	10
0.50	1.85	2.00	0.200	12	10
0.50	1.75	2.00	0.200	12	10
0.50	2.00	1.75	0.263	14	10
1.50	2.00	1.66	0.006	2	2
0.90	2.00	2.00	0.048	1	< 1
0.99	2.00	2.00	0.005	1	< .05

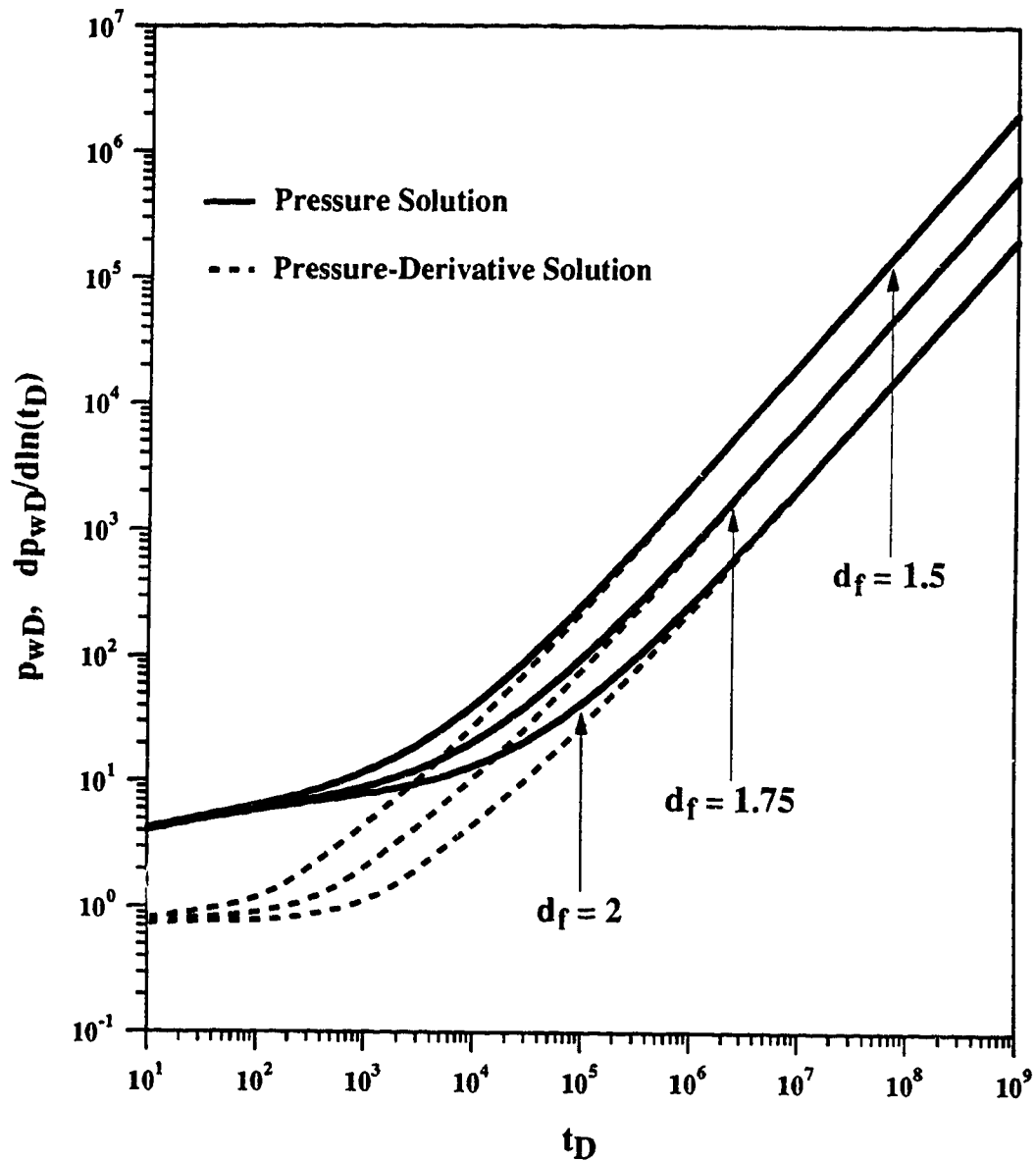
least within the range of values of the various parameters studied. Thus, so long as the magnitude of  $n$  is larger than 0.75, that of  $d_f$  is greater than 1.75 and that of  $d_s$  is larger than 1.50, the relative difference between the large-time analytical and numerical solutions would not be more than approximately 5%. More importantly, under these conditions, the relative difference between the slopes of the large-time analytical and numerical solutions would be even smaller.

### 10.1.3 Analytical Solutions: Finite Fractal Medium

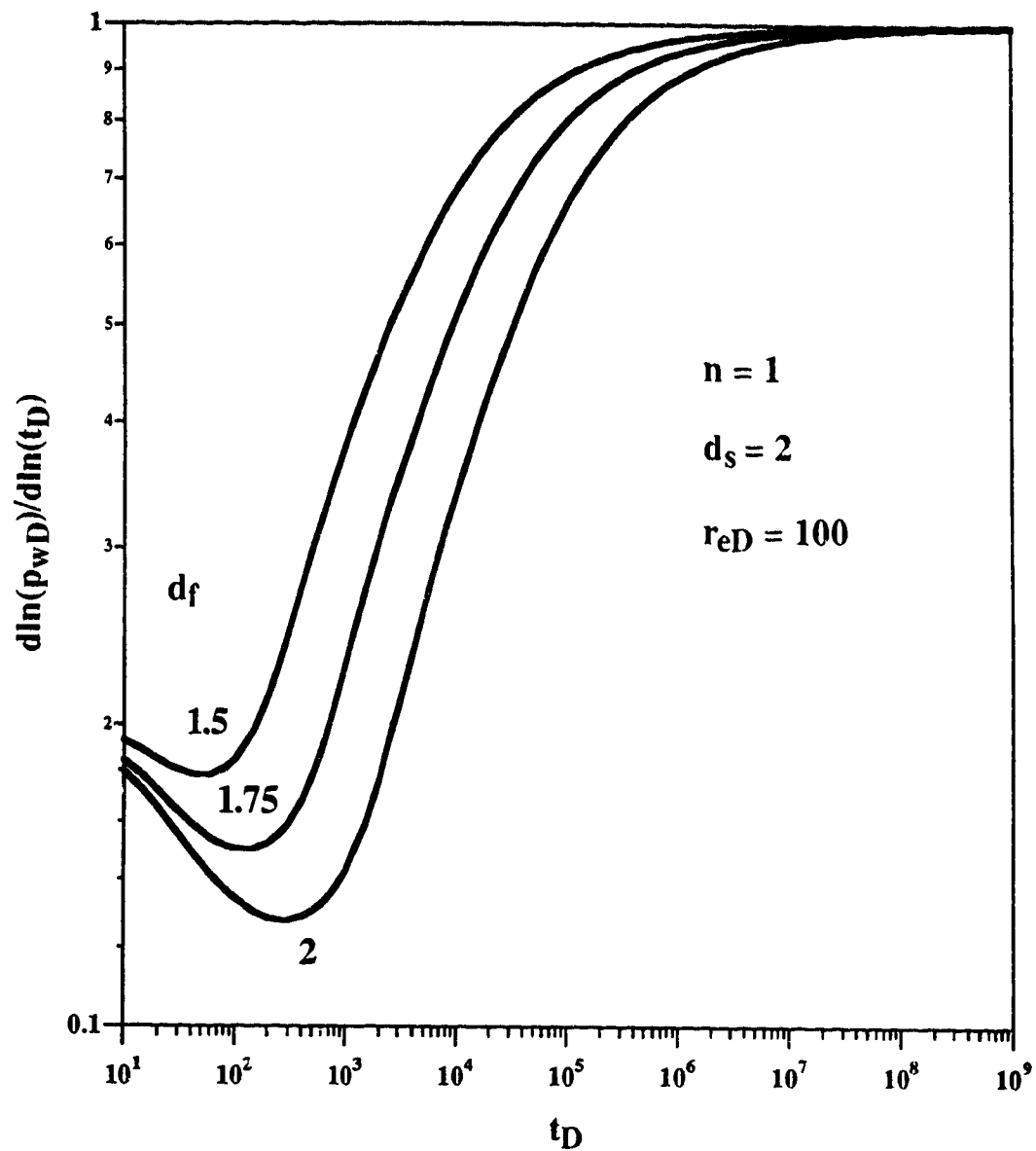
In this section, some of the results obtained for the case of a finite fractal flow medium are presented. Two different situations are considered here: the first case involves a bounded circular fractal reservoir with both closed and constant pressure outer boundaries, and the second case involves a two-zone composite reservoir situation with the inner zone being a fractal medium and the outer zone a homogeneous region. The results presented in this section pertain to a constant flow rate condition imposed at the wellbore.

Figure 10-19 is a graph of dimensionless pressure and pressure derivative for the case of a closed circular reservoir with  $n = 1$ ,  $d_s = 2$  and  $r_{eD} = 100$ . Three different plots of pressure and pressure derivative are displayed in Figure 10-19 for  $d_f = 1.5, 1.75$  and 2. The corresponding plots of  $d \ln(p_{wD})/d \ln(t_D)$  are displayed in Figure 10-20. Figure 10-19 shows that at early times, in the infinite-acting stage, the pressure behaviour is independent of  $d_f$ . With increasing time, the effect of the finite outer boundary is felt by the pressure transients; it is interesting to note that the smaller the value of  $d_f$ , the earlier is the time when the pressure transients respond to the boundary effects. A similar behaviour is also exhibited by the pressure derivative, which attains the same value as the pressure response at large times when pseudosteady-state is attained (as shown by the unit-slope line). This is also shown in the late-time behaviour of  $d \ln(p_{wD})/d \ln(t_D)$ .





**Figure 10-19: Plots of Pressure Drop and Pressure-Derivative for a Closed Circular System:  $n = 1$ ,  $d_s = 2$ ,  $r_{eD} = 100$**

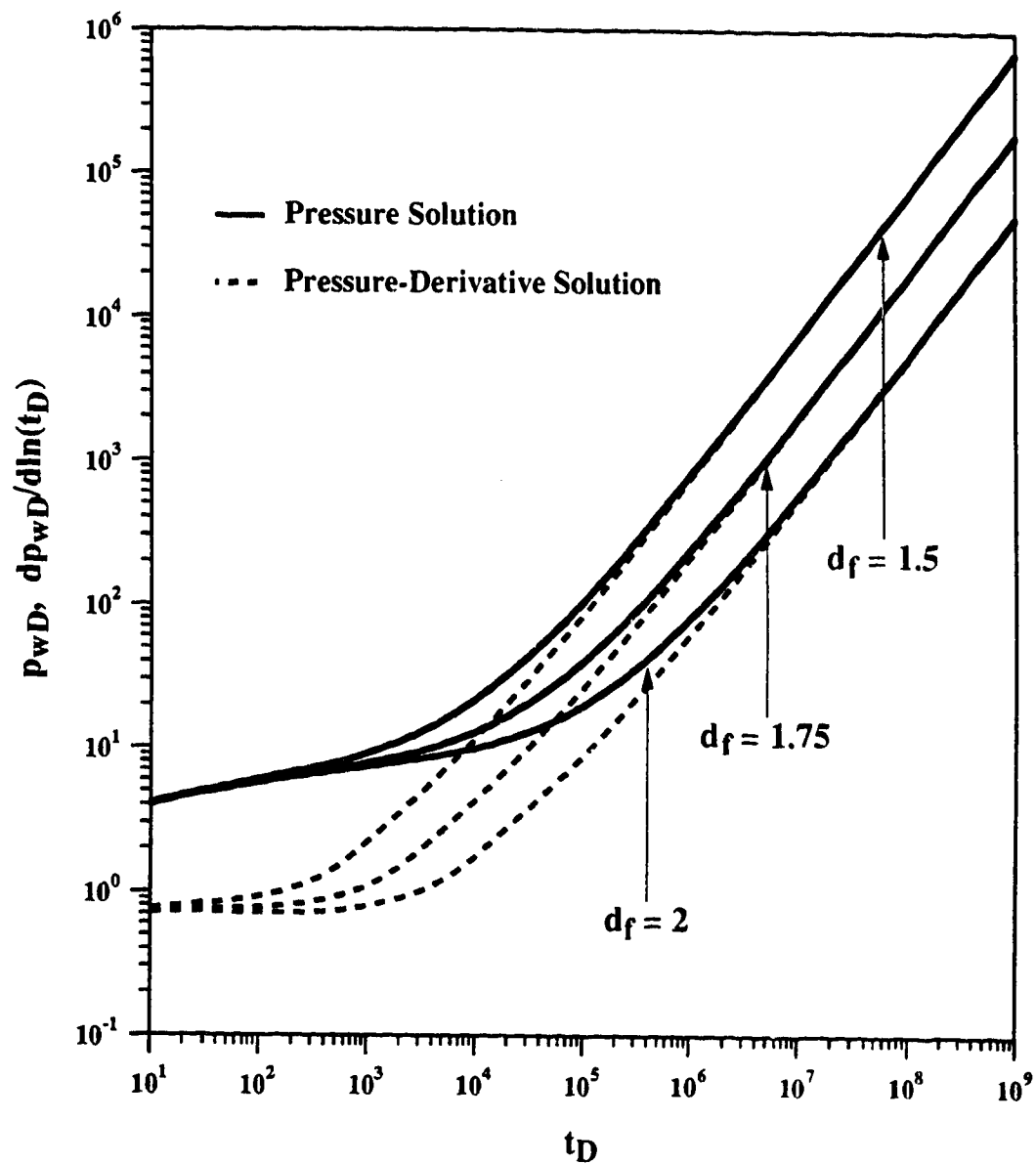


**Figure 10-20: Effect of  $d_f$  on  $d\ln(p_{wD})/d\ln(t_D)$  for a Closed Reservoir**

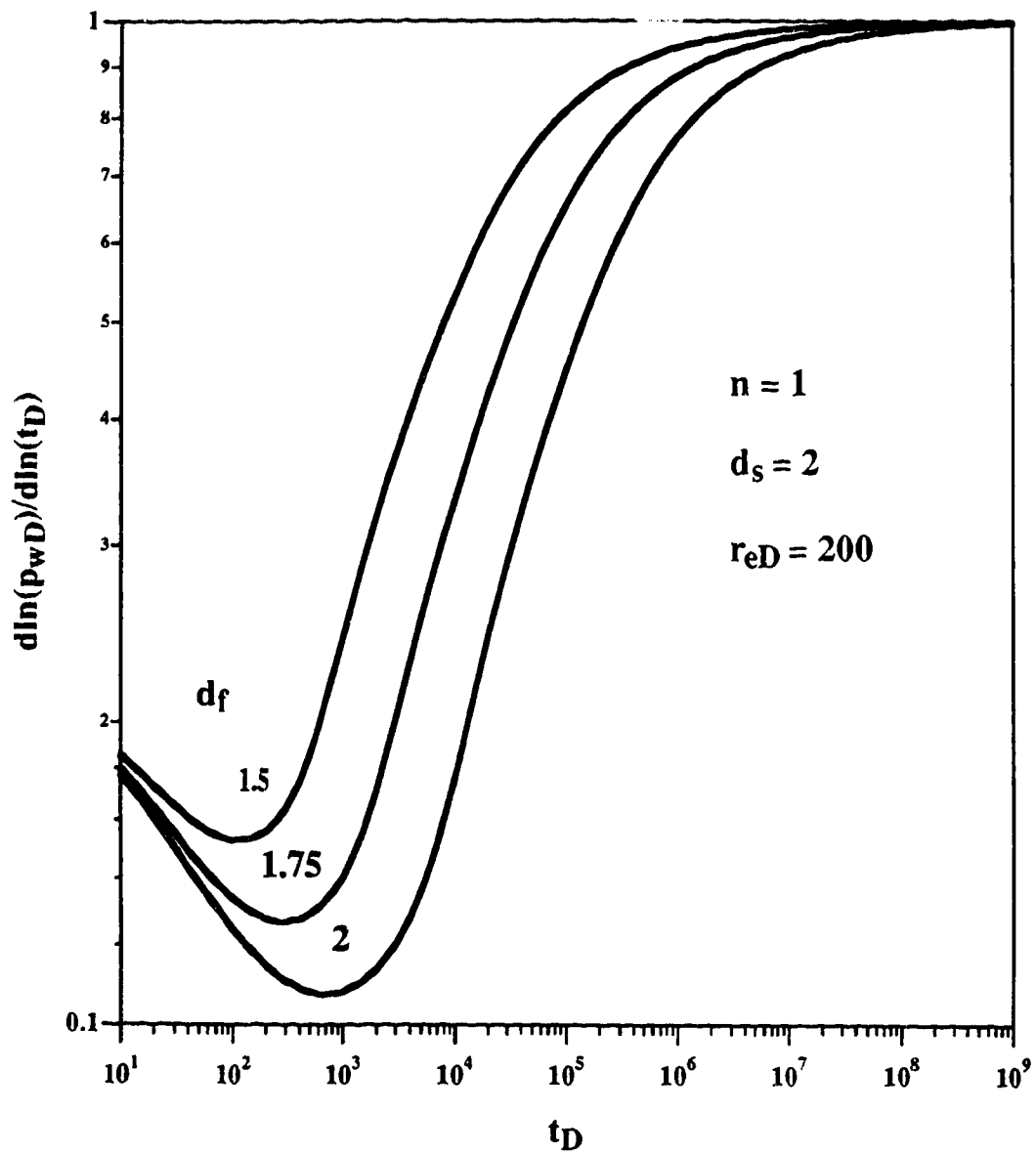
Figure 10-21 presents a graph of dimensionless pressure and pressure derivative for a closed reservoir with  $n = 1$ ,  $d_s = 2$  and  $r_{eD} = 200$ . Here also, the plots of pressure and pressure derivative are characterized by  $d_f$  values of 1.5, 1.75 and 2. The corresponding plots of  $d \ln(p_{wD})/d \ln(t_D)$  are shown in Figure 10-22. It may be seen from Figures 10-19 and 10-21 that the plots of pressure and pressure derivative for  $d_f = 2$  and  $r_{eD} = 100$  and those for  $d_f = 1.75$  and  $r_{eD} = 200$  are almost identical. In other words, for  $d_f < 2$ , the pressure response of the system may be misinterpreted to represent a smaller reservoir size if one assumes  $d_f$  to be equal to 2.

Figure 10-23 presents plots of pressure, pressure derivative and  $d \ln(p_{wD})/d \ln(t_D)$  solutions for a constant pressure outer boundary condition. The plots correspond to  $n = 1$ ,  $d_s = 2$  and  $r_{eD} = 200$  and  $d_f = 1.5, 1.75$  and 2. Here, at large times ( $t_D > 10^5$ ), the effect of  $d_f$  on the pressure response is similar as in the case of a closed reservoir. For the same value of  $r_{eD}$ , the large-time pressure solution is smaller for a smaller value of  $d_f$ . This may result in an underestimation of reservoir size if one assumes  $d_f = 2$ , when in reality  $d_f$  is less than 2. The large-time difference between the three plots is displayed more clearly by the pressure derivative plots which, however, show the same general trend of a sharp decrease with increasing time due to the gradual attainment of steady-state.

In the present study, the wellbore pressure solutions for the case of a composite reservoir will be displayed mainly by the pressure derivative response of the system. Because of its detail-enhancement capabilities, the pressure derivative has been used to a large extent in recent studies to analyze the behaviour of composite reservoirs of various geometries (Ambastha and Ramey, 1989; Stanislav et al., 1992). The results presented in this section are directed at studying the sensitivity of the response of the system to



**Figure 10-21: Plots of Pressure Drop and Pressure-Derivative for a Closed Reservoir:  $n = 1$ ,  $d_s = 2$ ,  $r_{eD} = 200$**



**Figure 10-22: Effect of  $d_f$  on  $\frac{d\ln(p_{wD})}{d\ln(t_D)}$  for a Closed Circular Reservoir**

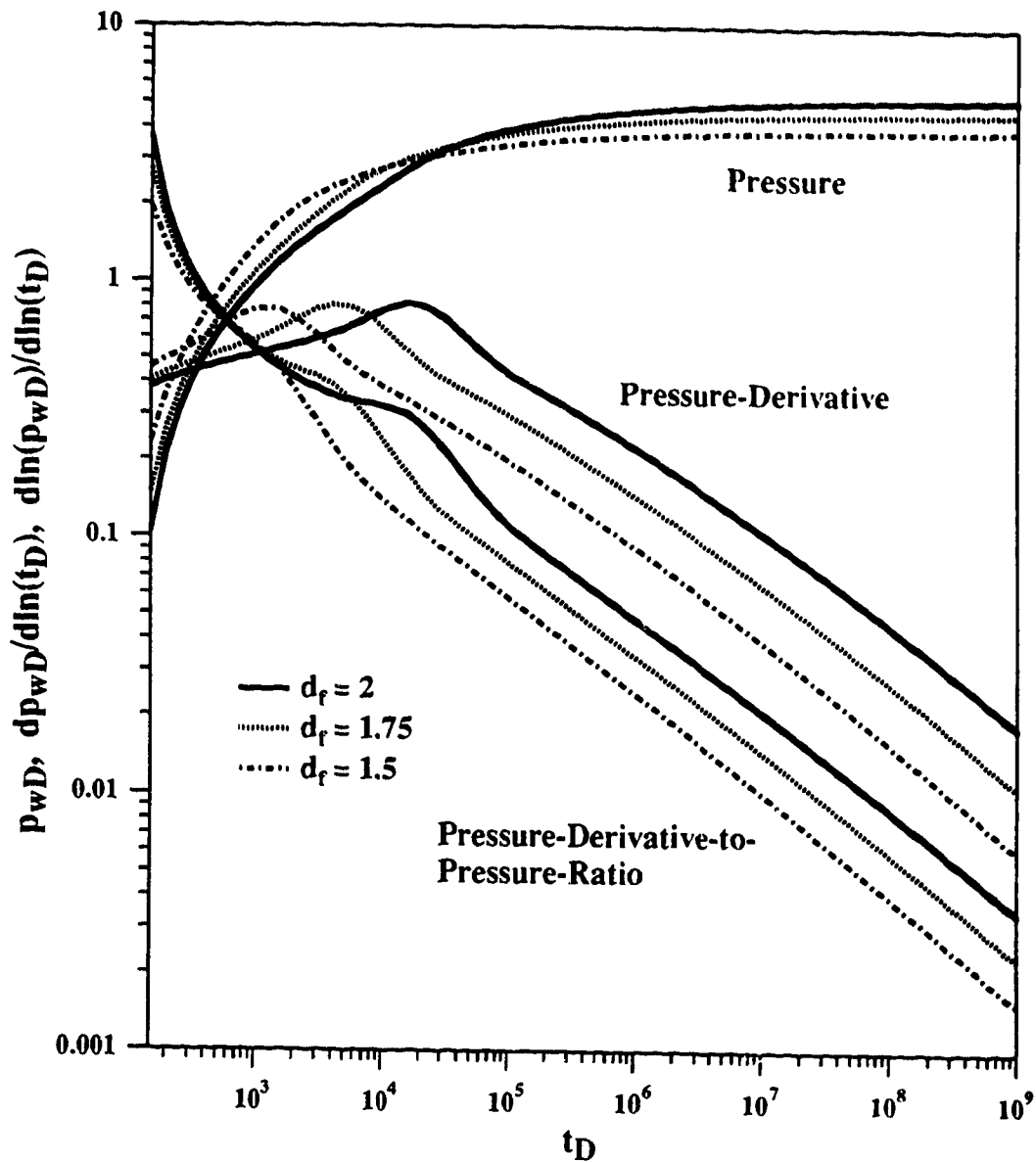


**Figure 10-23: Effect of  $d_f$  on the Pressure Behaviour of a Circular Reservoir with Constant Pressure Outer Boundary:  $n = 1$ ,  $d_s = 2$ ,  $r_{eD} = 200$**

parameters such as the dimensionless size of the inner region ( $a$ ), the permeability ratio ( $k_w/k'$ ), ratio of permeability-to-porosity-ratio ( $F = \frac{k_w/\phi_w}{k'/\phi'}$ ),  $d_f$ , and  $d_s$ .

The variation of dimensionless wellbore pressure with time is shown in Figure 10-24 for a two-zone composite system. The log-log plot is generated to illustrate the effects of permeability ratio and parameter  $F$  on the system response. Figure 10-24 shows that for a fixed value of permeability ratio, dimensionless pressure is higher at any time for higher values of the porosity ratio ( $\phi_w/\phi'$ ), even though the plots have similar shapes at relatively large times. Furthermore, for a fixed value of porosity ratio, the dimensionless pressure is significantly higher for higher values of the permeability ratio. The effects of permeability ratio and  $F$  on the system behaviour may be better illustrated by the derivative response, as shown in Figure 10-25. The following is apparent from Figure 10-25:

i) After the inner region flow is terminated, transitional flow occurs when the derivative goes through a maximum corresponding to the values of permeability ratio and  $F$ ; subsequently, the derivative declines and, at late times, it demonstrates the constant behaviour characteristic of an infinite homogeneous medium.

ii) The permeability ratio has a strong impact on the time when the maximum in the derivative occurs and also on the magnitude of the maximum derivative.

iii) The transition period seems to end sooner for the low permeability ratio case.

iv) The parameter  $F$  has a mild influence on when the maximum in the derivative occurs, but has a stronger influence on the value of the maximum derivative.

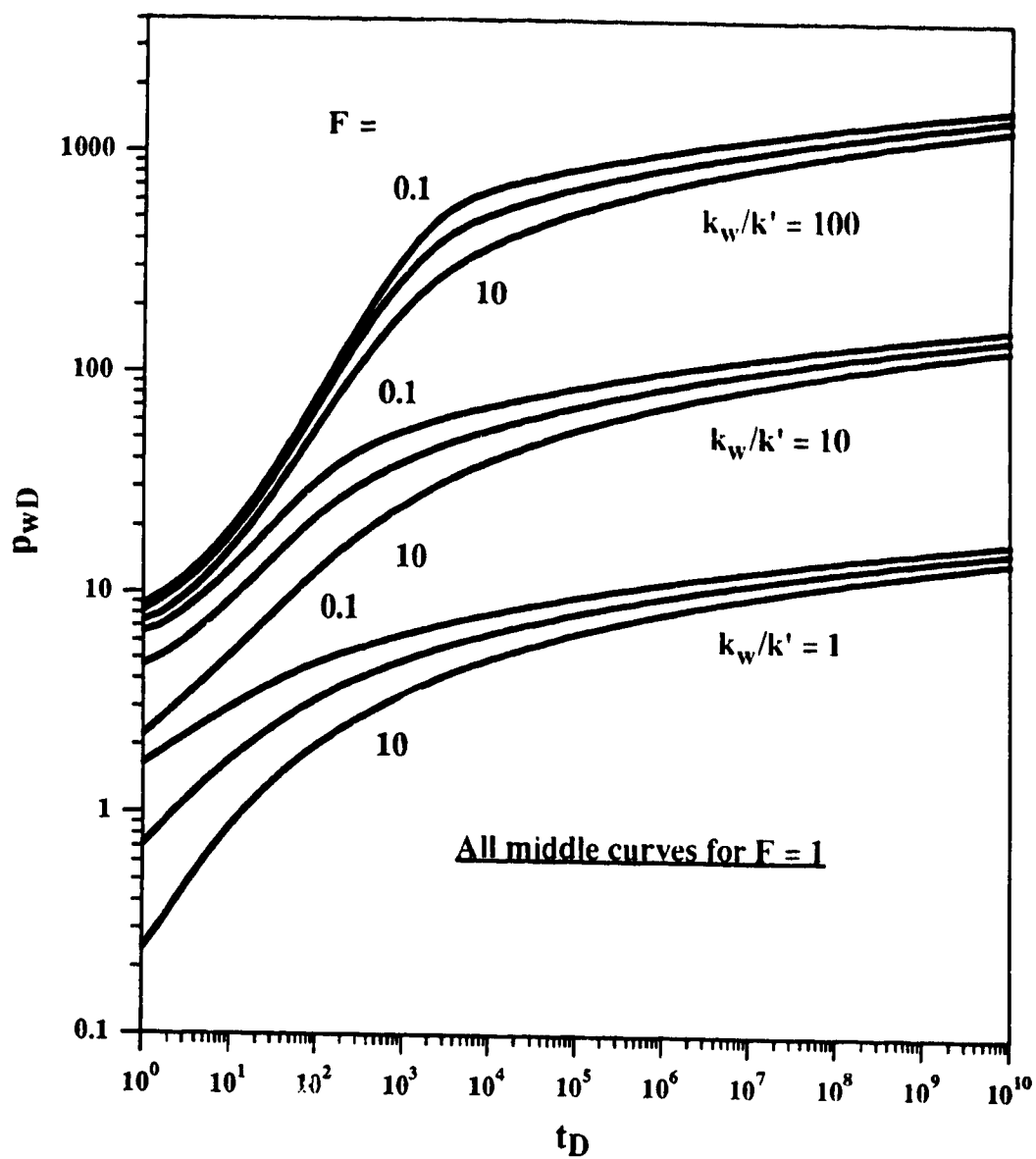


**Figure 10-24: Effect of Permeability and Diffusivity Ratios on Pressure Solution for a Composite System:  $n = 1$ ,  $d_f = 2$ ,  $d_s = 1.5$ ,  $a = 2$**



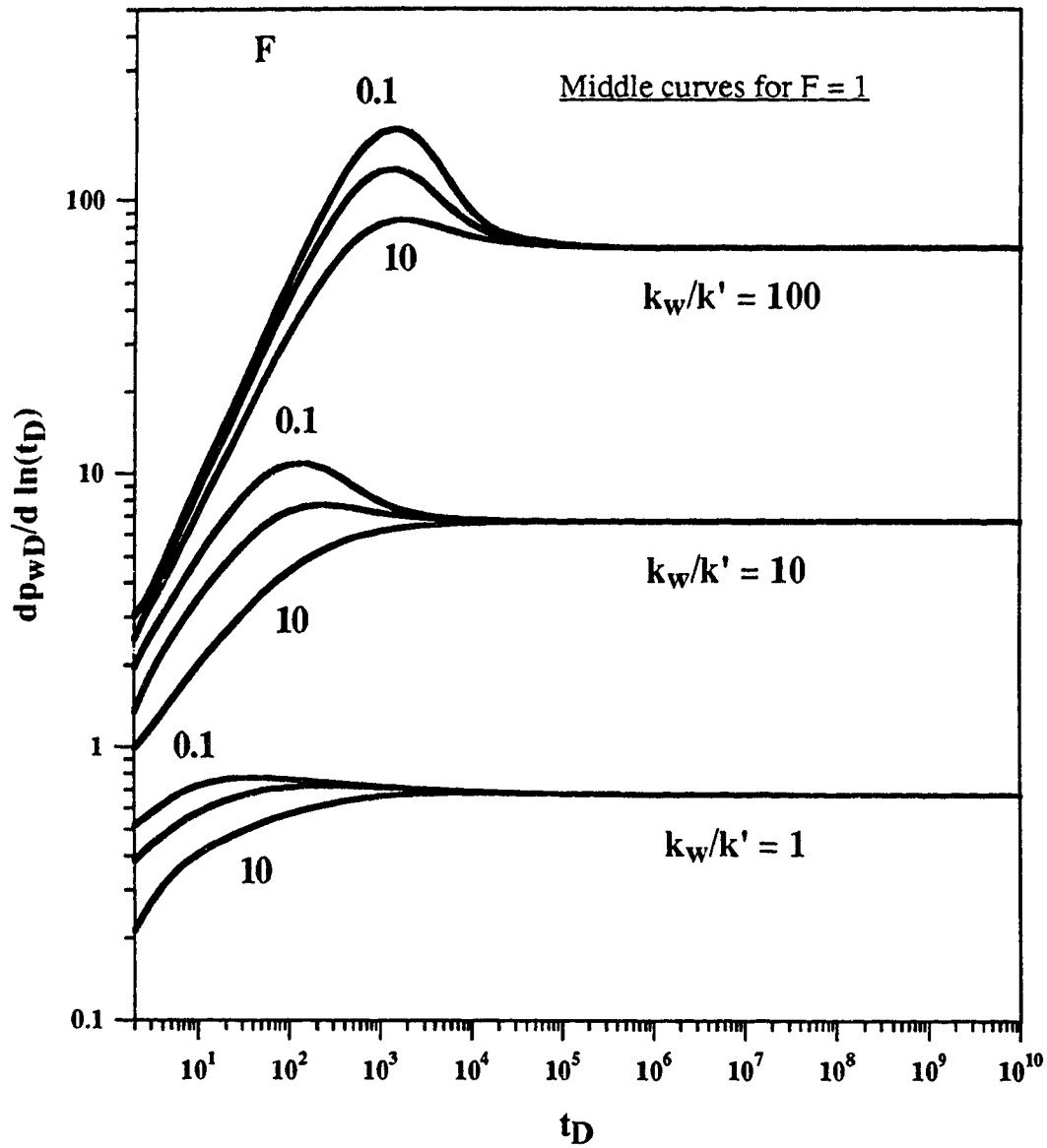


**Figure 10-25: Effect of Permeability and Diffusivity Ratios on Pressure Derivative for a Composite System:  $n = 1$ ,  $d_f = 2$ ,  $d_s = 1.5$ ,  $a = 2$**

Similar behaviour of derivative curves has also been observed for composite homogeneous reservoirs of cylindrical (Ambastha and Ramey, 1989) and elliptical (Stanislav et al., 1992) flow geometries.

Figures 10-24 and 10-25 correspond to  $n = 1$ ,  $d_f = 2$ ,  $d_s = 1.5$  and  $a = 2$ . Figure 10-26 presents a log-log plot of pressure derivative versus time identical in every respect to Figure 10-25, except that the former corresponds to  $a = 10$ . Comparing these two figures, it may be observed that even though the magnitude of the maximum derivative (during the transitional period) and the late-time constant value of the derivative are not affected by the value of  $a$ , the time when the maximum derivative is reached and that when the flattening out of the derivative takes place are dependent upon the magnitude of  $a$ . As expected, for larger values of  $a$ , the maximum in the derivative is reached later; also, for larger magnitudes of inner zone size, the time when the flattening out of the derivative begins is seen to increase.

Another aspect of the derivative plots that is of interest is its early-time behaviour. It has been shown by Ambastha and Ramey (1989) that, in the absence of wellbore storage and for a sufficiently large inner-zone size, an infinite-acting behaviour is shown by the derivative at early times (a flat derivative curve); obviously, the magnitude of this constant derivative value does not depend upon the permeability and porosity ratios, size of the inner zone, and so forth. For the case of an elliptical system, the early-time derivative plot would not consist of a zero-slope line, because of the non-cylindrical nature of flow at early times (Stanislav et al., 1992). It was not possible in this study to determine conclusively the behaviour of the derivative curves at very early times ( $t_D \leq 1$ ), because of some numerical instabilities in the calculation of the pressure derivative from the Laplace space solution at small times. However, it is not difficult to observe from Figures 10-25 and 10-26 that, at early times, the pressure derivative solutions would not exhibit a zero-slope derivative line; this is not difficult to visualize based on the discussions presented in previous sections

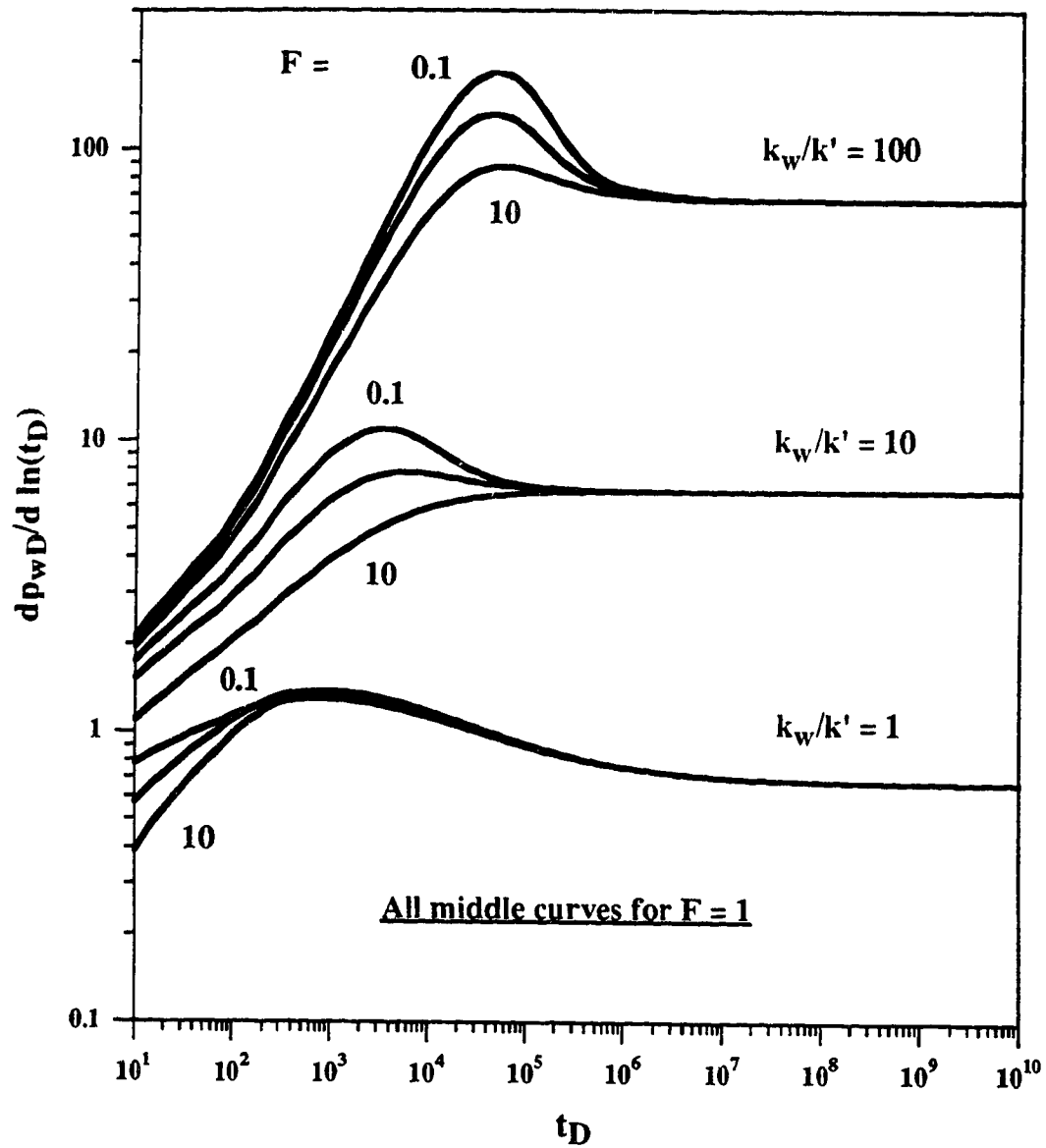
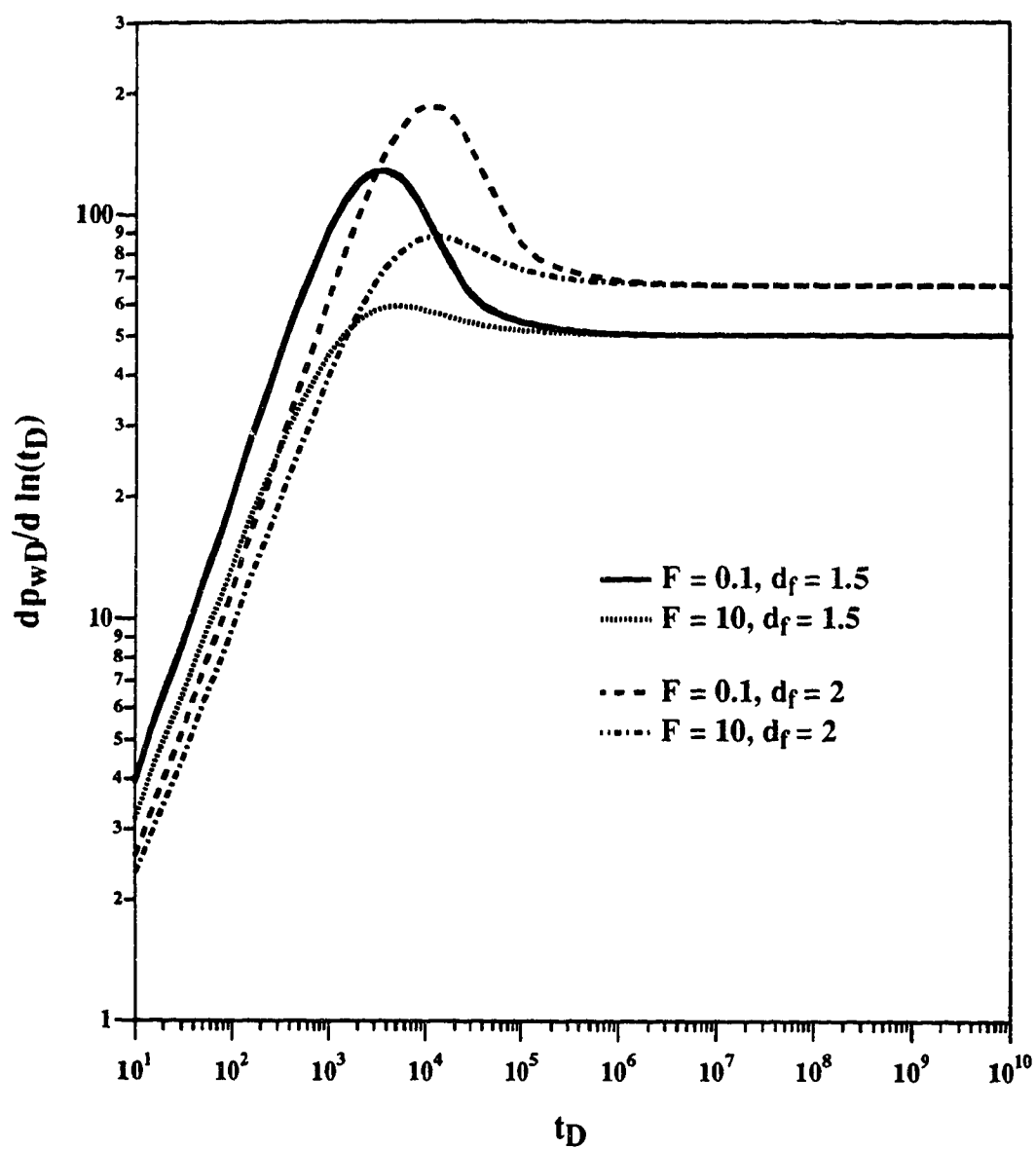


**Figure 10-26: Effect of Permeability and Diffusivity Ratios on Pressure Derivative for a Composite System:  $n = 1$ ,  $d_f = 2$ ,  $d_s = 1.5$ ,  $a = 10$**

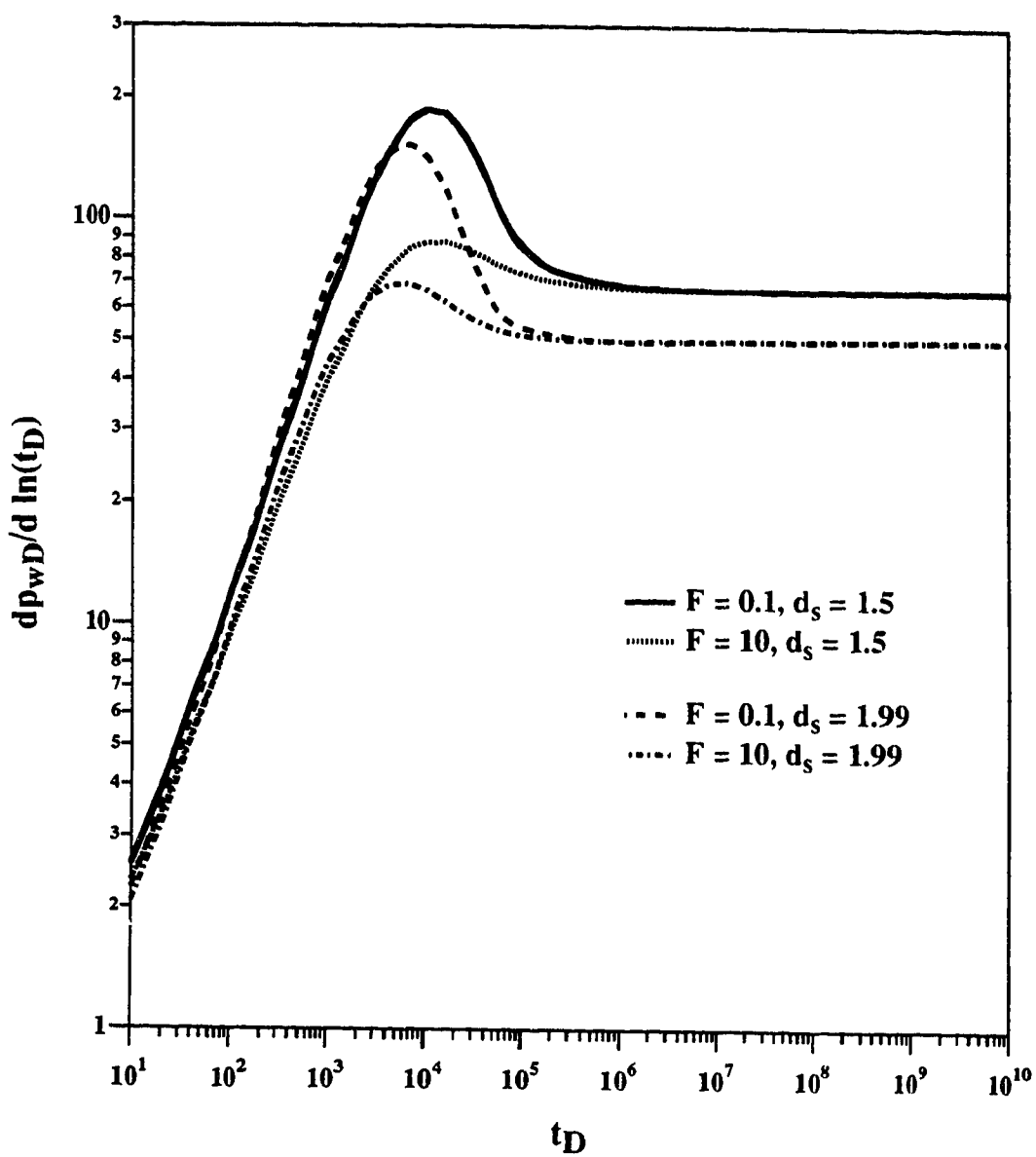
regarding the pressure derivative behaviour for a fractal medium. However, these early-time characteristics of pressure derivative are of little practical importance because of the presence of wellbore storage effects, which may obscure any early-time telltale "signature", as it were, of the system. On the other hand, at large enough times, the theoretical pressure derivative behaviour for different types of composite reservoirs are quite similar, as has been mentioned earlier. Thus, without a proper foreknowledge of the nature of the composite system, it is quite possible to match the field data with results from a model that does not represent the actual system at all.

Figures 10-24 through 10-26 were generated by assuming constant values of  $d_f$  and  $d_s$ . Figures 10-27 and 10-28 present the effects of  $a_f$  and  $a_s$ , respectively, on the pressure derivative behaviour of a composite system. Figure 10-27 shows that a smaller value of  $d_f$  may make the composite system appear as one with a smaller magnitude of permeability ratio, if it is assumed that  $d_f = 2$ . Similarly, it may be seen from Figure 10-28 that a smaller magnitude of  $d_s$  may be misinterpreted as the system having a higher permeability ratio, if it is incorrectly assumed that  $d_s = 2$ .

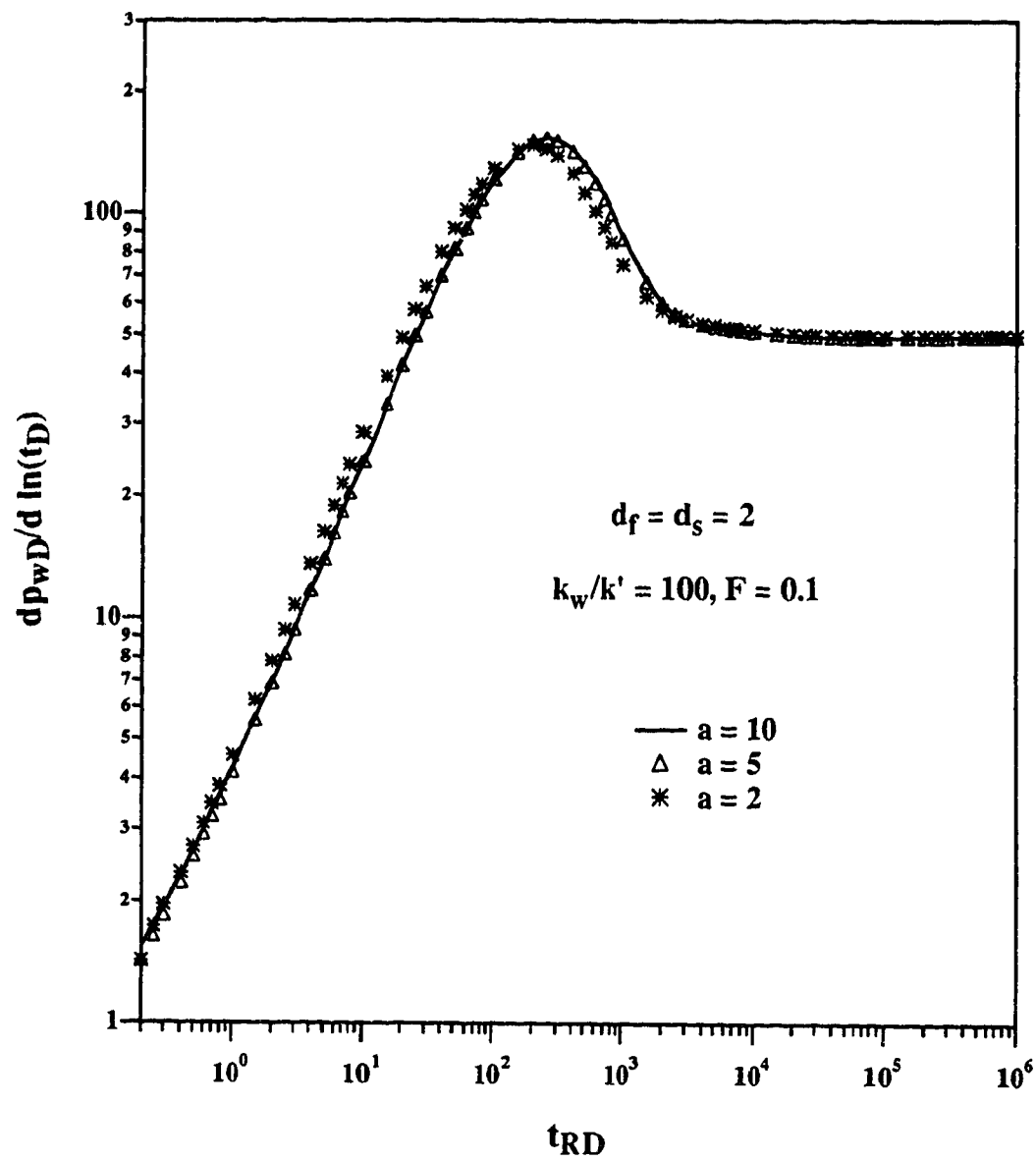
It has been shown in the previous graphs that the pressure derivative of a composite system depends upon a number of parameters. It was proposed in previous studies on pressure transient analysis of composite reservoirs (Ambastha and Ramey 1989; Stanislav *et al.*, 1992) that the time coordinate may be redefined as  $t_{RD} = t_D/a^2$ , in order to eliminate the dependence of the pressure behaviour on the size of the inner region. In this study also, the dimensionless time is redefined in a similar way, in order to investigate the possibility of removing the dependence of the pressure derivative on  $a$ . Figures 10-29 and 10-30 present derivative curves plotted against  $t_{RD}$ . In Figure 10-29, the values of  $d_f$  and  $d_s$  are the same, viz. 2. It is clear from Figure 10-29 that the correlation holds quite well for relatively large magnitudes of  $a$ . A similar observation was made also by Ambastha and Ramey (1989).



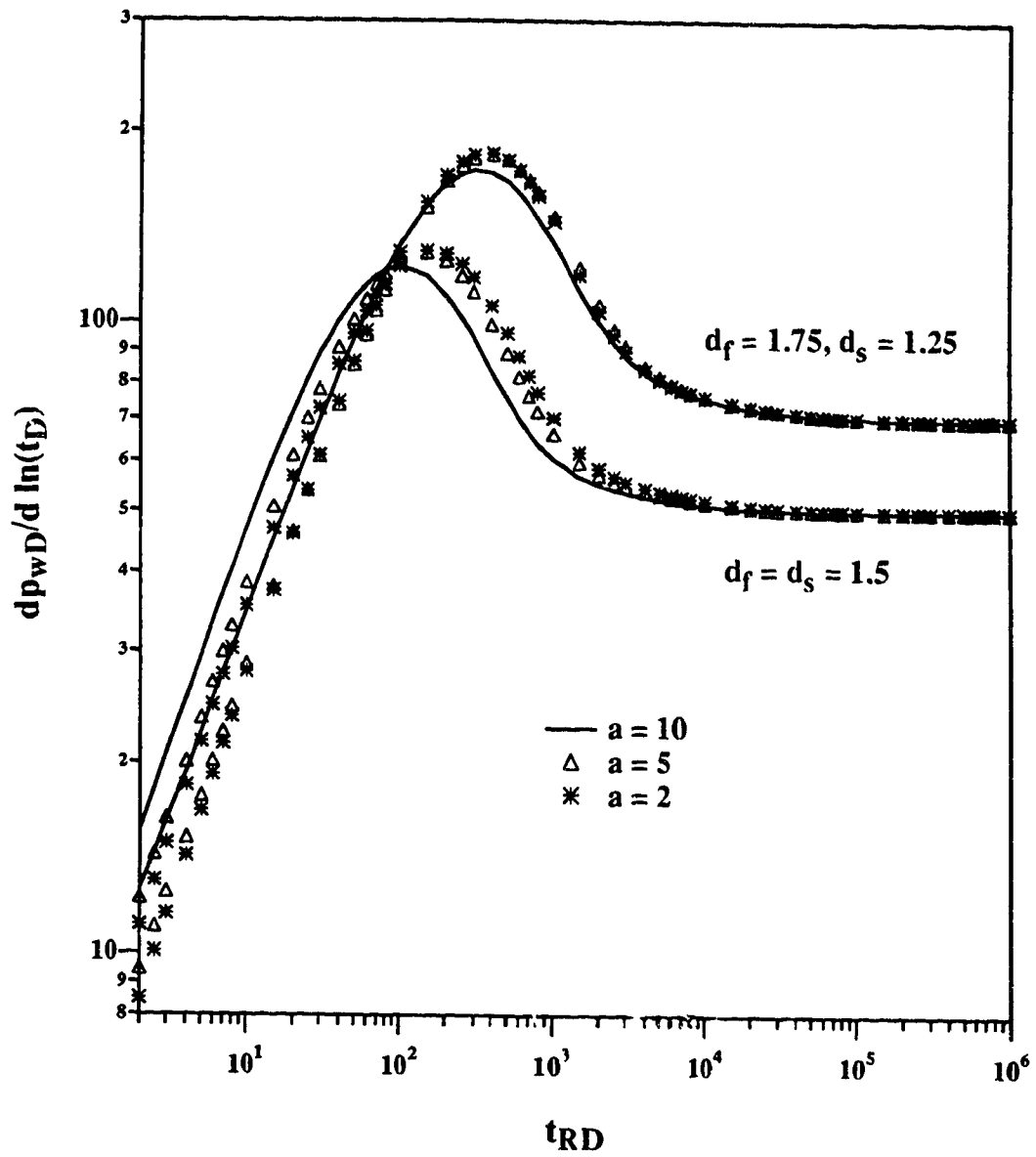
**Figure 10-27: Effect of  $d_f$  on Pressure Derivative for a Composite System:  $n = 1$ ,  $d_s = 1.5$ ,  $a = 5$ ,  $k_w/k' = 100$**



**Figure 10-28: Effect of  $d_s$  on Pressure Derivative for a Composite System:  $n = 1, d_f = 2, a = 5, k_w/k' = 100$**



**Figure 10-29: Pressure Derivative Behaviour for a Composite Reservoir: Different Inner-Zone Sizes**



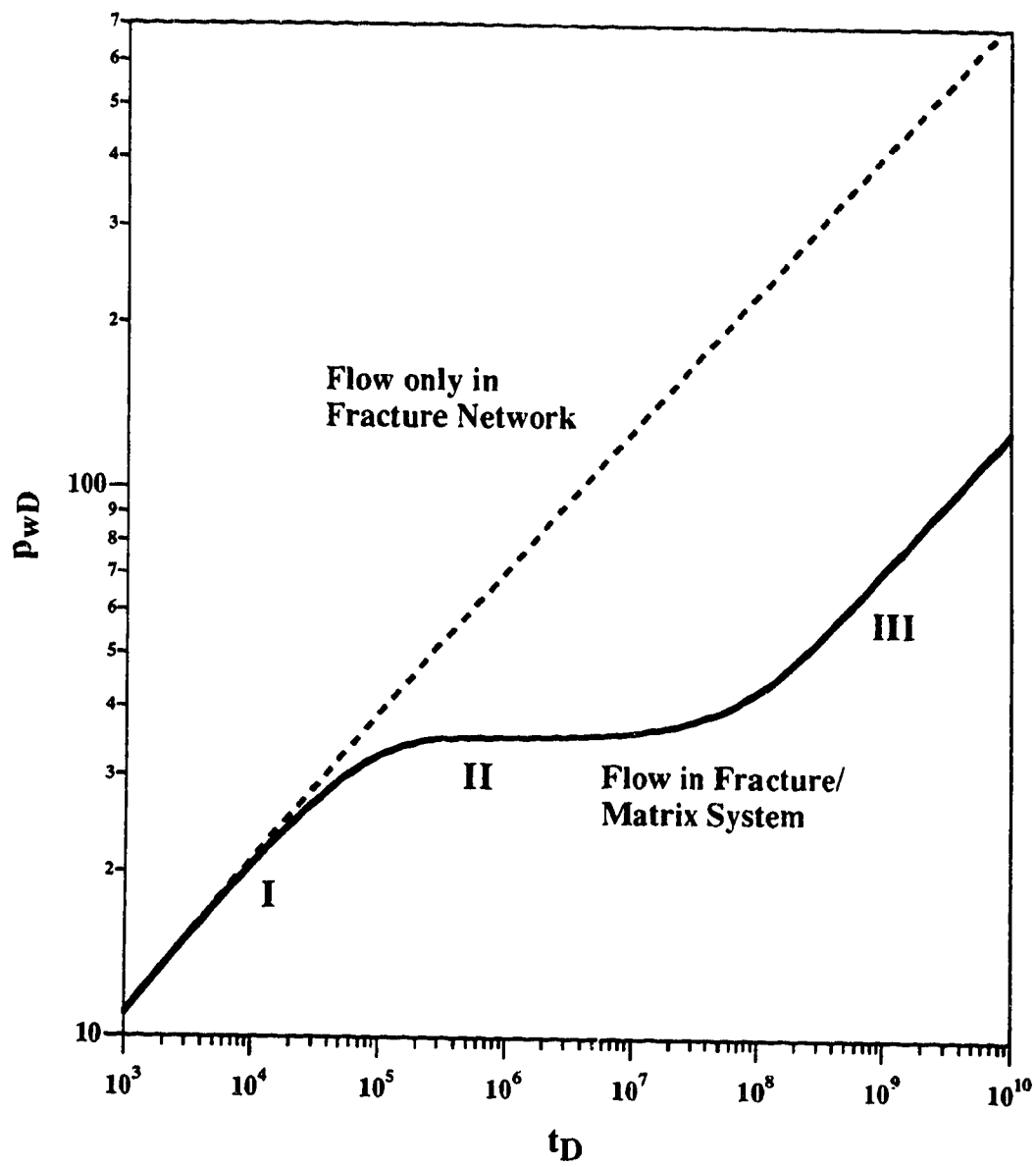
**Figure 10-30: Effect of  $d_f$  and  $d_s$  on Pressure Derivative for a Composite System:  $n = 1$ ,  $k_w/k' = 100$ ,  $F = 0.1$**



Figure 10-30 shows that for  $d_f = 1.75$  and  $d_s = 1.25$ , the correlation holds for  $a = 2$  and 5 and not for  $a = 10$ . Again, for  $d_f = d_s = 1.5$ , the correlation does not seem to work for the three values of  $a$ , at least for  $t_{RD} < 10^4$ . Thus, it is reasonable to conclude from Figures 10-29 and 10-30 that a correlation of pressure derivative versus  $t_{RD}$  does not work for all combinations of  $d_f$  and  $d_s$ , and alternative correlations must be sought for such composite reservoirs.

## 10.2 Transient Flow Through a Fractal Fracture/Homogeneous Matrix System

The previous sections dealt with the case of the matrix not participating in the system pressure response. This section presents a discussion of results obtained for the case of a fracture/matrix system (i.e., the matrix has connected porosity and is in pressure communication with the fracture network) with the fracture network being characterized by  $d_f = 2$  and  $d_s < 2$  and the matrix being homogeneous. The results of calculation of the dimensionless wellbore pressure for a constant rate condition at the wellbore and an infinite reservoir could be used to analyze the characteristics of pressure drawdown curves in such a double-porosity reservoir for single-well situations. Figure 10-31 presents a basic pattern of such pressure drawdown curves for an infinite system on a log-log plot. As Figure 10-31 shows, a complete curve may generally be represented by three different flow regimes or intervals. The early-time flow regime (interval I), characterized by the log-log straight line, exhibits a rapid drawdown in the fractal fracture system. Obviously, for flow only in the fracture network, the drawdown curve would maintain the same trend of interval I. However, for a fracture/matrix system, the transitional stage (shown by interval II) appears at the end of the first flow regime. The transitional stage involves a slower pressure drawdown in the fracture system because of increasing participation of the tighter matrix in the flow process. Interval III, the late-time straight line, develops after an equilibrium is reached between the fracture and matrix pressures. The straight line of interval III is parallel



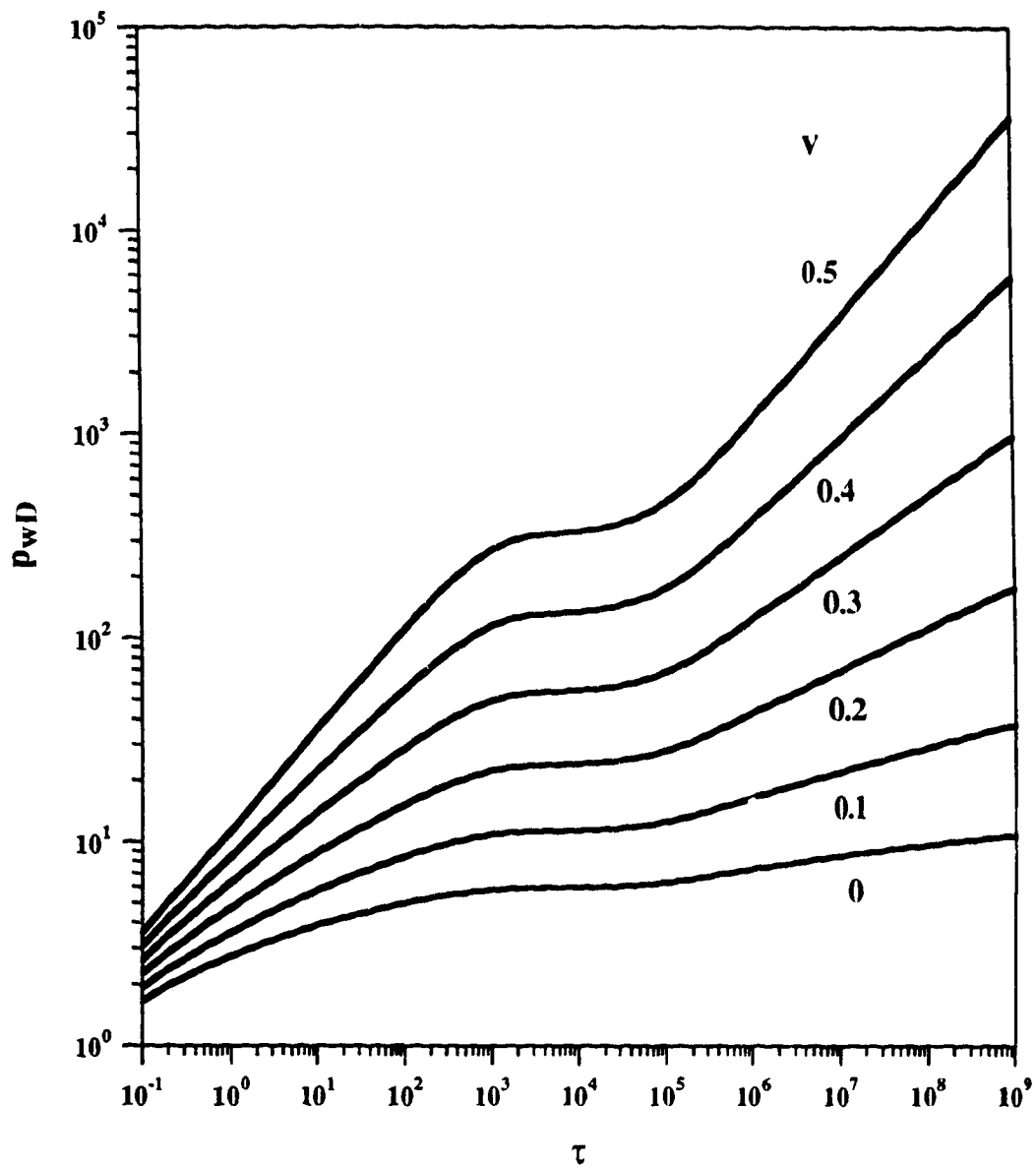
**Figure 10-31: Pressure Drawdown Curves  
for Single- and Double-Porosity Systems:**

$$d_s = 1.5, \omega = 10^{-3}, \lambda = 10^{-5}$$

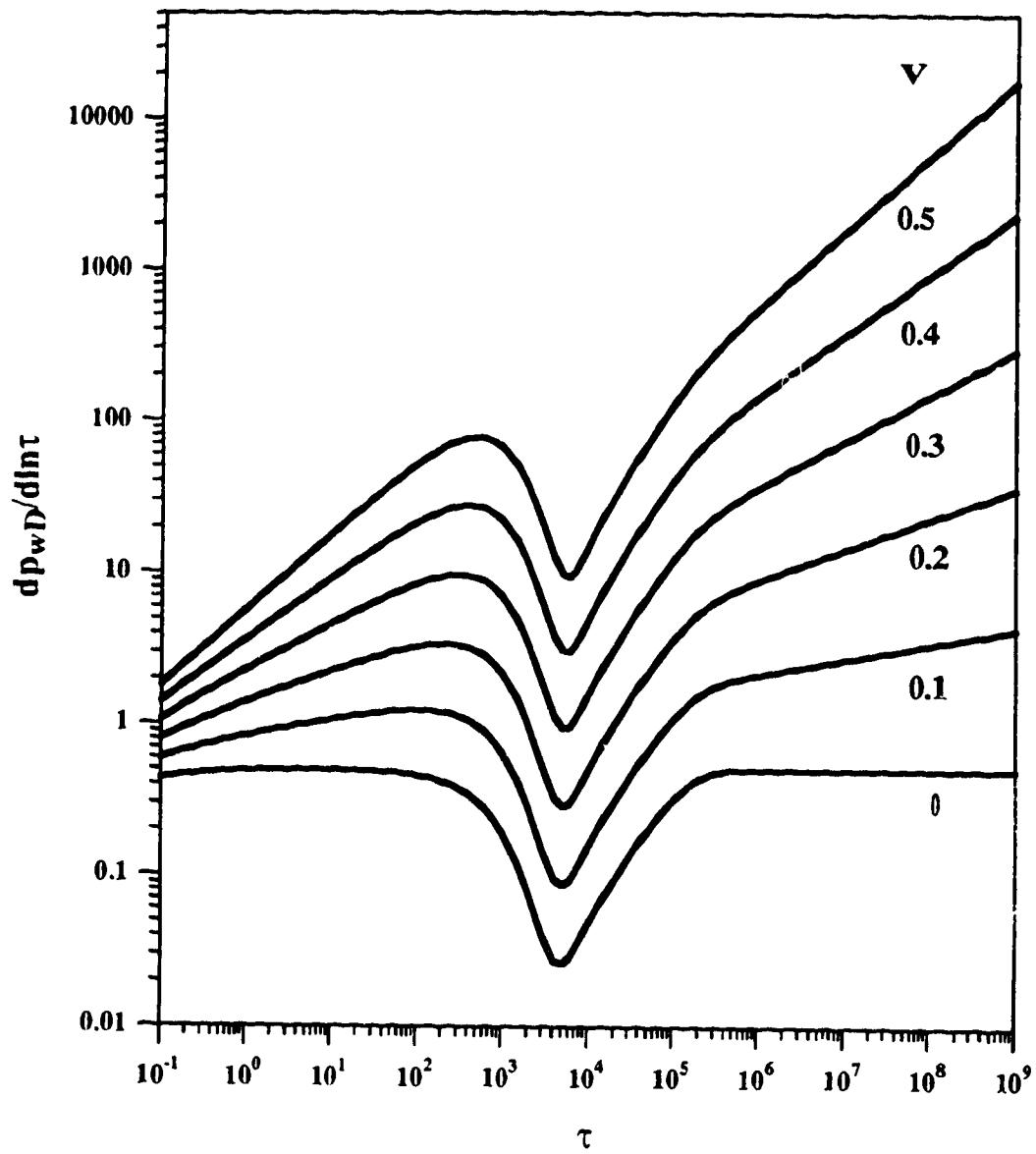
to that of interval I because of the assumption of  $d_f = 2$ . For  $d_f \neq 2$ , the slopes of these two straight lines would be different, even though the difference would be small (Chang and Yortsos, 1990). For a sufficiently large distance to the outer boundary, the pressure response would show the boundary effects after interval III.

Figure 10-32 presents sensitivity runs carried out to determine the effects of parameter  $\nu$  on the transient dimensionless pressure response. For the set of pressure curves presented in Figure 10-32, the values of  $\omega$  and  $\lambda$  are set to be 0.01 and  $10^{-5}$ , respectively. The characteristics of the "double-porosity" system are exhibited more clearly by the pressure derivative curves, as shown in Figure 10-33. The derivative curves (for  $\nu \neq 0$ ) show the typical power-law dependence on time of the late-time segments, as is expected for fractal systems. The well known "V" shaped derivative behaviour for the Warren and Root (1963) type double porosity system ( $\nu = 0$ ) appears to be quite similar to that for the fractal systems. However, the late-time pressure derivative for a homogeneous system stabilizes asymptotically to a finite value, unlike that for a fractal system. Figure 10-34 presents plots of the pressure derivative group,  $d \ln(p_{wD})/d \ln(\tau)$ , with values of  $\nu$  ranging from 0 to 0.5. Clearly, for large magnitudes of  $\nu$ , the values of the derivative group would stabilize at constant values of  $\nu$ , unlike the case of a homogeneous fracture/matrix system, where the derivative group would decrease indefinitely with increasing times. Identical results have been presented previously, by numerical means, in the study of Chang and Yortsos (1990).

Figure 10-35 presents the sensitivity of the wellbore pressure solutions to  $\omega$ , with  $\omega$  ranging from 0.001 (relatively small amount of storage in the fracture system) to 1 (flow only in the fractures). Figure 10-35 shows that the early- and late-time pressure curves have the same slopes irrespective of the magnitude of  $\omega$ ; the parameter  $\omega$ , however, has a strong influence on the duration of the transition period. As may be expected, the smaller the



**Figure 10-32: Plot of Pressure Drop for a Fracture /Matrix System:  $\omega = 0.01$ ,  $\lambda = 10^{-5}$**



**Figure 10-33: Plot of Pressure-Derivative for a Fracture/Matrix System:  $\omega = 0.01$ ,  $\lambda = 10^{-5}$**

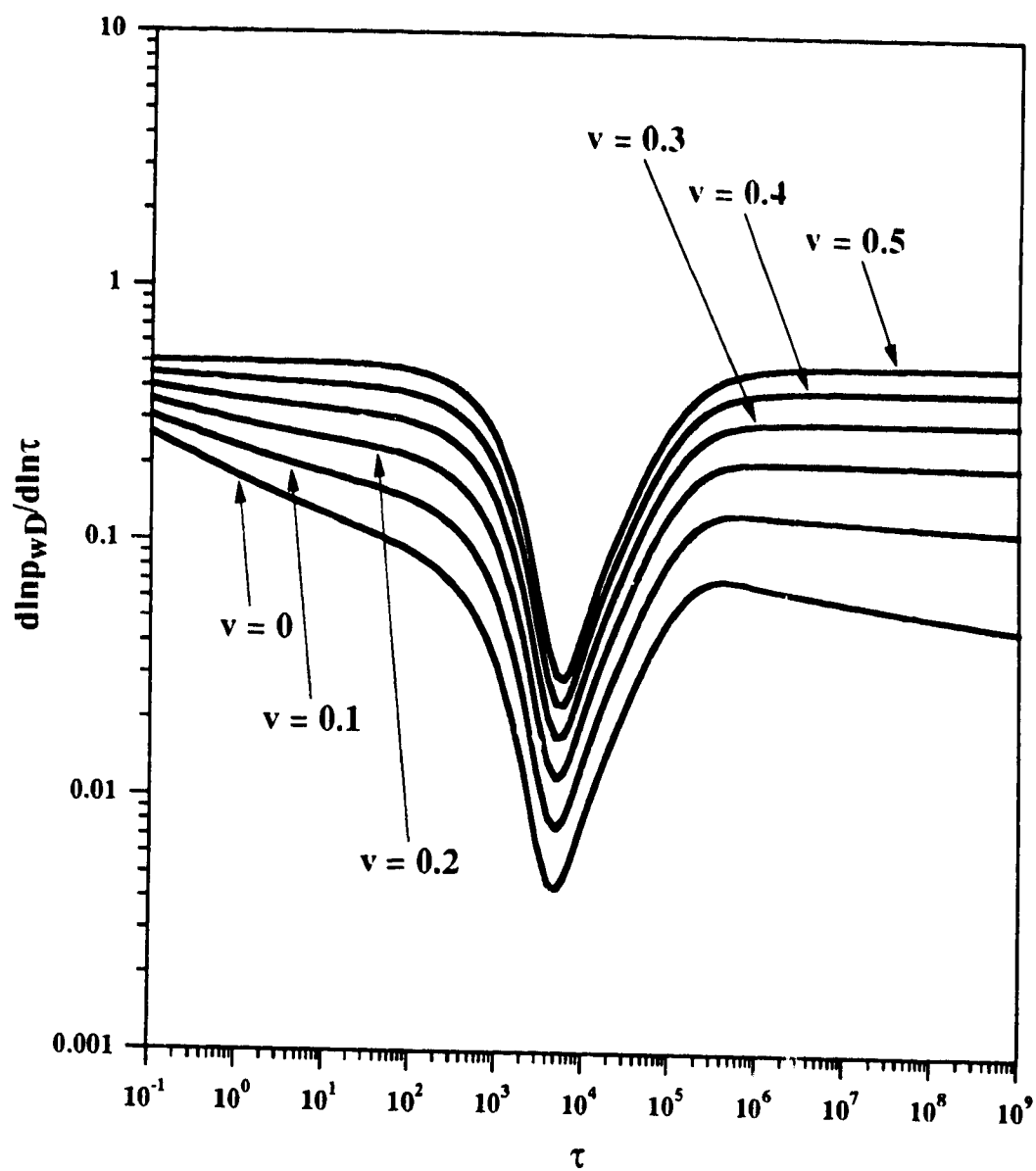


**Figure 10-34: Plot of  $\frac{d \ln(p_{wD})}{d \ln(\tau)}$  for a Fracture/Matrix System:  $\omega = 0.01$ ,  $\lambda = 10^{-5}$**

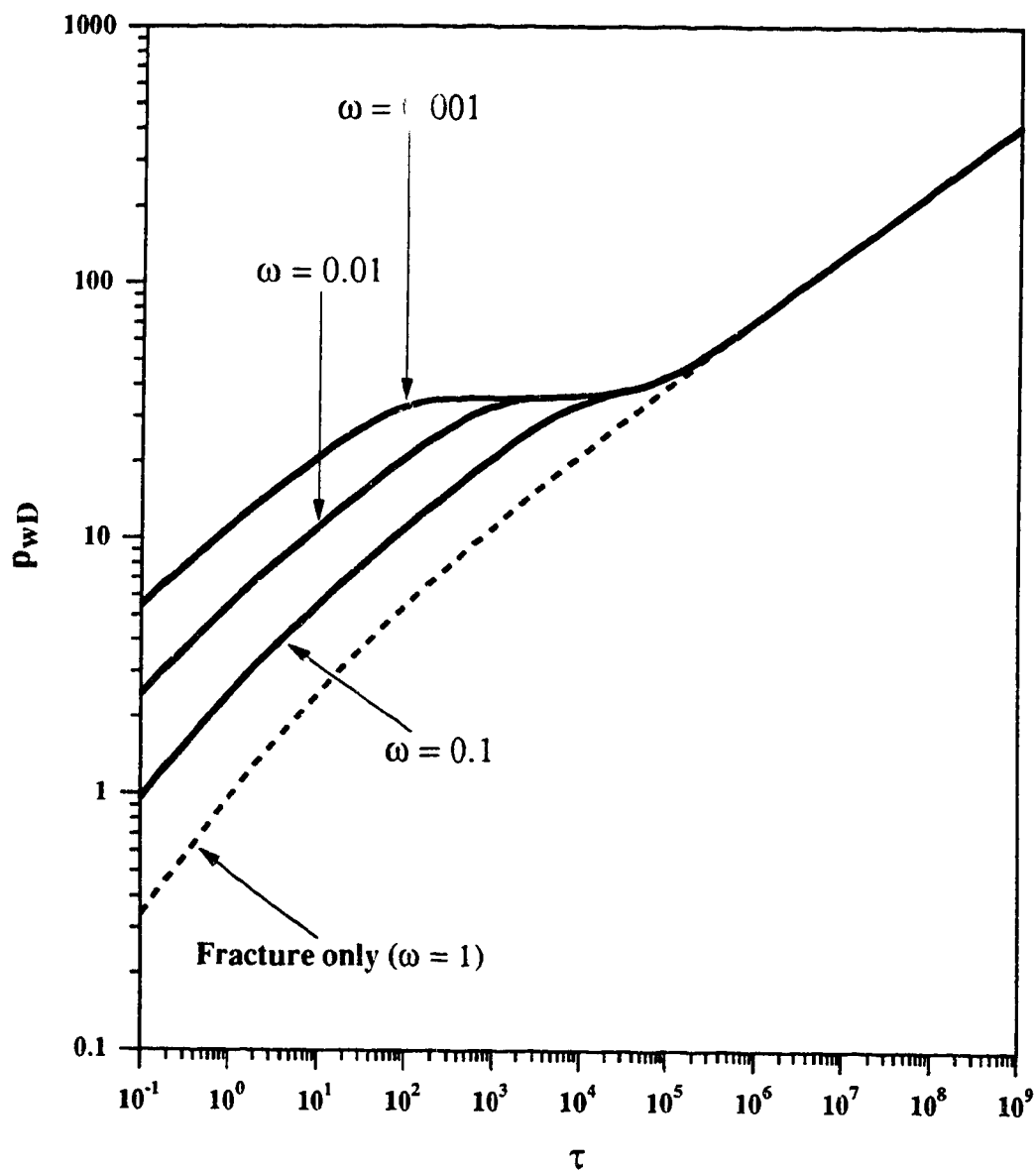


**Figure 10-35: Effect of  $\omega$  on Plot of  $p_{wD}$  versus  $\tau$  for Fracture/Matrix System:  $v = 0.25$ ,  $\lambda = 10^{-5}$**

magnitude of  $\omega$  relative to one, the earlier is the time when the transition stage sets in (so that the longer is the duration of the transition period) and the larger is the pressure drop between the early- and late-time segments. The effect of  $\omega$  on the pressure derivative is shown in Figure 10-36, for  $\nu = 0.25$  and  $\lambda = 10^{-5}$ . The transitional stage (when the pressure response shows a period of gradual decrease and subsequent increase in slope) appears as a dip in the derivative curve; the smaller the magnitude of  $\omega$ , the sharper is the minimum and the smaller is the value of  $\tau$  when the dip in the derivative takes place.

Figures 10-35 and 10-36 demonstrated the variation of the pressure and derivative responses, respectively, against  $\tau$ , where  $\tau$  has been defined as  $\tau = \omega t_D$ . Figures 10-37 and 10-38 are presented to study the effects of  $\omega$ , when the pressure and derivative responses are studied against dimensionless time  $t_D$ . Figure 10-37 shows that at early times, the curves for different values of  $\omega$  merge together, as, during this period, flow takes place only through the fracture system. At late times, the pressure curve for the fracture/matrix system in the log-log plot is parallel to the hypothetical straight line for  $\omega = 1$  (shown by the dotted line). This is strictly true only for  $d_f = 2$ , and for such a situation, the vertical distance between the two asymptotes depends only on two parameters, namely,  $\nu$  and  $\omega$ . However, when  $d_f \neq 2$ , the magnitude of the pressure drop not only depends on other parameters but is also time-dependent; therefore, when  $d_f \neq 2$ , it may not be possible to obtain a reliable estimate of the magnitude of  $\omega$  from an observed value of the vertical pressure drop. On the other hand, when  $d_f = 2$ , the late-time equations for wellbore pressure (Equation (5-47) for flow only in the fracture network and Equation (9-37) for flow in the fracture/matrix system) may be analyzed to show that the magnitude of the pressure drop varies with  $\nu \log(1/\omega)$ . Thus, knowing the magnitude of  $\nu$  and that of the vertical pressure drop, the value of  $\omega$  may be calculated.



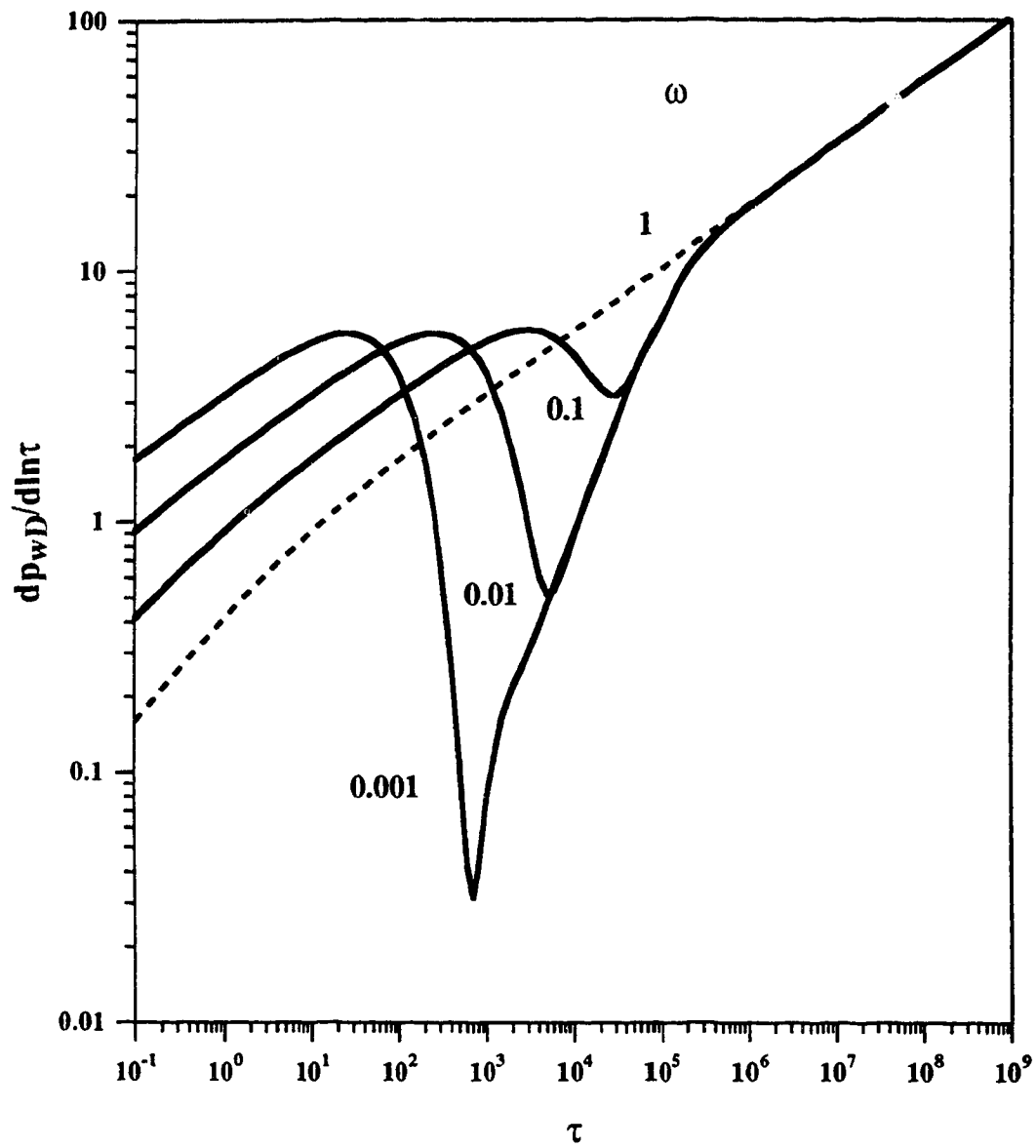


**Figure 10-36: Effect of  $\omega$  on  $\frac{dp_{wD}}{d\ln(\tau)}$  for Fracture/Matrix System:  $\nu = 0.25, \lambda = 10^{-5}$**

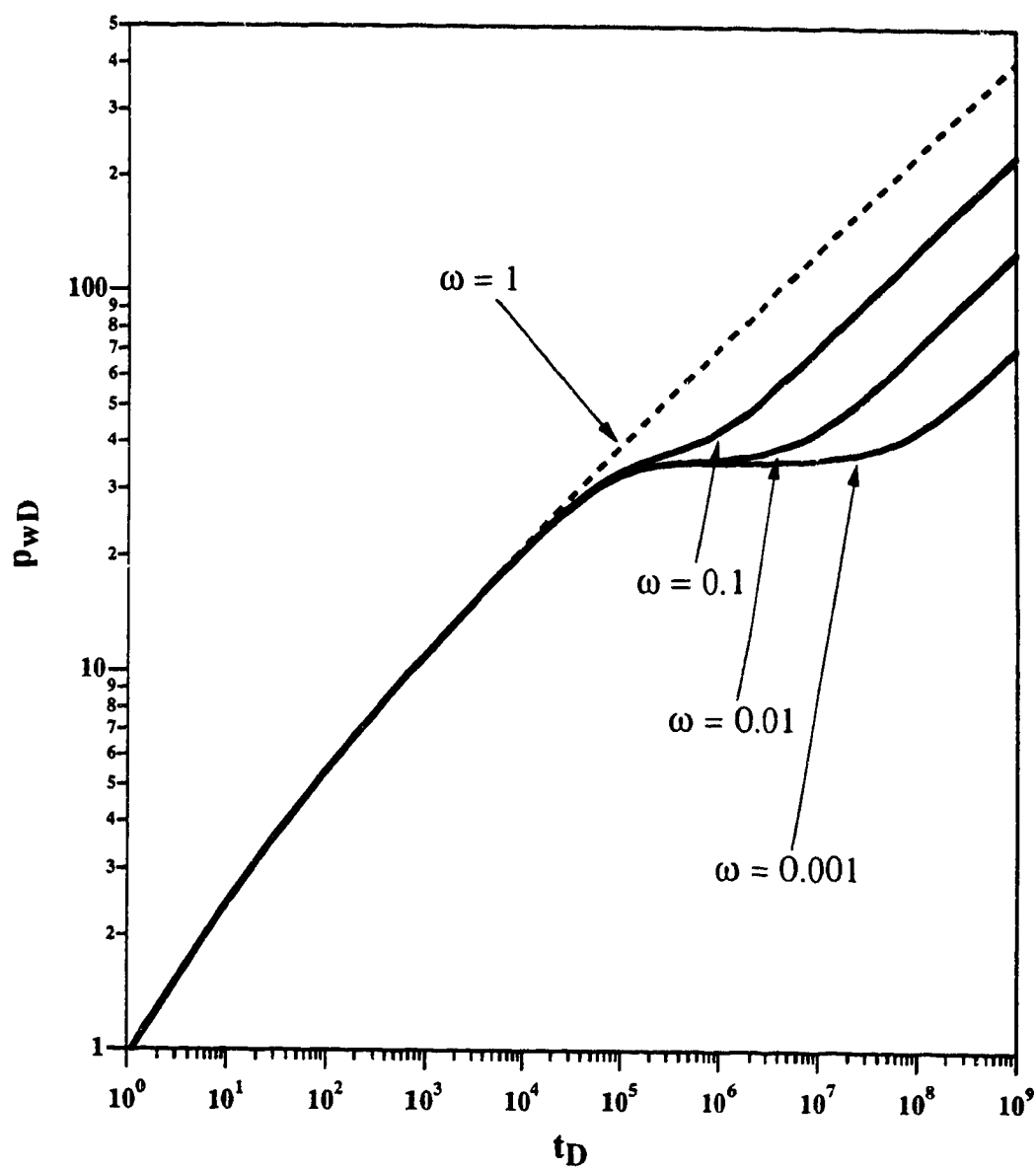


**Figure 10-37: Effect of  $\omega$  on Plot of  $p_{wD}$  vs.  $t_D$   
for Fracture/Matrix System:  $\nu = 0.25, \lambda = 10^{-5}$**

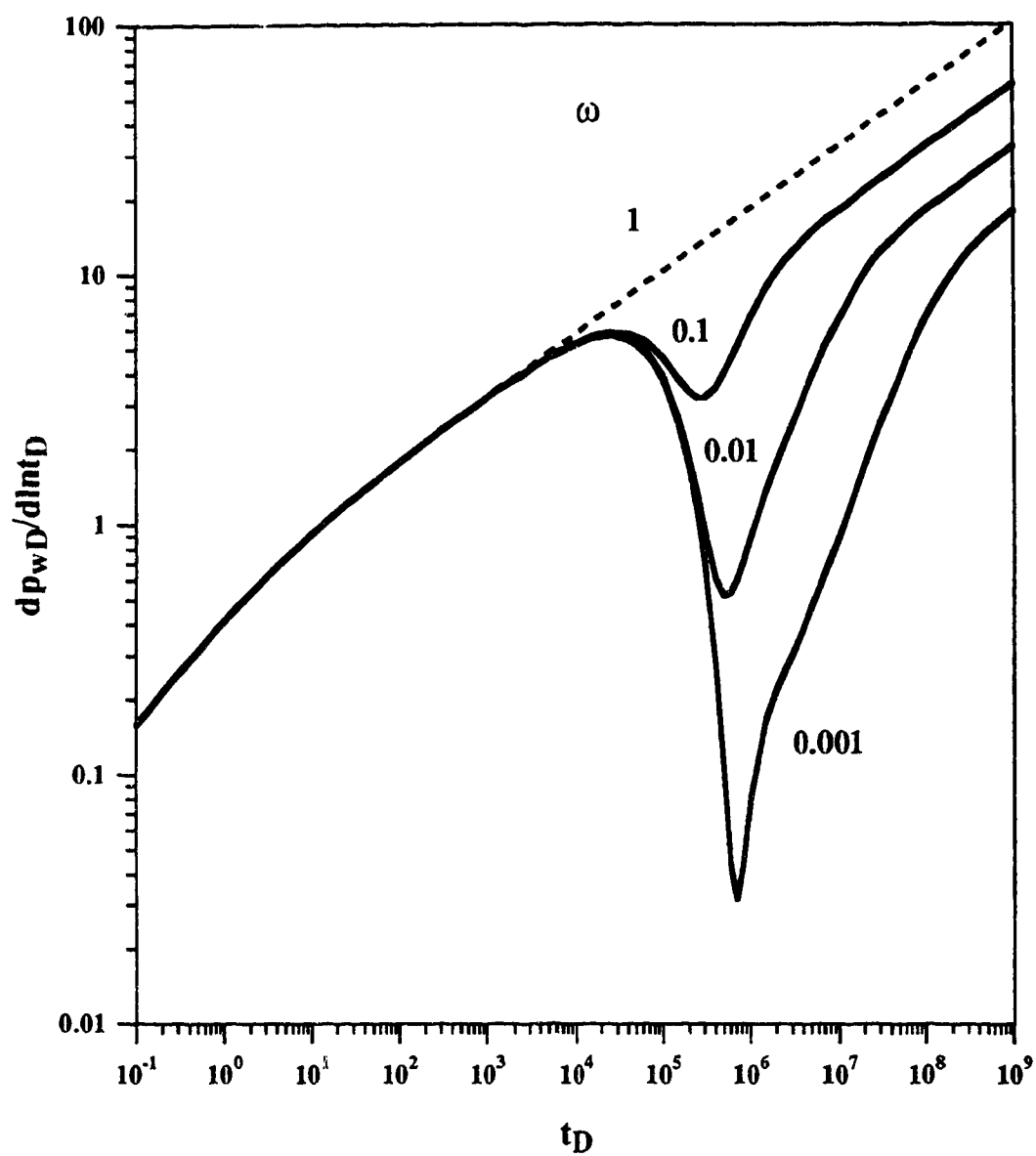


**Figure 10-38: Effect of  $\omega$  on Plot of Pressure-Derivative for Fracture/Matrix System:  $\nu = 0.25$ ,  $\lambda = 10^{-5}$**

Figure 10-38 shows the effect of  $\omega$  on the pressure derivative behaviour. It may be noted from Figure 10-38 that the parameter  $\omega$  has a weak influence on the dimensionless time when the pressure derivative reaches its minimum. This time, however, is strongly influenced by the parameter  $\lambda$ , as is shown in Figures 10-39 and 10-40. The parameter  $\lambda$  indicates the strength of the exchange rate between the matrix and the fracture system (Chang and Yortsos, 1990) and, therefore, the smaller the magnitude of  $\lambda$ , the later is the onset of the transitional stage. It has been found in the present study, that within the ranges of the various parameters studied, the time when the wellbore pressure derivative reaches its minimum during flow in a fracture/matrix system depends on  $\lambda$  and, to some extent, on  $\omega$ . The following empirical relationship is found to hold between this time and the parameters  $\lambda$  and  $\omega$ :  $t_D = \ln(1/\omega)/\lambda$ .

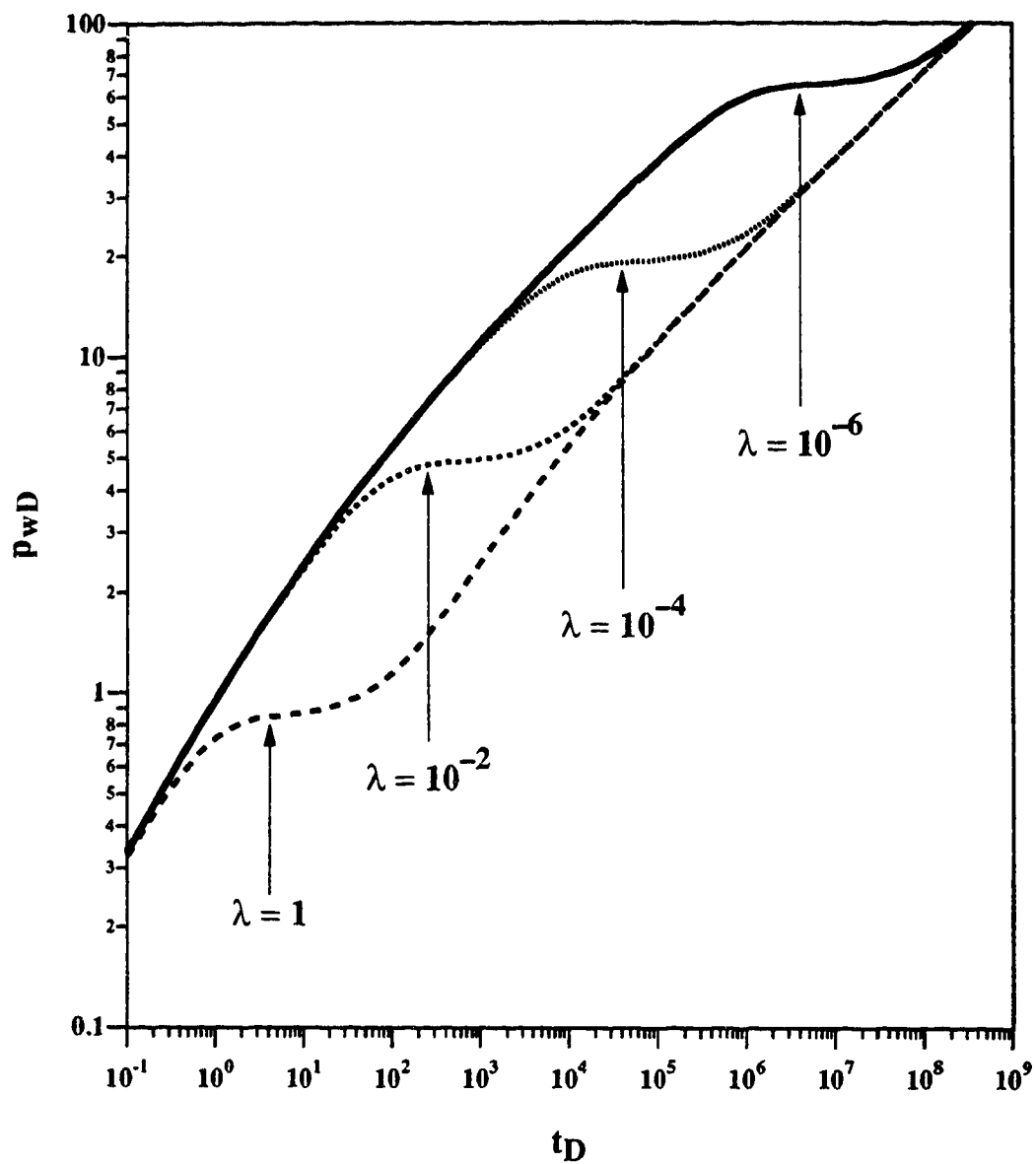


**Figure 10-39: Effect of  $\lambda$  on Pressure Solution for a Fracture/Matrix System:  $\omega = 0.01$ ,  $\nu = 0.25$**

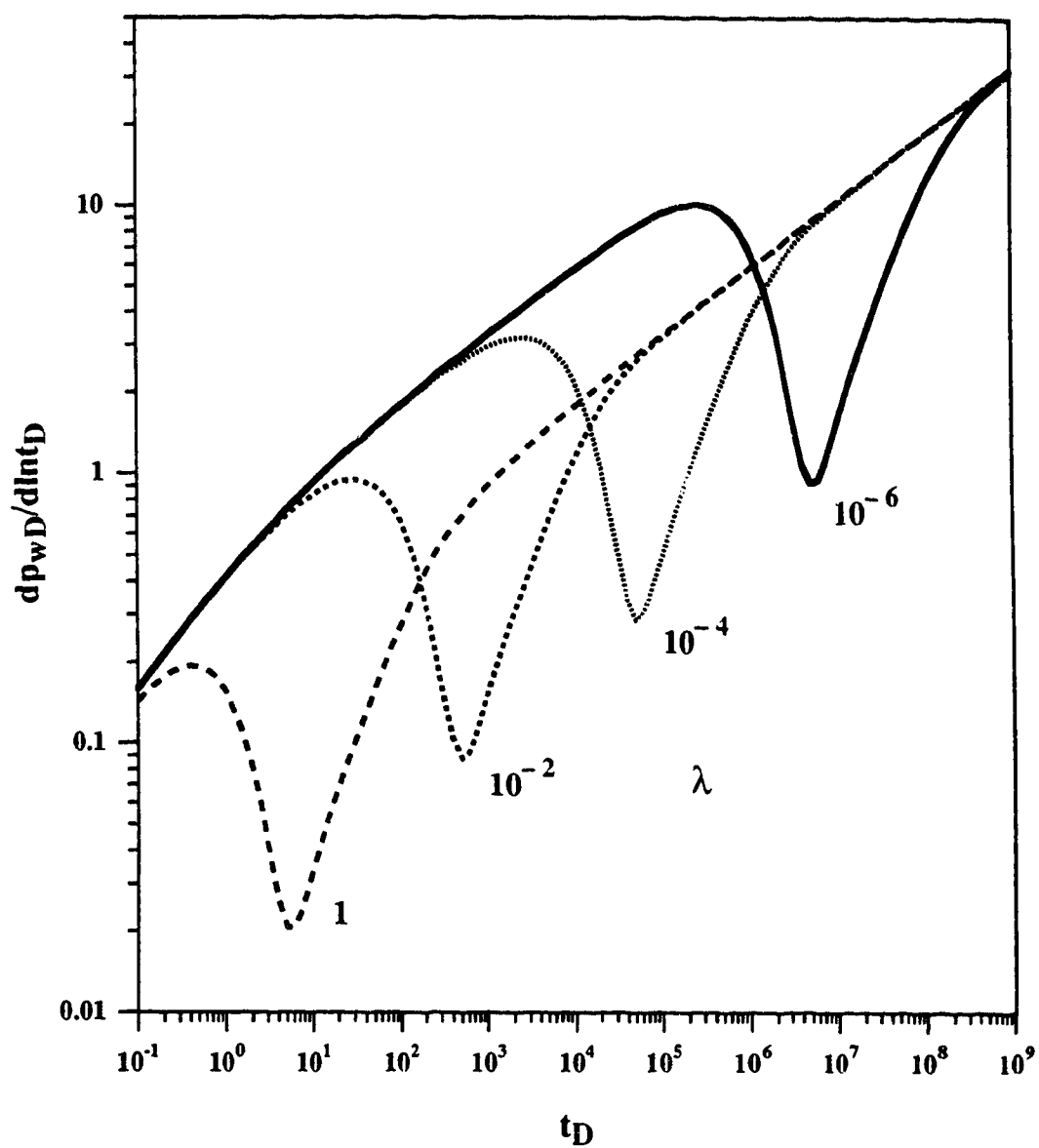


**Figure 10-40: Effect of  $\lambda$  on Pressure-Derivative for a Fracture/Matrix System:  $\nu = 0.25$ ,  $\omega = 0.01$**

## Chapter XI

### CONCLUSIONS

A mathematical model describing the single-phase transient flow of a slightly compressible, non-Newtonian, power-law fluid in a fractal fracture network has been presented. The nonlinear partial differential equation governing such flows has been shown to reduce to the standard diffusivity equation as a limiting case. Approximate analytical solutions of the governing equation, with constant rate and constant pressure inner boundary conditions, have been presented for infinite and finite systems and for a composite reservoir case. Analytical solutions have also been presented for a special case of the flow situation where the matrix participates in the flow process along with the fracture network. Numerical solutions of the rigorous flow equation were compared with the approximate analytical solutions for flow in an infinite fractal reservoir.

Based on the results obtained in this study, the following conclusions can be drawn:

- i) log-log plots of wellbore pressure and pressure derivative may be used as diagnostic plots to identify either the fractal nature of a reservoir or the power-law characteristics of the flowing fluid;
- ii) for power-law flow in a fractal reservoir, the slopes of late-time straight lines in the log-log pressure-drawdown plots will depend on both the flow behaviour index of the power-law fluid ( $n$ ) and the spectral dimension of the fractal reservoir ( $d_f$ ). It is necessary to analyze the late-time behaviour of both transient pressure and rate data to calculate the values of  $n$  and  $d_f$  under such flow situations;
- iii) the approximate analytical solution for pressure-drawdown behaviour in an infinite fractal system is seen to be within acceptable error, when the parameters have the following ranges:  $0.75 \leq n \leq 1$ ,  $1.75 \leq d_f \leq 2$ , and  $1.50 \leq d_s \leq 2$ ;

- iv) the large-time pressure response of a finite, areally heterogeneous system with a fractal structure may be misinterpreted to represent a smaller reservoir size if analyzed using methods derived for homogeneous systems;
- v) methods presented in previous studies for the analysis of composite reservoirs may result in gross misinterpretation of the nature of the flow system if the inner region of the composite system consists of a fractal medium. The analysis of drawdown data from such reservoirs with techniques that do not account for the fractal characteristics of the inner zone can lead to incorrect reservoir property estimates;
- vi) for Newtonian flow in a reservoir comprising a fractal fracture network and a homogeneous matrix, the spectral dimension,  $d_f$ , and the interporosity flow parameters,  $\omega$  and  $\lambda$ , may be estimated provided  $d_f = 2$  and the magnitude of  $\sigma$  is small.

One can make many recommendations for further research in this area. The more important ones are:

- i) to validate the analytical models presented in this study for finite and composite reservoirs by comparing the analytical solutions with rigorous numerical results and to subsequently define the ranges of magnitudes of the various parameters within which the analytical solutions compare favourably with the numerical ones;
- ii) to investigate the pressure transient behaviour of a fractal fracture/homogeneous matrix system for non-Newtonian fluids using numerical techniques;
- iii) to develop extensions of the methods presented in this study to multiple well situations and interference testing. It has been shown (Chang and Yortsos, 1992) that approaches based on Green's functions may be appropriate for such purposes;
- iv) to develop an understanding of the relationship, if any, between theories developed for a fractional dimension medium (e.g., Barker, 1988; Doe, 1991) and those for a fractal object.



## REFERENCES

- Abdassah, D. and Ershaghi, I. (1986): "Triple-Porosity Systems for Representing Naturally Fractured Reservoirs", *Soc. Pet. Eng. Form. Eval.*, (April) 113-27.
- Abramowitz, M. and Stegun, I. A. (1972): *Handbook of Mathematical Functions with Formulas, Graphs, and Mathematical Tables*, Dover Publications, Inc., New York.
- Acuña, J. A. and Yortsos, Y. C. (1991): "Numerical Construction and Flow Simulation in Networks of Fractures Using Fractal Geometry", SPE Paper 22703, 66th Annual Technical Conference and Exhibition of the SPE, Oct. 6-9, Dallas, TX.
- Acuña, J. A., Ershaghi, I. and Yortsos, Y. C. (1992a): "Fractal Analysis of Pressure Transients in the Geysers Geothermal Field", paper presented at the 17th Annual Workshop Geothermal Reservoir Engineering, Jan. 29-31, Stanford, CA.
- Acuña, J. A., Ershaghi, I. and Yortsos, Y. C. (1992b): "Practical Application of Fractal Pressure Transient Analysis of Naturally Fractured Reservoirs", SPE Paper 24705, 67th Annual Technical Conference and Exhibition of the SPE, Oct. 4-7, Washington, DC.
- Ambastha, A. K. and Ramey, H. J., Jr. (1989): "Thermal Recovery Well Test Design and Interpretation", *Soc. Pet. Eng. Form. Eval.*, (June) 173-80.
- Balberg, I., Berkowitz, B. and Drachsler, G. E. (1991): "Application of a Percolation Model to Flow in Fractured Hard Rocks", *Jour. Geoph. Res.*, **96**(B6) 10.015-10.021.
- Barker, J. A. (1988): "A Generalized Radial Flow Model for Hydraulic Tests in Fractured Rock", *Water Resour. Res.*, **24**(10) 1796-1804.

- Barnes, H. A. (1989): "Shear-Thickening ('Dilatancy') in Suspensions of Nonaggregating Solid Particles Dispersed in Newtonian Liquids", *Jour. Rheol.*, **33**(2) 329-66.
- Beier, R. A. (1990a): "Pressure Transient Field Data Showing Fractal Reservoir Structure", CIM/SPE Paper 90-4, International Technical Meeting of the Pet. Soc. of CIM and the SPE, June 10-13, Calgary, AB.
- Beier, R. A. (1990b): "Pressure Transient Model of a Vertically Fractured Well in a Fractal Reservoir", SPE Paper 20582, 65th Annual Technical Conference and Exhibition of the SPE, Sept. 23-26, New Orleans, LA.
- Berkowitz, B. and Balberg, I. (1993): "Percolation Theory and Its Application to Groundwater Hydrology", to be published in *Water Resour. Res.*
- Bondor, P. L., Hirasaki, G. J. and Tham, M. J. (1972): "Mathematical Simulation of Polymer Flooding in Complex Reservoirs", *Soc. Pet. Eng. Jour.*, (Oct.) 369-82.
- Carslaw, H. S. and Jaeger, J. C. (1959): *Conduction of Heat in Solids* (2nd edition), Oxford University Press, Oxford.
- Chang, J. and Yortsos, Y. C. (1990): "Pressure-Transient Analysis of Fractal Reservoirs", *Soc. Pet. Eng. Form. Eval.*, (March) 31-38.
- Chang, J. and Yortsos, Y. C. (1992): "Comments on Pressure-Transient Analysis of Fractal Reservoirs", *Soc. Pet. Eng. Form. Eval.*, manuscript submitted.
- Christopher, R. H. and Middleman, S. (1965): "Power-Law Flow Through a Packed Tube", *I. & E. C. Fundamentals*, **4**(4) 422-26.

- Doe, T. W. (1991): "Fractional Dimension Analysis of Constant-Pressure Well Tests", SPE Paper 22702, 66th Annual Technical Conference and Exhibition of the SPE, Oct. 6-9, Dallas, TX.
- Doung, A. N. (1989): "A New Set of Type Curves for Well-Test Interpretation with the Pressure/Pressure-Derivative Ratio, *Soc. Pet. Eng. Form. Eval.*, 264-272.
- Gaitonde, N. Y. and Middleman, S. (1967): "Flow of Viscoelastic Fluids Through Porous Media", *I. & E. C. Fundamentals*, 6(1) 145-47.
- Gogarty, W. B. (1967): "Rheological Properties of Pseudoplastic Fluids in Porous Media", *Soc. Pet. Eng. Jour.*, (June) 149-59.
- Harris, J. (1977): *Rheology and Non-Newtonian Flow*, Longman, London.
- Ikoku, C. U. (1978): "Transient Flow of Non-Newtonian Power-Law Fluids in Porous Media", Ph.D. dissertation, Stanford University, Stanford, CA.
- Ikoku, C. U. and Ramey, H. J., Jr. (1979): "Transient Flow of Non-Newtonian Power-Law Fluids in Porous Media", *Soc. Pet. Eng. Jour.*, (June) 164-74.
- Ikoku, C. U. and Ramey, H. J., Jr. (1980): "Wellbore Storage and Skin Effects During the Transient Flow of Non-Newtonian Power-Law Fluids in Porous Media", *Soc. Pet. Eng. Jour.*, (Feb.) 25-38.
- Ikoku, C. U. and Ramey, H. J., Jr. (1982): "Pressure Behaviour During Polymer Flow in Petroleum Reservoirs", *Jour. Ener. Resour. Tech.*, 104 149-56.
- Long, J. C. S., Majer, E. L., Martel, S. J., Karasaki, K., Peterson, J. E., Jr., Davey, A. and Hestir, K. (1990): *Hydrologic Characterization of Fractured Rocks – An*

*Interdisciplinary Methodology*, Report LBL-27863, Lawrence Berkeley Laboratory, Berkeley, CA (Nov.).

McKinley, R. M., Jahns, H. O., Harris, W. W. and Greenkorn, R. A. (1966): "Non-Newtonian Flow in Porous Media", *A. I. Ch. E. J.*, (Jan.) 17-20.

Murtha, J. A. and Ertekin, T. (1983): "Numerical Simulation of Power-Law Fluid Flow in a Vertically Fractured Reservoir", SPE Paper 12011, 58th Annual Technical Conference and Exhibition of the SPE, Oct. 5-8, San Francisco, CA.

Odch, A. S. and Yang, H. T. (1979): "Flow of Non-Newtonian Power-Law Fluids Through Porous Media", *Soc. Pet. Eng. Jour.*, (June) 155-63.

Olarewaju, J. S. (1992): "A Reservoir Model of Non-Newtonian Fluid Flow", SPE 25301 (unsolicited manuscript).

Orbach, R. (1986): "Dynamics of Fractal Networks", *Science*, (Feb. 21) 814-19.

O'Shaughnessy, B. and Procaccia, I. (1985): "Diffusion on Fractals", *Phys. Rev. A*, **32**(5) 3073-83.

Pascal, H. and Pascal, F. (1985): "Flow of Non-Newtonian Fluid Through Porous Media", *Int. Jour. Eng. Sci.*, **23**(5) 571-85.

Poon, D. C. and Kisman, K. (1992): "Non-Newtonian Effects on the Primary Production of Heavy Oil Reservoirs", *Jour. Can. Pet. Tech.*, **31**(7) 55-59.

Sabet, M. A. (1991): *Well Test Analysis*, Gulf Publishing Company, Houston.

- Sahimi, M. and Yortsos, Y. C. (1990): "Application of Fractal Geometry to Porous Media: A Review", SPE Paper 20476, 65th Annual Technical Conference and Exhibition of the SPE, Sept. 23-26, New Orleans, LA.
- Savins, J. G. (1969): "Non-Newtonian Flow Through Porous Media", *I. & E. C.*, (Oct.) 18-47.
- Schowalter, W. R. (1978): *Mechanics of Non-Newtonian Fluids*, Pergamon Press, Oxford.
- Stanislav, J. F., Easwaran, C. V. and Kokal, S. L. (1992): "Elliptical Flow in Composite Reservoirs", *Jour. Can. Pet. Tech.*, **31**(10) 47-50.
- Stehfest, H. (1970): "Numerical Inversion of Laplace Transform", *Commun. ACM*, **13**(1) 47-49.
- Streltsova, T. D. (1988): *Well Testing in Heterogeneous Formations*, John Wiley and Sons, New York.
- Torok, J. S. and Advani, S. H. (1987): "Non-Newtonian Fluid Flow in a Reservoir – An Application to Hydraulic Fracturing", *Jour. Ener. Resour. Tech.*, **109** 6-10.
- van Everdingen, A. F. and Hurst, W. (1949): "The Application of the Laplace Transformation to Flow Problems in Reservoirs", *Trans. Am. Inst. Min. Metall.*, **186** 305-324.
- van Poolen, H. K. and Jargon, J. R. (1969): "Steady-State and Unsteady-State Flow of Non-Newtonian Fluids Through Porous Media", *Soc. Pet. Eng. Jour.*, (March) 80-88.

- Vongprachai, S. and Raghavan, R. (1987): "Pressure Falloff Behaviour in Vertically Fractured Wells: Non-Newtonian Power-Law Fluids", *Soc. Pet. Eng. Form. Eval.*, (Dec.) 573-89.
- Warren, J. E. and Root, P. J. (1963): "The Behaviour of Naturally Fractured Reservoirs", *Soc. Pet. Eng. Jour.*, (Sept.) 245-55.
- Yortsos, Y. C. (1991): *Modification of Chemical and Physical Factors in Steamflood to Increase Heavy Oil Recovery*, Technical Report for the U. S. Department of Energy, Ch. 9.

## Appendix A

### COMPUTER PROGRAM FOR GENERATING DIMENSIONLESS PRESSURES FOR POWER-LAW FLOW IN AN INFINITE FRACTAL RESERVOIR

```

C      **      THE PROGRAM LISTED HERE IS DEVELOPED      **
C      **      TO CALCULATE DIMENSIONLESS WELLBORE      **
C      **      PRESSURE RESPONSE IN LAPLACE SPACE DURING  **
C      **      THE PRODUCTION OF A NON-NEWTONIAN, POWER- **
C      **      -LAW TYPE FLUID AT A CONSTANT RATE FROM   **
C      **      AN INFINITE RESERVOIR EXHIBITING FRACTAL  **
C      **      DISTRIBUTIONS OF POROSITY AND PERMEABILITY. **
C      **
C      **      THIS PROGRAM COMPUTES THE DIMENSIONLESS    **
C      **      PRESSURE RESPONSE AND ITS DERIVATIVE USING **
C      **      NUMERICAL LAPLACE TRANSFORM INVERSION WITH **
C      **      THE STEHFEST ALGORITHM (STEHFEST, 1970).   **
C      **
C      *****      MAIN PROGRAM      *****
C
C      *****      DEFINITION OF VARIABLES      *****
C      *****
C
C      **      INPUT VARIABLES      *****
C
C      AN --> DIMENSIONLESS FLOW BEHAVIOUR INDEX (POWER-
C              LAW PARAMETER)
C      DS --> DIMENSIONLESS SPECTRAL DIMENSION
C      S --> LAPLACE VARIABLE
C      T(J) --> ARRAY OF DIMENSIONLESS TIME
C      TD --> DIMENSIONLESS TIME
C
C      **      OUTPUT VARIABLES      *****
C
C      PWD(J) --> VECTOR OF THE WELLBORE PRESSURE DROP
C      DPWDL(J) --> VECTOR OF THE SLOPE OF THE WELLBORE
C                  PRESSURE RESPONSE
C
C      *****
C
C      IMPLICIT REAL*8 (A-H, O-Z)
C
C      DIMENSION TDST(10), TD(100),
C      # PWD(100), DPWDL(100)
C
C      COMMON/THE/AN,DS
C
C      DATA TDST/1.00D0,1.50D0,2.00D0,2.50D0,3.00D0,4.00D0,5.00D0,
C      # 6.00D0,7.00D0,8.00D0/
C      M=777
C      N=8
C      READ (5,*) AN,DS
C      CALCULATE THE VALUES OF TD
C      ITD=0
C      DO 20 J=1,8
C      DO 20 K=1,10

```

```

      ITD=ITD+1
      TDI=TDST(K)*(10.0D0**(J-1))
      TD(ITD)=TDI
20    CONTINUE
      NTD=ITD-1
      WRITE (6,30) AN,DS
30    FORMAT ('The values of n =',1E9.4,2X,'and ds =',1E9.4)
      WRITE (6,40)
40    FORMAT (3X,'tD',5X,'PwD',5X,'dPwD/dlntD')
C
C
      DO 50 J=1,NTD
      T=TD(J)
      CALL INVERT(T,M,N,PD,PDP)
      PWD(J)=PD
      DPWDL(J)=T*PDP
C
C      PRINT OUT COLUMNS OF TD, PWD AND DPWDL VALUES
C
      WRITE (6,60) T,PWD(J),DPWDL(J)
60    FORMAT (1E12.6,5X,1E12.6,5X,1E12.6)
50    CONTINUE
      STOP
      END
C
C      THE STEHFEST ALGORITHM
C      *****
C      SUBROUTINE INVERT(TD,M,N,PD,PDP)
C      THIS SUBROUTINE COMPUTES NUMERICALLY
C      THE LAPLACE TRANSFORM INVERSE OF ANY FUNCTION
C      IN LAPLACE SPACE, F(S).
C      COURTESY OF: ANIL K. AMBASTHA (PET E 668; 1991)
C
      IMPLICIT REAL*8(A-H,O-Z)
      DIMENSION G(50), H(50), V(25)
C
C      NOW IF THE ARRAY V(I) WAS COMPUTED BEFORE, THE PROGRAM
C      GOES DIRECTLY TO THE END OF THE SUBROUTINE TO CALCULATE
C      F(S).
C
      IF (N.EQ.M) GO TO 17
      M=N
      DLOGTW=0.6931471805599453DC0
      NH=N/2
C
C      THE FACTORIALS OF 1 TO N ARE CALCULATED INTO ARRAY G.
C
      G(1)=1.D0
      DO 1 I=2,N
      G(I)=G(I-1)*I
1    CONTINUE
C
C      TERMS WITH K ONLY ARE CALCULATED INTO ARRAY H.
C
      H(1)=2.D0/G(NH-1)
      DO 6 I=2,NH
      FI=I
      IF (I-NH) 4,5,6
4    H(I)=FI**NH*G(2*I)/(G(NH-I)*G(I)*G(I-1))
      GO TO 6
5    H(I)=FI**NH*G(2*I)/(G(I)*G(I-1))
6    CONTINUE
C
C      THE TERMS (-1)**NH+1 ARE CALCULATED.
C      FIRST THE TERM FOR I=1
      SN=2*(NH-NH/2*2)-1

```



```

C
C     THE REST OF THE SN'S ARE CALCULATED IN THE MAIN ROUTINE.
C
C     THE ARRAY V(I) IS CALCULATED.
C     DO 7 I=1,N
C
C     FIRST SET V(I) =0
C     V(I)=0.D0
C
C     THE LIMITS FOR K ARE ESTABLISHED.
C     THE LOWER LIMIT IS K1=INTEG((I+1/2))
C     K1=(I+1)/2
C
C     THE UPPER LIMIT IS K2=MIN(I,N/2)
C     K2=I
C     IF (K2-NH) 8,8,9
C     K2=NH
C     THE SUMMATION TERM IN V(I) IS CALCULATED.
C
C     DO 15 K=K1,K2
C     IF (2*K-I) 12,13,12
C     IF (I-K) 11,14,11
C     V(I)=V(I)+H(K)/(G(I-K)*G(2*K-I))
C     GO TO 15
C     V(I)=V(I)+H(K)/G(I-K)
C     GO TO 15
C     V(I)=V(I)+H(K)/G(2*K-I)
C     15 CONTINUE
C
C     THE V(I) ARRAY FINALLY CALCULATED BY WEIGHTING
C     ACCORDING TO S
C     V(I)=SN*V(I)
C
C     THE TERM SN CHANGES ITS SIGN EACH INTERATION.
C     SN=-SN
C     7 CONTINUE
C
C     THE NUMERICAL APPROXIMATION IS CALCULATED.
C     17 PD=0.D00
C     PDP=0.D00
C     A=DLOGTW/TD
C     DO 19 I=1,N
C     ARG=A*I
C     C/LL LAP(ARG,PWDL,PDPL)
C     PD=PD+V(I)*PWDL
C     PDP=PDP+V(I)*PDPL
C     19 CONTINUE
C     PD=PD*A
C     PDP=PDP*A
C     18 RETURN
C     END
C
C     SUBROUTINE LAP HAS THE FUNCTIONS THAT ARE OF INTEREST;
C     THE DIMENSIONLESS PRESSURE AND DIMENSIONLESS PRESSURE
C     DERIVATIVE FUNCTIONS ARE EXPRESSED IN TERMS OF THE
C     LAPLACE VARIABLE, S, WHICH CORRESPONDS TO VARIABLE
C     "ARG" IN SUBROUTINE "INVERT".
C
C     SUBROUTINE LAP(S,PWDL,PDPL)
C     IMPLICIT REAL*8(A-H,O-Z)
C     COMMON/THE/AN,DS
C     A=2.0D0*DSQRT(S)/(AN+1.0D0-DS*(AN-1.0D0))
C     V1=1.00d00-DS/(AN+1.0D0-DS*(AN-1.0D0))
C     V2=1.0D0-V1

```

```

      IF (V1 .EQ. 0.0D00) GOTO 66
C
      NN=1
      CALL DBSKES (V1,A,NN,BK1)
      CALL DBSKES (V2,A,NN,BK2)
      ANUM=BK1/DEXP(A)
      ADEN=BK2*S*DSQRT(S)/DEXP(A)
      GOTO 67
66     ANUM=DBSK0E(A)/DEXP(A)
      ADEN=DBSK1E(A)*S*DSQRT(S)/DEXP(A)
67     PWDL=ANUM/ADEN
      PDPL=S*PWDL
C
      RETURN
      END

```

## Appendix B

### COMPUTER PROGRAM FOR NUMERICAL SOLUTION OF THE NONLINEAR PARTIAL DIFFERENTIAL EQUATION FOR FLOW OF A POWER-LAW FLUID IN AN INFINITE FRACTAL RESERVOIR

```

C      **      THE PROGRAM LISTED HERE USES THE DOUGLAS-      **
C      **      JONES PREDICTOR-CORRECTOR METHOD FOR THE      **
C      **      NUMERICAL SOLUTION OF THE NONLINEAR      **
C      **      PARTIAL DIFFERENTIAL EQUATION GOVERNING      **
C      **      THE TRANSIENT FLOW OF A NON-NEWTONIAN      **
C      **      POWER-LAW FLUID IN AN INFINITE FRACTAL      **
C      **      RESERVOIR.      **
C      **      **
C      **      AT TIME TD=0, THE DIMENSIONLESS PRESSURE      **
C      **      IS ZERO EVERYWHERE. THE FLOW RATE INTO THE      **
C      **      FINITE-RADIUS WELLBORE IS CONSTANT, AND      **
C      **      PRESSURE AT THE OUTER BOUNDARY IS ZERO AS      **
C      **      THE DISTANCE TO THE OUTER BOUNDARY TENDS      **
C      **      TO A VERY LARGE VALUE.      **
C      **      **
C      **      THE WELLBORE PRESSURE IS PRINTED AT EVERY      **
C      **      TIME-STEP AFTER CONVERGENCE IS ACHIEVED AT      **
C      **      THE CORRECTOR STAGE.      **
C
C      *****      MAIN PROGRAM      *****
C
C      *****      DEFINITION OF VARIABLES      *****
C      *****
C
C      ** INPUT VARIABLES *****
C
C      AN --> DIMENSIONLESS FLOW BEHAVIOUR INDEX (POWER-
C      LAW PARAMETER)
C      DELTD --> SIZE OF THE TIME-STEP
C      DF --> DIMENSIONLESS FRACTAL DIMENSION
C      DS --> DIMENSIONLESS SPECTRAL DIMENSION
C      DX --> SPATIAL INCREMENT
C      EPSILON --> MAXIMUM ALLOWABLE RELATIVE DIFFERENCE IN PRESSURES
C      FROM TWO DIFFERENT ITERATION LEVELS
C      N --> NUMBER OF SPATIAL INTERVALS INTO WHICH THE SYSTEM
C      IS DIVIDED BY THE GRID POINTS
C      TD --> DIMENSIONLESS TIME
C      TDMAX --> MAXIMUM VALUE OF DIMENSIONLESS TIME CONSIDERED
C
C      ** OUTPUT VARIABLES *****
C
C      IC --> ITERATION COUNTER
C      P(1) --> REQUIRED WELLBORE PRESSURE SOLUTION AT THE
C      CURRENT VALUE OF TIME TD
C      *****
C
C      IMPLICIT REAL*8(A-H, O-Z)
C
C      DIMENSION A(1001), B(1001), C(1001), D(1001), P(1001),

```

```

1          PHALF(1001), PNEW(1001)
C
  READ (5,*) N, DX, DELTD, TDMAX
  READ (5,*) AN, DF, DS, EPSILON
  WRITE (6,'(2(A,G12.6))')
+ 'AN = ', AN, ', DF = ', DF
  WRITE (6,'(2(A,G12.6))')
+ 'DS = ', DS, ', EPSILON = ', EPSILON
C
  PRINT *, ' '
C
  N1 = N + 1
  A3 = (DF/DS) * (AN + 1.0D0) / AN
  A2 = (DF/DS) ** ((AN + 1.0D0) / AN)
  A1 = AN * (DF - A3)
  DX2 = DX * DX
  ALPHA = 2.0D0 * DX2 / DELTD
  C1 = A3 * DX
  C2 = (AN - 1.0D0) / AN
  C2N = -C2
  C3 = (DF/DS) * C2
  C4 = DX * DF / DS
  C5 = A2 * ALPHA
  C6 = A1 * DX
C
C  SETTING INITIAL AND BOUNDARY CONDITIONS...
DO 10 I = 1, N1
  P(I) = 0.0D0
  PHALF(I) = 0.0D0
10
C
C  PERFORM CALCULATIONS OVER SUCCESSIVE TIME-STEPS
TD = 0.0D0
20  TD = TD + DELTD
C
C  NOW BEGINS THE PREDICTOR; THE COEFFICIENT ARRAYS A, B, C AND
C  RIGHT-HAND SIDE VECTOR D ARE SET AND PRESSURES AT THE END OF
C  HALF OF THE TIME-STEP, PHALF, ARE COMPUTED.
C
  B(1) = -(2.0D0+C3*C5)
  D(1) = C4 * C6 - C3 * C5 * P(1) - 2.0D0 * C4
  A(1) = 0.0D0
  C(1) = 2.0D0
C
  DO 60 I = 2, N
    IP1 = I + 1
    IM1 = I - 1
    AIM1 = IM1
    DP1 = (P(IM1) - P(IP1)) / (2.0D0*DX)
    IF (DP1 .LE. 0.0D00) GO TO 30
    PD1 = 1.0D00 / DP1
    B(I) = -(2.0D0+C5*DEXP(C1*AIM1)*(PD1**C2N))
    D(I) = A1 * DX2 * DP1 - C5 * DEXP(C1*AIM1) * (PD1**C2N) * P(I)
    GO TO 50
30  CONTINUE
    IF (TD .EQ. DELTD) THEN
      B(I)=-2.0D0
      D(I)=0.0D0
      GO TO 50
    ENDIF
C
  NN = I - 1
  CALL TRISOL(1, NN, A, B, C, D, PNEW)

```

```

C      DO 40 J = NN + 1, N
40      PNEW(J) = P(J)
C
      GO TO 70
50      CONTINUE
      A(I) = 1.0D0
      C(I) = 1.0D0
60      CONTINUE
C
      C(N) = 0.0D0
C
      CALL TRISOL(1, N, A, B, C, D, PNEW)
C
70      DO 80 I = 1, N
80      PHALF(I) = PNEW(I)
C
C      THE CORRECTOR BEGINS NOW; IN THIS STAGE ALSO THE COEFFICIENT
C      ARRAYS A, B AND C AND THE RIGHT-HAND SIDE VECTOR D ARE SET;
C      SUBSEQUENTLY, THE PRESSURES AT THE END OF THE TIME-STEP
C      ARE CALCULATED.
C
      IC = 0
      D(1) = -2.0D0 * PHALF(2) + 2.0D0 * PHALF(1) - C3 * C5 * P(1) + 2.
10D0 * C4 * C6 - 4.0D0 * C4
90      IC = IC + 1
C
      DO 130 I = 2, N
      IP1 = I + 1
      IM1 = I - 1
      AIM1 = IM1
      DP2 = (PHALF(IM1) - PHALF(IP1)) / (2.0D0 * DX)
      IF (DP2 .LE. 0.0D00) GO TO 100
      PD2 = 1.0D00 / DP2
      B(I) = -(2.0D0 + C5 * DEXP(C1 * AIM1) * (PD2 ** C2N))
      D(I) = -(PHALF(IM1) + PHALF(IP1) - 2.0D00 * PHALF(I)) - C5 * DEXP(
1      C1 * AIM1) * (PD2 ** C2N) * P(I) + 2.0D0 * A1 * DX2 * DP2
      GO TO 120
C
100      CONTINUE
      NN = I - 1
      CALL TRISOL(1, NN, A, B, C, D, PNEW)
C
      DO 110 J = NN + 1, N
110      PNEW(J) = PHALF(J)
C
      GO TO 140
C
120      CONTINUE
130      CONTINUE
C
      CALL TRISOL(1, N, A, B, C, D, PNEW)
C
C      CHECK FOR CONVERGENCE
140      DIFF1 = (PNEW(1) - PHALF(1)) / PNEW(1)
      IF (DABS(DIFF1) .LE. EPSILON) GO TO 160
C
      DO 150 I = 1, N
150      PHALF(I) = PNEW(I)
C
      GO TO 90
160      CONTINUE
C
      DO 170 I = 1, N

```

```

170 P(I) = PNEW(I)
C
C PRINT CURRENT VALUE OF TIME, THE NUMBER OF ITERATIONS
C REQUIRED AND THE WELLBORE PRESSURE VALUE.
WRITE (6, '(A,G12.6,A,I3)') 'TD = ', TD, ', IC = ', IC
WRITE (6, '(A,G12.6)') 'P(1): ', P(1)
IF (TD .LE. TDMAX) GO TO 20
STOP
END

C
C
SUBROUTINE TRISOL(I, N, A, B, C, D, PRESS)
C SUBROUTINE FOR SOLVING A SYSTEM OF LINEAR SIMULTANEOUS
C EQUATIONS WITH A TRIDIAGONAL COEFFICIENT MATRIX.
IMPLICIT REAL*8 (A - H, O - Z)
DIMENSION A( , B(*), C(*), D(*), PRESS(*), BETA(1001),
1 GAMMA(1001)
BETA(I) = B(I)
GAMMA(I) = D(I) / BETA(I)
IP1 = I + 1

C
DO 10 K = IP1, N
BETA(K) = B(K) - A(K) * C(K - 1) / BETA(K - 1)
GAMMA(K) = (D(K) - A(K) * GAMMA(K - 1)) / BETA(K)
10 CONTINUE
C
PRESS(N) = GAMMA(N)
M = N - 1

C
DO 20 J = 1, M
K = N - J
PRESS(K) = GAMMA(K) - C(K) * PRESS(K + 1) / BETA(K)
20 CONTINUE
C
RETURN
END

```

## Appendix C

### COMPUTER PROGRAM FOR GENERATING DIMENSIONLESS PRESSURES FOR POWER-LAW FLOW IN A FINITE FRACTAL RESERVOIR

```

C      **      THE PROGRAM LISTED HERE IS DEVELOPED      **
C      **      TO CALCULATE DIMENSIONLESS WELLBORE      **
C      **      PRESSURE AND DERIVATIVE RESPONSE IN      **
C      **      LAPLACE SPACE DURING THE PRODUCTION      **
C      **      OF A NON-NEWTONIAN, POWER--LAW TYPE      **
C      **      FLUID AT A CONSTANT RATE FROM A FINITE   **
C      **      FRACTAL RESERVOIR.                      **
C      **
C      **      THIS PROGRAM COMPUTES THE DIMENSIONLESS   **
C      **      PRESSURE RESPONSE AND ITS DERIVATIVE USING **
C      **      NUMERICAL LAPLACE TRANSFORM INVERSION WITH **
C      **      THE STEHFEST ALGORITHM (STEHFEST, 1970).  **
C      **
C      *****      MAIN PROGRAM      *****
C
C      *****      DEFINITION OF VARIABLES      *****
C      *****
C      ** INPUT VARIABLES *****
C
C      AN --> DIMENSIONLESS FLOW BEHAVIOUR INDEX (POWER-
C              LAW PARAMETER)
C      DF --> DIMENSIONLESS FRACTAL DIMENSION
C      DS --> DIMENSIONLESS SPECTRAL DIMENSION
C      RED --> DIMENSIONLESS RADIUS TO OUTER BOUNDARY
C      S --> VARIABLE OF LAPLACE TRANSFORM W. R. T. TIME, TD
C      T(J) --> ARRAY OF DIMENSIONLESS TIME
C      TD --> DIMENSIONLESS TIME
C
C      ** OUTPUT VARIABLES *****
C
C      PWD(J) --> VECTOR OF THE WELLBORE PRESSURE DROP
C      DPWDL(J) --> VECTOR OF THE SLOPE OF THE WELLBORE
C                  PRESSURE RESPONSE
C
C      *****
C
C      IMPLICIT REAL*8 (A-H, O-Z)
C
C      DIMENSION TDST(10), TD(200),
C      * PWD(200), DPWDL(200)
C
C      COMMON/TH/AN, DF, DS, RED
C
C      DATA TDST/1.0D0,1.5D0,2.0D0,2.5D0,3.0D0,4.0D0,5.0D0,6.0D0,
C      * 7.0D0,8.0D0/
C      M=777
C      N=8
C      READ (5,*) AN,DF,DS,RED

```

```

C      CALCULATE THE VALUES OF TD
      ITD=0
      DO 10 J=3,10
      DO 10 K=1,10
      ITD=ITD+1
      TDI=TDST(K)*(10.0D0**(J-1))
      TD(ITD)=TDI
10     CONTINUE
      NTD=ITD-1
      WRITE (6,20) AN,DF
20     FORMAT ('The value of n =',1E9.4,2X,'and df =',1E9.4)
      WRITE (6,30) DS,RED
30     FORMAT ('The value of ds =',1E9.4,2X,'and reD =',1E9.4)
      WRITE (6,40)
40     FORMAT (3X,'tD',3X,'PwD',3X,'dPwD/dlntD')
C
C
      DO 50 J=1,NTD
      T=TD(J)
      CALL INVERT(T,M,N,PD,PDP)
      PWD(J)=PD
      DPWDL(J)=T*PDP
C
C      PRINT OUT COLUMNS OF TD, PWD AND DPWDL VALUES
C
      WRITE (6,60) TD(J),PWD(J),DPWDL(J)
60     FORMAT (1E12.6,3X,1E12.6,3X,1E12.6)
50     CONTINUE
      STOP
      END

```



```

C      *** CLOSED OUTER BOUNDARY CASE      *****
C
C      SUBROUTINE LAP HAS THE FUNCTIONS THAT ARE USED TO
C      CALCULATE THE DIMENSIONLESS PRESSURE AND PRESSURE
C      DERIVATIVE FUNCTIONS IN TERMS OF THE LAPLACE VARIABLE,
C      S, AND THE SYSTEM PARAMETERS.
C
      SUBROUTINE LAP(S,PWDL,PDPL)
      IMPLICIT REAL*8(A-H,O-Z)
      COMMON/THE/AN, DF, DS, RED
      PIE=3.14159265359D00
      ALPHA=2.0D0*DSQRT(S)/(AN+1.0D0-DS*(AN-1.0D0))
      BETA=((DF/DS)*(AN+1.0D0)-DF*(AN-1.0D0))/2.0D00
      V1=1.00D00-DS/(AN+1.0D0-DS*(AN-1.0D0))
      V2=1.00D00-V1
      ARGU1=ALPHA*(RED**BETA)
      ARGU2=V2*PIE
C
      NN=1
      CALL DBSKES(V2,ARGU1,NN,BK1)
      CALL DBSIES(V2,ARGU1,NN,BI1)
      T1=BI1/DEXP(ARGU1)+2.0D0*DSIN(ARGU2)*BK1/PIE/DEXP(ARGU1)
      T6=T1
      CALL DBSKES(V1,ALPHA,NN,BK2)
      T2=BK2/DEXP(ALPHA)
      CALL DBSIES(V1,ALPHA,NN,BI3)
      T3=BI3/DEXP(ALPHA)
      T4=BK1/DEXP(ARGU1)
      T7=T4
      CALL DESKES(V2,ALPHA,NN,BK5)
      T5=BK5/DEXP(ALPHA)
      CALL DBSIES(V2,ALPHA,NN,BI6)
      T8=BI6/DEXP(ALPHA)+2.0D0*DSIN(ARGU2)*T5/PIE
C
C      CALCULATE THE PRESSURE SOLUTION, AS GIVEN IN EQUATION (7-27)
C
      PWDL=(T1*T2+T3*T4)/(T5*T6-T7*T8)/S/DSQRT(S)
      PDPL=S*PWDL
      RETURN
      END

```

```

C      *** CONSTANT PRESSURE OUTER BOUNDARY CASE      *****
C
C      SUBROUTINE LAP HAS THE FUNCTIONS THAT ARE USED TO
C      CALCULATE THE DIMENSIONLESS PRESSURE AND PRESSURE
C      DERIVATIVE FUNCTIONS IN TERMS OF THE LAPLACE VARIABLE,
C      S, AND THE SYSTEM PARAMETERS.
C
      SUBROUTINE LAP(S,PWDL,PDPL)
      IMPLICIT REAL*8(A-H,O-Z)
      COMMON/THE/AN, DF, DS, RED
      PIE=3.14159265359D00
      ALPHA=2.0D0*DSQRT(S)/(AN+1.0D0-DS*(AN-1.0D0))
      BETA=((DF/DS)*(AN+1.0D0)-DF*(AN-1.0D0))/2.0D00
      V1=1.00D00-DS/(AN+1.0D0-DS*(AN-1.0D0))
      V2=1.00D00-V1
      ARGU1=ALPHA*(RED**BETA)
      ARGU2=V2*PIE
C
      NN=1
      CALL DBSIES(V1,ARGU1,NN,BI1)
      T1=BI1/DEXP(ARGU1)
      T6=T1
      CALL DBSKES(V1,ALPHA,NN,BK2)
      T2=BK2/DEXP(ALPHA)
      CALL DBSIES(V1,ALPHA,NN,BI3)
      T3=BI3/DEXP(ALPHA)
      CALL DBSKES(V1,ARGU1,NN,BK4)
      T4=BK4/DEXP(ARGU1)
      T7=T4
      CALL DBSKES(V2,ALPHA,NN,BK5)
      T5=BK5/DEXP(ALPHA)
      CALL DBSIES(V2,ALPHA,NN,BI8)
      T8=BI8/DEXP(ALPHA)+2.0D0*DSIN(ARGU2)*T5/PIE
C
C      CALCULATE THE PRESSURE SOLUTION, AS GIVEN IN EQUATION (7-27)
C
      PWDL=(T1*T2-T3*T4)/(T5*T6+T7*T8)/S/DSQRT(S)
      PDPL=S*PWDL
      RETURN
      END

```